

UNIVERSITAT POLITÈCNICA DE CATALUNYA  
PONTIFICIA UNIVERSIDAD CATÓLICA DEL PERÚ  
CENTRE TECNOLÒGIC DE TELECOMUNICACIONS DE CATALUNYA

**X-Band Substrate Integrated Waveguide  
Cavity-backed Patch Antenna  
Self-Oscillating Mixer**

By

Renzo Díaz Portilla

A thesis submitted in partial fulfillment  
for the degree of Engineer

in the

Escola Tècnica Superior d'Enginyeria de Telecomunicacions de Barcelona  
Departament de Teoria del Senyal i Comunicacions

October 2010

# Abstract

The work is focused on designing, measuring and testing an active substrate integrated waveguide (SIW) cavity-backed patch antenna self-oscillating mixer (SOM). The cavity-backed antenna structure permits to overcome potential problems such as heat dissipation, unwanted surface wave modes and at the same time may provide better phase noise performance of the SOM.

Full-wave FEM-based analysis and harmonic balance (HB) and matrix conversion (CM) simulations are used to design the passive antenna and the active antenna self-oscillating mixer, whose frequency responses have been evaluated for different values of certain geometrical parameters. Compact, single substrate prototypes are presented. These low cost implementations could be useful in radar and communication applications.

# Agradecimientos

A mis padres y hermanos por siempre haberme apoyado en todos los proyectos que he emprendido a lo largo de mi vida. Sus consejos, compañía y amor incondicional han sido vitales para que todas las metas trazadas hayan sido más fáciles de alcanzar. Muchas gracias por todo.

A aquellos amigos y profesores que a lo largo de la carrera me han acompañado y han influido en mi desarrollo tanto profesional como personal. Haber estado presentes a lo largo de estos años y haber compartido un sinfín de anécdotas ha sido muy importante y estaré siempre agradecido por todo ello. Especialmente a las personas con las que compartí una nueva etapa en Barcelona: Javier, Bruce, Oscar, Jesús y Omar; como también aquellos que me acompañaron desde antes: Laura, George, Cesar, Ozzy, Gustavo, Alfredo, Andrew y Andrés. Muchas gracias por su apoyo y amistad.

A aquellas personas que creyeron en mí y en el desarrollo de este proyecto. Sin duda su amistad, colaboración y amabilidad hicieron que este trabajo haya sido una de las mejores experiencias que he tenido y crearon uno de los mejores entornos donde he podido trabajar. Por ello agradezco a Apóstolos, Selva y especialmente a Ana por todo el apoyo brindado.

# Contents

<b>Abstract</b> .....	<b>1</b>
<b>Acknowledgements</b> .....	<b>2</b>
<b>Contents</b> .....	<b>3</b>
<b>List of Figures</b> .....	<b>5</b>
<b>List of Tables</b> .....	<b>8</b>
<b>1. Introduction</b> .....	<b>9</b>
1.1. Overview .....	10
<b>2. State of the Art</b> .....	<b>11</b>
2.1. Receiving Phased Arrays based on Coupled SOMs.....	11
2.2. A brief Background Information .....	12
2.2.1. Substrate Integrated Waveguide (SIW) Technology .....	12
2.2.2. Cavity-backed Patch Antenna.....	14
2.2.2.1. Patch Antenna .....	14
2.2.2.2. Cavity-Backed Antenna.....	15
2.2.3. Self-Oscillating Mixers (SOM).....	15
<b>3. Simulation methods</b> .....	<b>17</b>
3.1. Harmonic Balance.....	17
3.2. Finite Element Method (FEM).....	20
3.3. Conversion Matrix .....	21
<b>4. SIW Cavity-Backed Patch Antenna design</b> .....	<b>25</b>
4.1. SIW Cavity-Backed Patch Antenna Structure .....	25
4.1.1. Description.....	25
4.1.2. Relevant parameters of SIW Cavity-Backed Patch Antenna .....	28
4.2. Simulation Setup and Design Process .....	29
4.2.1. Antenna dimensions.....	29
4.2.2. Design and Simulation process.....	30
4.3. Simulation Results .....	42
4.3.1. Finding a good SIW Cavity-Backed Patch Antenna Structure .....	42
4.3.2. Results of the SIW Cavity-Backed Patch Antenna Structure .....	44
<b>5. SOM Active Integrated Antenna design</b> .....	<b>50</b>

5.1. SOM Active Integrated Antenna structure .....	50
5.1.1. Description.....	50
5.2. Simulation Setup and Design Process .....	52
5.2.1. Circuit dimensions .....	52
5.2.2. Design and Simulation process.....	54
5.2.2.1. Finding the oscillation frequency.....	54
5.2.2.2. Self-Oscillating Mixer simulation .....	59
<b>6. Fabrication and measurements.....</b>	<b>64</b>
6.1. Fabrication process.....	64
6.2. Measurement results.....	68
6.2.1. $S_{11}$ Parameter of the Passive Antenna .....	68
6.2.2. Oscillation frequency of the SOM .....	69
6.2.3. Radiation Pattern Measurements Process and Results .....	71
6.2.3.1. Comparison procedure.....	71
6.2.3.2. Measurement Process of the Radiation Pattern .....	74
6.2.3.3. Passive Antenna.....	77
6.2.3.4. Active antenna.....	79
6.2.4. Gain of the SOM.....	81
<b>7. Conclusions and future work .....</b>	<b>82</b>
<b>Bibliography .....</b>	<b>83</b>

# List of Figures

Figure 2.1: Topology of an SIW guide realized on a dielectric substrate .....	13
Figure 2.2: Rectangular-patch antenna configuration .....	15
Figure 3.1: Harmonic Balance representation of the circuit .....	18
Figure 3.2: Representation of a non-linear circuit.....	18
Figure 3.3: General model .....	21
Figure 4.1: Front view of the SIW cavity-backed patch antenna.....	26
Figure 4.2: Rear view of the SIW cavity-backed patch antenna .....	27
Figure 4.3: Passive antenna structure .....	29
Figure 4.4: Box that represents the substrate structure .....	30
Figure 4.5: Adding project variables .....	31
Figure 4.6: Substrate dimensions and position .....	32
Figure 4.7: Substrate attributes .....	32
Figure 4.8: Substrate structure .....	32
Figure 4.9: Subtracting the rectangles.....	33
Figure 4.10: Defining the subtraction.....	33
Figure 4.11: Ground plane and patch.....	33
Figure 4.12: Assign the correct behavior.....	34
Figure 4.13: Variables for the cooper plane design and feed line design .....	34
Figure 4.14: Rectangles that represent the feed line and the ground plane .....	35
Figure 4.15: Joining the rectangles.....	36
Figure 4.16: Bottom part of the substrate .....	36
Figure 4.17: Variables for the metalized via holes design.....	37
Figure 4.18: Representation of the metalized via holes .....	37
Figure 4.19: Metalized via hole attribute (Perfect conductor).....	38
Figure 4.20: Preview of the SIW cavity-backed antenna.....	38
Figure 4.21: Air box and wave port representation .....	39
Figure 4.22: Box and rectangle attributes.....	39
Figure 4.23: Adding a solution setup .....	40
Figure 4.24: Adding a frequency sweep .....	40
Figure 4.25: Far field radiation sphere setup.....	41
Figure 4.26: Resonant frequency variation versus the stub length .....	42

Figure 4.27: Changing feed line length.....	43
Figure 4.28: Simulated 3D radiation pattern.....	44
Figure 4.29: Simulated E-plane co-polar radiation pattern in a polar plot (a) and rectangular plot (b).....	45
Figure 4.30: Simulated E-plane cross-polar radiation pattern in a polar plot (a) and rectangular plot (b).....	46
Figure 4.31: Simulated H-plane co-polar radiation pattern in a polar plot (a) and rectangular plot (b).....	47
Figure 4.32: Simulated H-plane cross-polar radiation pattern in a polar plot (a) and rectangular plot (b).....	48
Figure 4.33: Directivity .....	49
Figure 5.1: Active antenna oscillating mixer structure.....	51
Figure 5.2: Active antenna oscillating mixer structure .....	53
Figure 5.3: OscTest element .....	54
Figure 5.4: Osc Test results representation .....	55
Figure 5.5: Auxiliary generator schematic .....	57
Figure 5.6: AuxG conditions setup in Harmonic Balance .....	57
Figure 5.7: Variables to optimize .....	58
Figure 5.8: Harmonic Balance results after the optimization.....	59
Figure 5.9: Small signal set up .....	60
Figure 5.10: Small-signal voltage source .....	61
Figure 5.11: Defining gain equation .....	61
Figure 5.12: Gain goal .....	61
Figure 5.13: Generating the layout .....	62
Figure 5.14: Circuit layout .....	63
Figure 6.1: Exporting all data into a Gerber file type .....	65
Figure 6.2: Fixing A25N substrate into the work surface of the LPFK milling machine .....	65
Figure 6.3: Before I removed the unwanted cooper .....	66
Figure 6.4: Removing the unwanted copper using a cutter and following the marks made by the milling machine .....	66
Figure 6.5: SOM Active Integrated Antenna: Rear view (a) and front view (b).....	67
Figure 6.6: SIW cavity-backed antenna: Rear view (a) and front view (b).....	67
Figure 6.7: $S_{11}$ parameter plot .....	68
Figure 6.8: Oscillation frequency's behavior according the drain voltage .....	69
Figure 6.9: Oscillation frequency injecting 0.4 volt in the drain terminal.....	70
Figure 6.10: Oscillation frequency injecting 1.5 volts in the drain terminal .....	70
Figure 6.11: Transmission and reception scheme for standard horn antenna measurement ....	71

Figure 6.12: Transmission and reception scheme to SIW cavity-backed antenna measurement .....	72
Figure 6.13: Transmission and reception scheme for SOM Active Integrated Antenna measurement.....	73
Figure 6.14: $L_{IF}$ and $L_{RF}$ measurement.....	74
Figure 6.15: Measuring E-plane co-polar .....	74
Figure 6.16: Measuring E-plane cross-polar .....	75
Figure 6.17: Measuring H-plane co-polar .....	75
Figure 6.18: Measuring H-plane cross-polar.....	76
Figure 6.19: Rotational platform of the anechoic chamber .....	76
Figure 6.20: Measured E-plane co-polar radiation patter.....	77
Figure 6.21: Measured E-plane cross-polar radiation pattern .....	77
Figure 6.22: Measured H-plane co-polar radiation pattern .....	78
Figure 6.23: Measured H-plane cross-polar radiation pattern .....	78
Figure 6.24: Measured E-plane co-polar radiation pattern.....	79
Figure 6.25: Measured E-plane cross-polar radiation pattern.....	80
Figure 6.26: Measured H-plane co-polar radiation pattern .....	80
Figure 6.27: Measured H-plane cross-polar radiation pattern.....	81
Figure 6.28: Conversion Gain of the self-oscillating mixer .....	81

## List of Tables

Table 4.1: Substrate parameters .....	27
Table 4.2: Antenna dimensions.....	29
Table 4.3: Relevant characteristics of the designed antenna .....	49
Table 5.1: Parameters of the circuit.....	52
Table 5.2: Values for the OscTest simulation.....	55
Table 5.3: Optimized variables .....	58
Table 5.4: Optimized variables in order to obtain a reasonable conversion gain .....	62
Table 6.1: Passive antenna results.....	79

## Chapter 1:

# Introduction

At the beginning of the century, wireless communications began a long road full of prosperous progress. Since Marconi's proposals until today, the technologies used for wireless communications have progressed very fast. These advances have always had as its purpose the low power consumption, miniaturization of components and, above all, maximum efficiency.

With the advent of transistors, circuits have achieved high performance and current receivers have widely reduced their size. The transistors have enabled many applications such as amplifiers, oscillators, mixers, among others. Without doubt, this nonlinear device allows a wide range of important applications to the development of wireless communications.

Nowadays, in microwave communications, receivers have achieved a great reduction of their size maintaining its efficiency. This is due to the use of the transistor and other technologies that complement each other.

One of them is the use of microstrip technology to design passive circuits. Microstrip is widely used due to its compact size and easy integration. But with frequency increasing as an open structure a microstrip circuit shows undesirable radiation. To solve these kinds of problems we can use SIW technology.

The SIW technology is important because any non-planar waveguide like structure (including classical rectangular waveguide) can be synthesized into planar form, which can be seamlessly integrated with conventional printed planar circuits (including transitions, active components and antennas). This is one of the major advantages of SIW technology, because allow us to fabricate a complete circuit in planar form. Moreover, it is possible to mount one or more chips on the same substrate, reducing losses and parasitics. Using the SIW technology, one can optimize an antenna structure and integrate it with different components.

With the use of the SIW technology, we can propose a better antenna structure. The SIW technology allows us to make cavity-backed antennas. These kinds of antennas have better performance because suppress the propagation of surface wave, increase the bandwidth,

decrease end-fire radiation, decrease cross-polarization radiation and increase the applicable frequency range.

This project is focused on designing, measuring and testing an active SIW cavity-backed antenna integrating a self-oscillating mixer.

## **1.1. Overview**

The issues related to the optimized design of the SIW cavity-backed patch antenna and of the self-oscillating mixer are presented in this report as follows:

- Chapter 2 describes the state of the art of microwave receivers based on coupled SOMs. It also presents a brief description of the technologies used in this project.
- Chapter 3 describes the simulations methods used in this project.
- Chapter 4 describes the design and the simulation process of the SIW cavity-backed antenna. It also presents the simulation results.
- Chapter 5 describes the design and the simulation process of the SIW cavity-backed antenna integrating a self-oscillating mixer and also presents the simulation results.
- Chapter 6 presents the fabrication process and the measurement process. It presents the final results and the comparison between the simulations results and the fabrication results.
- Chapter 7 presents the conclusions and the future work

## Chapter 2

# State of the Art

This chapter presents a brief description of the target application of this project: Receiving phased arrays based on coupled SOMs. It also explains some concepts that were applied to develop this project: First, a brief description about SIW technology and its benefits is explained; in the same way, the characteristics of cavity-backed patch antenna are described; finally, some characteristics of self-oscillating mixers and their advantages with respect to the use of common down converters are presented.

It is worth noting that joint use of those technologies is important to develop this project. Because of that, this chapter is essential to acquire basic notions that were used to design and fabricate the compact active SIW cavity-backed patch antenna SOM.

### 2.1. Receiving Phased Arrays based on Coupled SOMs

Active phased antenna arrays have a number of advantages due to their compact size, light weight, low cost and energy efficiency. They are perfect to applications as power combining, beam-forming and adaptive beam-forming. An active antenna mostly consists of a passive radiating element and an active circuit integrated in the same substrate.

In the design of a phased array based on coupled SOMs each element of the phased array allows the double functionality of variable phase shifters and down-converters. Therefore, the single SOM has to be designed before the complete phased array is implemented. In this work, in order to be able to scan the beam of the receiving array in a wide range, the incoming RF signal (from the antenna) will be mixed with the 2<sup>nd</sup> harmonic of the SOM. To achieve a good performance, the SOM has to be designed to present conversion gain ( $G_c$ ) at the chosen output frequency  $f_f$ . The complete phased array using SOMs can be externally injection locked to improve stability.

In the proposed phased array, the SOMs oscillate at the same frequency and their relative phases can be electronically set, for example by controlling their free-running (uncoupled) frequencies. The relative phases of the radiating elements ultimately define the main beam direction of the array and, generally, the shape of the radiation pattern.

This project presents the design of the single element that will be used to implement receiving phased arrays based on coupled SOMs. Here an X-Band SIW Cavity-Backed Antenna Self-Oscillating Mixer is studied and manufactured.

## **2.2. A brief Background Information**

This section explains some concepts that are applied to develop this project. They are important to understand the design and the fabrication process that will be explained in the next chapters.

### **2.2.1. Substrate Integrated Waveguide (SIW) Technology**

The deployment of microwave integration technologies is critical for the evolution of wireless systems and applied electromagnetics in the next few years. Current waveguides allow us to obtain high-performance in microwave system. This classical waveguide has a non-planar structure that forces the designers to make hybrids schemes of planar and non-planar structures. However, a number of design techniques of planar circuits integrated with non-planar circuits have been reported that may not be so attractive for widespread applications because the designs proposed to date present themselves a real challenge for mass-production with respect to microwave integration and packaging. In this context, substrate integrated waveguide (SIW) technology emerges to offer a compact, flexible and cost-effective solution for integrating planar and non-planar circuits.

Thanks to SIW technology, any non-planar waveguide like structure can be synthesized into planar form, which can be seamlessly integrated with conventional printed planar circuits. This is one of the major advantages of SIW technology, because allow us to fabricate a complete circuit in planar form. Moreover, it is possible to mount one or more chip on the same substrate, reducing losses [1].

The SIW technology has been applied to several microwave components, including active circuits, passive components and antennas. Concerning the passive circuits, most of the classical microwave components have been implemented in SIW technology. This allows us to obtain components with a substantial reduction in size; moreover, their losses are lower than in the corresponding microstrip devices, and there are no radiation and packaging problems. SIW technology was also used to implement several active components, thus exploiting the advantage of an easy integration of the active elements with the waveguide components [1].

The SIW is synthesized through the use of arrays of metallized via hole in the substrate (Fig. 2.1). Those two rows of metallized holes in the substrate create equivalent electrical walls into which electromagnetic waves or field are confined. To design a good SIW structure, we have to follow some simple design steps. The parameters necessary for the design of the guide are:

the diameter  $D$  of the holes, the spacing  $b$  between the holes and the spacing  $W$  between the two rows of via holes; and the rule of design are:

$$b \leq 2D \quad (2.1)$$

$$D < \lambda_g/5 \quad (2.2)$$

One of the major issues in the design of SIW components is related to minimization of losses. As rectangular waveguides, SIW structures exhibit conductor losses due to the finite conductivity of metallic walls and dielectric losses due to the loss tangent of dielectric substrate. Those kinds of losses in SIW can be minimized. We just have to modify geometrical parameters, namely the substrate thickness  $h$ , the diameter  $D$  of the metal vias and their longitudinal spacing  $b$  (Figure 2.1).

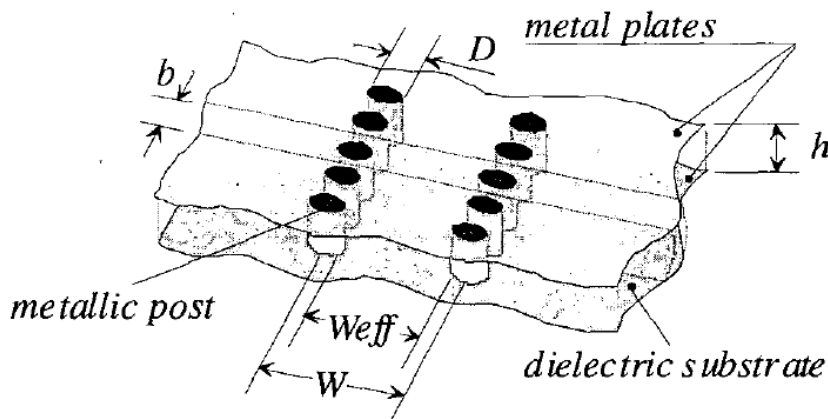


Figure 2.1: Topology of an SIW guide realized on a dielectric substrate

The thickness  $h$  plays an important role. Increasing  $h$  (while keeping the other physical dimensions unchanged) determines a very important reduction in the conductor loss. But, in the other hand, has no effect on the dielectric loss. In general, radiation loss is not affected by the substrate thickness (at least, as long as  $h$  is smaller than a half wavelength) [2].

Another important geometrical parameter is the diameter  $d$ . The conductor loss slightly decreases when increasing the diameter  $d$  of the vias. However, the dielectric loss is practically independent on the diameter  $d$ . A similar behavior is observed with longitudinal spacing  $b$ . When decreasing the value of  $b$ , the conductor loss decreases (because of the increased metal surface) and the dielectric loss practically remains unchanged. For those two parameters, we have to use the condition 2.1 to keep a small radiation loss [2].

Finally, SIW technology is a very promising candidate for the integration of microwave circuits and systems in the next decade. SIW allow us to integrate active circuits, passives

components and radiating elements on the same substrate. Moreover, SIW technology offers low loss, flexible and cost effective solutions for implementing microwave circuits. For those reason, this project used SIW technology.

## 2.2.2. Cavity-backed Patch Antenna

In the last few years, with rapid development of wireless communications, low profile antenna with good radiation performance and better isolation from feed network are in great demand, especially in space application such as satellite, aircraft and radar. Cavity backed patch antenna, for their attractive characteristics, are very suitable for those applications and have been studied by many researches. In this chapter, we describe patch antennas, their profits and losses; and we present as a solution the cavity-back patch antenna.

### 2.2.2.1. Patch Antenna

A patch antenna consists of a thin metallic patch, usually made of copper or gold, placed over a dielectric substrate which has a conducting ground plane at the bottom of it. Patch antennas have many profits like low profile, light-weight antennas most suitable for aerospace and mobile applications, they can be designed to operate over a large range of frequencies (1-40 GHz), easy integration with linear or planar arrays and they can generate linear, dual and circular polarizations. Patch antennas have low-cost fabrication and they are fabricated using printed circuit board etching that makes them useful to create integrated active antennas. Patch antennas could take any kind of shape and configuration, but in this project was decided to use a rectangular patch antenna.

The basic patch antenna elements are a thin conductor of dimensions  $L \times W$  (rectangular patch), a dielectric substrate with a permittivity constant  $\epsilon_r$ , loss tangent  $\tan \delta$  and thickness  $h$  backed and a conducting ground plane. We can see the configuration in Figure 2.2. The material covered in this section is from [3] and [4]

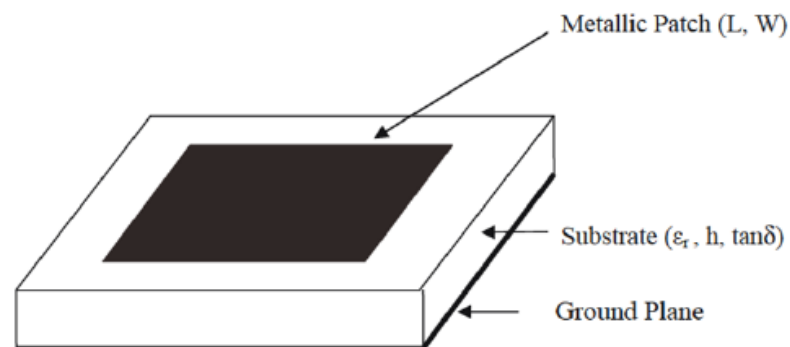


Figure 2.2: Rectangular-patch antenna configuration

### **2.2.2.2. Cavity-Backed Antenna**

One of the most serious limitations of patch antennas is the narrow bandwidth. One solution is to increase the thickness of the substrate. However, thick substrate causes the propagation of surface wave. This is a serious problem in patch antenna because surface wave reduce the antenna efficiency and gain, limit the bandwidth, increase end-fire radiation, increase cross-polarization radiation and limit the applicable frequency range. The radiation efficiency of the antenna decreases due to power carried away by the surface wave [from 5]. To avoid these undesired effects, one of the suitable choices is to place the patch antenna into a metallic cavity to suppress the surface waves: cavity-backed antennas.

The characteristics of cavity-backed antennas as reported in literature are summarized as follows:

- Cavities can suppress surface waves and mutual coupling in thick substrates and act as heat sinks in a high-powered large transmit array [6].
- Including stacked patch antenna configuration in a cavity further increases the bandwidth of patch antennas [7], [8].
- Inclusion of high-permittivity superstrates on the cavitybacked patch antenna improves the antenna gain significantly [9], [10].
- In a phased array antenna, cavities can prevent scan blindness, yield less coupling and improve good matching over wider scan angles [11]–[12].
- Standard microstrip patch antennas exhibit zero field strength near the horizon. A patch antenna in a cavity enclosure can improve the radiation near and beyond the horizon; thus, a truly omnidirectional radiation pattern can be achieved [13].
- Gain and radiation patterns can be changed significantly by placing the patch antenna into a cavity enclosure and changing the shape of the enclosure [14].
- Introducing a cavity on an aperture coupled patch antenna, cross-polar levels in radiation patterns, and mutual coupling between antenna elements can be improved [15].
- Patch with metallic cavity filled with dielectric material reduces the antenna dimensions. Up to 30% reduction in antenna diameter is achieved [16].

For those characteristics, a cavity-backed patch antenna was chosen, using SIW technology to suppress propagation of surface wave.

### **2.2.3. Self-Oscillating Mixers (SOM)**

Nowadays, transmitter and receiver require efficient frequency converters with low power consumption, small size and low cost. The self-oscillating mixer is a very attractive frequency converter to fulfill all these requirements.

Usually, the local oscillator (LO) signal is externally introduced to the mixer circuit. In the case of the self-oscillating mixer (SOM) one can use a transistor that will provide both the local oscillator signal and the at the same time perform the mixing process. This allows avoiding the use of any external LO signal and designing a more compact and efficient circuit. As we are using an active device it is possible to obtain conversion gain.

A self-oscillating mixer can be seen as an oscillator with a frequency  $f_{LO}$ . Then a external signal at  $f_{RF}$  is introduced into the circuit. One has to design first the oscillator circuit at  $f_{LO}$ . Then when introducing the RF signal at  $f_{RF}$ , the mixing process occurs and one can obtain the intermodulation products of  $f_{LO}$  and  $f_{RF}$  [17], [18].

In order to design a self-oscillation mixer, one must use a nonlinear analysis. The problem is that designers often have little control of the self-oscillating frequency, conversion gain and output power and there is a lack of optimization tools. Because of that, it is important to choose a correct simulation method to obtain a good design of the self-oscillation mixer.

Finally, the self-oscillating mixer approach simplifies the circuitry of the entire receiver system. Allow us to get conversion gain without amplifier stages, decrease power consumption and have a double function in only one circuit. For those characteristics, it was chosen to make the project.

## Chapter 3:

# Simulation methods

Nowadays communications systems have evolved, reaching a better efficiency and greater complexity. In this context, RF circuits and microwave circuits have been improving their characteristics. To design RF circuits and microwave circuits, we need to use powerful simulation tools that permit us to make an optimal and reliable design.

We have to take in mind that the design of non-linear circuits increases the complexity of the design. This increase is due to multiple mathematical solutions that require an additional analysis to verify the stability of the circuit.

Because of the difficulty involved in designing RF and microwave circuits, the designer has to choose a correct simulation method. The election of one simulation method depends of the circuit characteristics and of the working regime.

This chapter explains three simulations methods that were used to design the self-oscillating mixer (SOM) cavity-backed antenna: Harmonic balance (HB), conversion matrix (CM) and finite element method (FEM).

### 3.1. Harmonic Balance

The harmonic-balance is a technique that uses frequency-domain descriptions for the linear circuits while keeping the necessary time-domain descriptions for the non-linear circuits. HB analysis allows us to calculate the steady-state frequency response of a RF and microwave circuits due to the employment of Fourier series expansions for the circuit variables. This is an advantage because permit us to decrease the simulation time. But, on the other hand, we can have some difficulties because the solutions are not necessarily stable due to different steady-state solutions may coexist for the same parameter values.

To obtain the HB equations, the circuit under analysis has to be partitioned into its linear and non-linear parts (Figure 3.1) [19]. The unknowns are the voltages between the linear block and the non-linear block, but to simplify the resolution we only take the control variables from the non-linear block. This allows us to decrease the number of unknowns. The representation of the non-linear block is shown in Figure 3.2 [20].

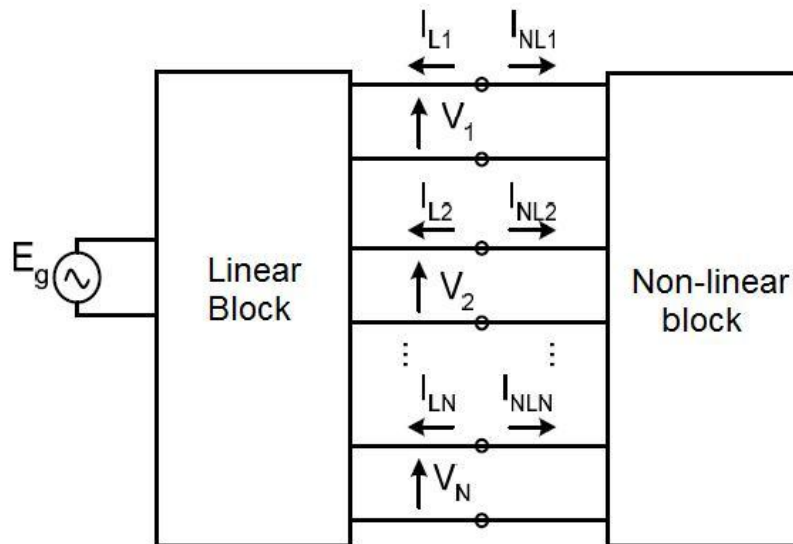


Figure 3.1: Harmonic Balance representation of the circuit

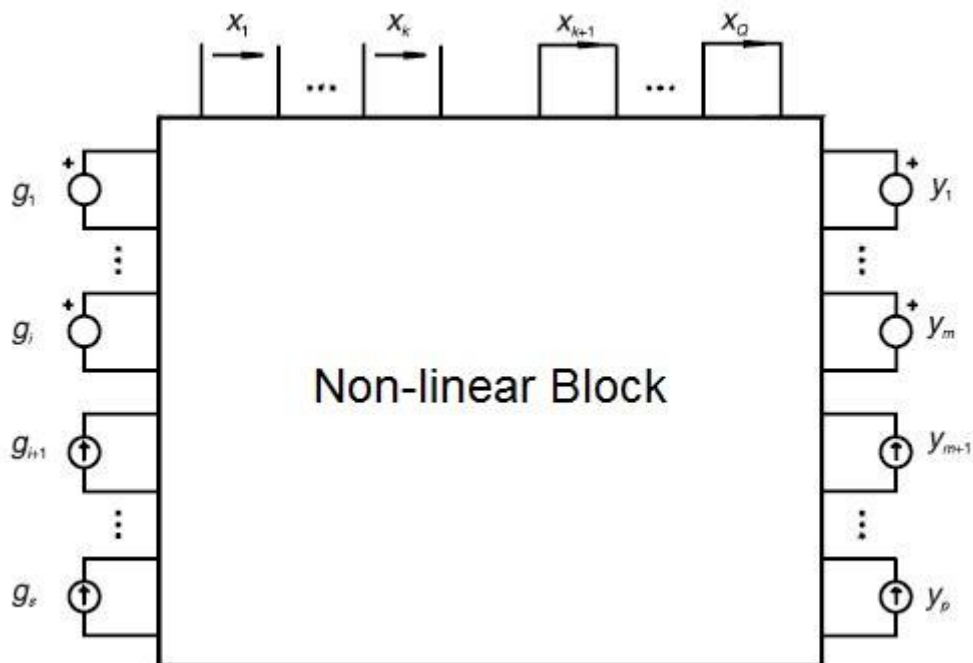


Figure 3.2: Representation of a non-linear circuit

In Figure 3.2, three different kinds of elements can be distinguished:  $x(t)$ , a vector with the control variables of the independent sources;  $y(t)$ , considered a vector of non-linear dependent sources; and  $g(t)$ , a vector of the independent generators.

The components of the three vectors ( $x$ ,  $y$  and  $g$ ) can be expanded in a Fourier series that have an infinite number of harmonics components ( $N$ ). In practice, the series have to be truncated to a limited number of harmonic components. The use of the Fourier series with a limited number of harmonic determines the HB to periodic and quasi-periodic regimes.

Once the Fourier series has been established, the three vectors  $\bar{x}(t)$ ,  $\bar{y}(t)$  and  $g(t)$  can be translated to the frequency domain, obtaining the three new vectors  $\bar{X}$ ,  $\bar{Y}$  and  $\bar{G}$ . Then, Kirchhoff's laws to the circuit in Figure 3.2 have to be applied. Equating the total node currents and branch voltages, a matrix relationship is obtained:

$$\bar{H}(\bar{X}) = [A_x]\bar{X} - [A_y]\bar{Y}(\bar{X}) - [A_g]\bar{G} = 0 \quad (3.2)$$

where  $[A_x]$ ,  $[A_y]$  and  $[A_g]$  are frequency-dependent linear matrix and their order are defined as  $Q \times Q$ ,  $Q \times P$  and  $Q \times S$  ( $Q$ : number of control variables of the independent sources;  $P$ : number of non-linear dependent sources;  $S$ : number of independent generators). In this way, the number of equation generated by the HB are defined as  $(2N + 1)Q$  with the same number of unknowns.

To solve equation 3.2, we have to use a numerical method: Newton-Raphson. This is an interactive method that minimizes the norm of the error vector  $\bar{H}$ . A threshold value in the norm of this vector  $\|\bar{H}\| = \varepsilon$  is initially imposed and the algorithm converges when  $\|\bar{H}\|$  value is lower than  $\varepsilon$ . The algorithm starts with an initial value  $\bar{X}_0$  (determined from the values of the external generators) that allows us to calculate  $\bar{Y}_0$ . With both values ( $\bar{X}_0$  and  $\bar{Y}_0$ ) and knowing the linear matrix, we can calculate the  $\|\bar{H}\|$  value. If the algorithm does not converge, we can use another initial value (e.g.  $\bar{X}_1$ ) and repeat the procedure.

The Newton-Raphson algorithm may be difficult to implement in the case of very large circuits. To minimize this problem, the matrix factorization required for the Jacobian inversion has to be used.

The obtained HB solution does not need to be stable, because of this method does not calculate the transient solution of the circuit. But, the HB solution can converge into a mathematical solution that coexists with a real stable-solution.

### 3.2. Finite Element Method (FEM)

The finite element method is a numerical technique which gives approximate solutions to differential equations. In FEM, a problem has to be defined in geometrical space to be subdivided into a finite number of smaller regions where each subdivision has its own characteristics and need not be orthogonal. Over each element, the unknown variables are approximated using known functions. The functions use to be linear or higher-order polynomial expansions. The election of a function depends on the geometrical locations of the elements. The equations are integrated over each element and the solution summed over the entire problem domain. The solution of these equations is achieved using linear algebra techniques. [21]

A general example will be considered to explain the steps that we need to model a structure with this method [22]:

- In a first step, we have to determine the element properties from the geometric material and loading data. Each element shown in Figure 3.3(a) [22] has its own number and nodal connection. For this example:

Element	1	connection	1	3	4
	2		1	4	2
	3		2	5	
	4		3	6	7 4
	5		4	7	8 5

Assuming that properties are found in global coordinates we can enter each component in its position (Figure 3.3(b)) [22]. The single coefficient or the submatrix ( $K_{ab}$ ) is represented by the shaded square.

- In a second step, we have to define the final equations. Figure 3.3(c) [22] shows the result where the non-zero coefficients are indicated by shading. If the matrices are symmetric, we only need to find the half above the diagonal. All the non-zero coefficients are confined within a band or profile because, in a first instance, they can be calculated for the nodal connections.
- In a third step, the prescribed boundary conditions have to be inserted into the final assembled matrix.
- The final step solves the resulting equation system. The technique to solve the equation depends of the computer program that is used.

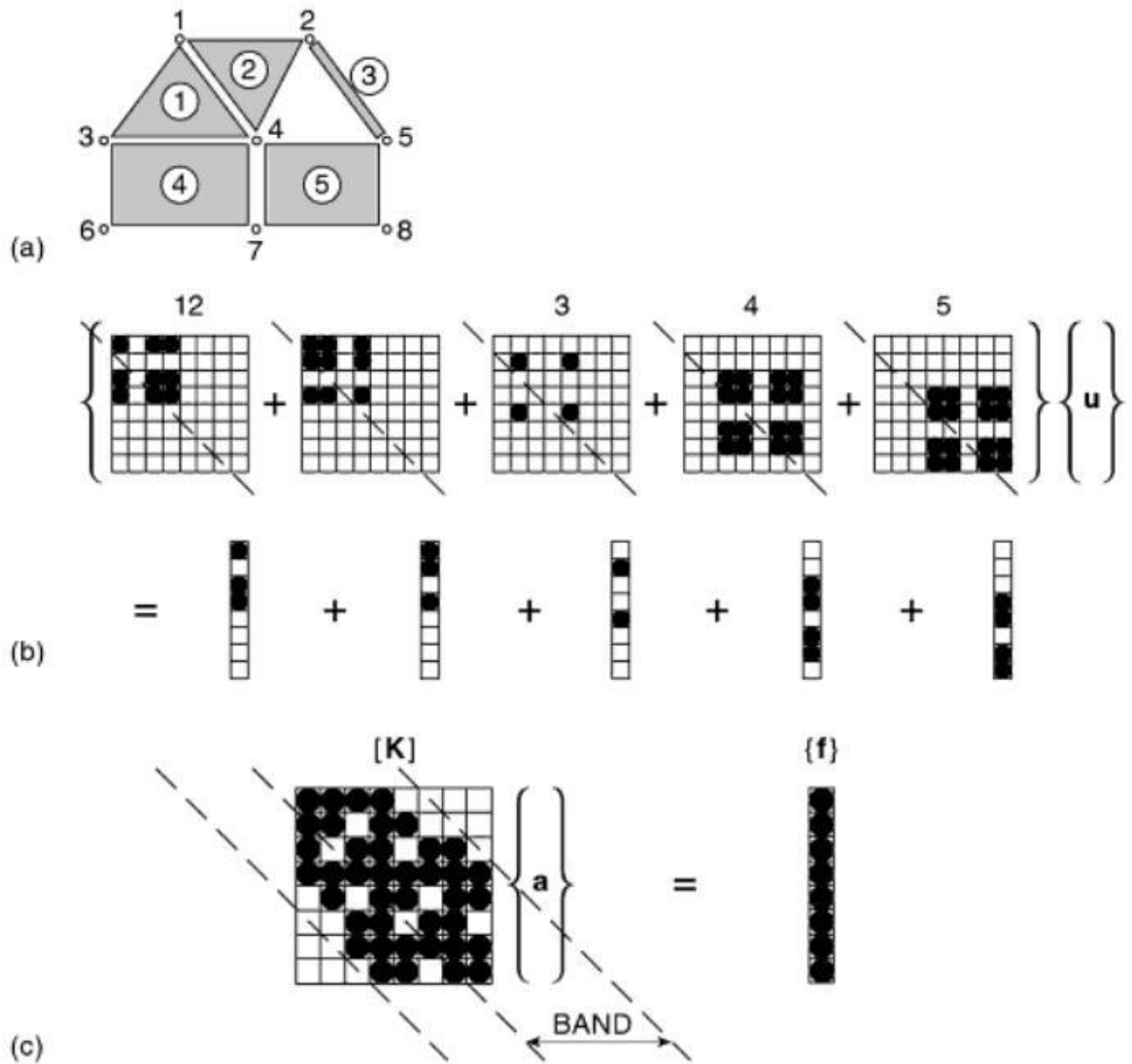


Figure 3.3: General model

### 3.3. Conversion Matrix

The conversion matrix [19] is a method that is used in circuits which involve large signals and small signals. Usually, the large signal drives the nonlinear element(s) into nonlinear operation and the small signal applies a small perturbation to the nonlinear operating regime. If the small signal has small enough amplitude, it can be linearized around a point of the large signal.

In a conversion matrix analysis, the large signal is periodic with a periodic frequency  $f_0$ . If we make a harmonic balance simulation, the steady state solution, that we obtain, has harmonics of the type:  $kf_0$ , where  $k = -NH \dots NH$ . In this description,  $NH$  represents the number of harmonics which the series has been truncated. We introduced a small signal with frequency  $f$  that is not

harmonically related with  $f_0$ . If the amplitude of this signal is small enough, the harmonic balance equations can be linearized around the large signal solutions in  $kf_0$ . In the circuit emerge frequency components of the type:  $kf_0 + f$ .

Next we can see the application of the method to a nonlinear parallel circuit. The nonlinearity is represented by a nonlinear dependence of a current source. The state variable is the voltage  $V$ . If we write the circuit equation, we have:

$$Y_L(k\omega_0 + \omega)v^p + i^p(t) = i_{g(t)} \quad (3.3)$$

where  $v^p(t)$  and  $i^p(t)$  are the voltage and the current affected by the perturbation of the small signal source.

$$\begin{aligned} v^p(t) = & v_0(t) + \Delta V_{DC} e^{j\omega t} + V_1^u e^{j(\omega_0 + \omega)t} + \Delta V_1^{1*} e^{j(-\omega_0 + \omega)t} \\ & + \Delta V_2^u e^{j(2\omega_0 + \omega)t} + \Delta V_2^{1*} e^{j(-2\omega_0 + \omega)t} + \dots \end{aligned} \quad (3.4)$$

Once the small signal source has been introduced, the current of the circuit can be written as shown in 3.11. The current can be represented by a Taylor series around  $v_0(t)$ .

$$\begin{aligned} i^p(t) = & i_0(t) + \Delta I_{DC} e^{j\omega t} + \Delta I_1^u e^{j(\omega_0 + \omega)t} + \Delta I_1^{1*} e^{j(-\omega_0 + \omega)t} + \\ & + \Delta I_2^u e^{j(2\omega_0 + \omega)t} + \Delta I_2^{1*} e^{j(-2\omega_0 + \omega)t} + \dots = \\ = & i_0(t) + \left[ \frac{\partial I_{DC}}{\partial V_{DC}} + \frac{\partial I_1^{1*}}{\partial V_{DC}} + \frac{\partial I_1^u}{\partial V_{DC}} + \dots \right] \Delta V_{DC} e^{j\omega t} + \\ & + \left[ \frac{\partial I_{DC}}{\partial V_1^u} + \frac{\partial I_1^u}{\partial V_1^u} + \frac{\partial I_1^{1*}}{\partial V_1^u} + \dots \right] \Delta V_1^u e^{j(\omega_0 + \omega)t} + \\ & + \left[ \frac{\partial I_{DC}}{\partial V_1^{1*}} + \frac{\partial I_1^u}{\partial V_1^{1*}} + \frac{\partial I_1^{1*}}{\partial V_1^{1*}} + \dots \right] \Delta V_1^{1*} e^{j(-\omega_0 + \omega)t} + \dots \end{aligned} \quad (3.5)$$

To write these equations, we have taken into account  $N$  harmonics in the steady-state periodic solution. Therefore, the elements  $-\omega$ ,  $-k\omega_0 \pm \omega$  are complex conjugates of the terms  $\omega$ ,  $k\omega_0 \pm \omega$ . In the formulation we have used the components  $\omega$ ,  $k\omega_0 + \omega$  and  $-k\omega_0 + \omega$  to represent the circuit variables. In this way,  $-k\omega_0 + \omega$  represents the voltage and it will be the complex conjugate of the lower sideband of the term  $k\omega_0 - \omega$ . Therefore, the term  $k\omega_0 + \omega$  is called  $\Delta V_k^u$  and the term  $-k\omega_0 + \omega$  as  $\Delta V_k^{1*}$ . in the same way we represents the current. The relations between the current and the voltage are given by the matrix conversion:

$$\begin{bmatrix} \Delta I_{DC} \\ \Delta I_1^{1*} \\ \Delta I_1^u \\ \Delta I_2^{1*} \\ \Delta I_2^u \\ \vdots \\ \Delta I_N^{1*} \\ \Delta I_N^u \end{bmatrix} = \begin{bmatrix} \frac{\partial I_{DC}}{\partial V_{DC}} & \frac{\partial I_{DC}}{\partial V_1^{1*}} & \frac{\partial I_{DC}}{\partial V_1^u} & \frac{\partial I_{DC}}{\partial V_2^{1*}} & \frac{\partial I_{DC}}{\partial V_2^u} & \dots & \frac{\partial I_{DC}}{\partial V_N^{1*}} & \frac{\partial I_{DC}}{\partial V_N^u} \\ \frac{\partial I_1^{1*}}{\partial V_{DC}} & \frac{\partial I_1^{1*}}{\partial V_1^{1*}} & & & & & & \\ \frac{\partial I_1^u}{\partial V_{DC}} & & \ddots & & & & & \\ \frac{\partial I_2^{1*}}{\partial V_{DC}} & & & \ddots & & & \vdots & \vdots \\ \frac{\partial I_2^u}{\partial V_{DC}} & & & & \ddots & & & \\ \vdots & & & & & \ddots & & \\ \frac{\partial I_N^{1*}}{\partial V_{DC}} & & & & & & \frac{\partial I_N^{1*}}{\partial V_N^{1*}} & \frac{\partial I_N^{1*}}{\partial V_N^u} \\ \frac{\partial I_N^u}{\partial V_{DC}} & & & \dots & & & \frac{\partial I_N^u}{\partial V_N^{1*}} & \frac{\partial I_N^u}{\partial V_N^u} \\ \frac{\partial I_N^u}{\partial V_{DC}} & & & \dots & & & \frac{\partial I_N^u}{\partial V_N^{1*}} & \frac{\partial I_N^u}{\partial V_N^u} \end{bmatrix} \begin{bmatrix} \Delta V_{DC} \\ \Delta V_1^{1*} \\ \Delta V_1^u \\ \Delta V_2^{1*} \\ \Delta V_2^u \\ \vdots \\ \Delta V_N^{1*} \\ \Delta V_N^u \end{bmatrix} \quad (3.6)$$

$$\Delta \bar{I} = [G] \Delta \bar{V} \quad (3.7)$$

where [G] is the matrix conversion and their coefficients can be calculated as:

$$g(t) = \left. \frac{\partial i}{\partial v} \right|_o (t) = \sum_k g_k e^{jk\omega_o t} \quad (3.8)$$

$$g_k = \left. \frac{\partial i}{\partial v} \right|_{k-j} = \frac{\partial I^k}{\partial V^j} \quad (3.9)$$

Therefore, [G] can be defined as:

$$[G] = \begin{bmatrix} g_0 & g_1 & g_{-1} & g_2 & \dots & \dots & g_N & g_{-N} \\ g_{-1} & g_0 & g_{-2} & g_1 & & & g_{N-1} & g_{-N-1} \\ g_1 & g_2 & g_0 & g_3 & & & & \vdots \\ g_{-2} & g_{-1} & g_{-3} & g_0 & & & & \vdots \\ \vdots & & & & \ddots & & & \vdots \\ \vdots & & & & & \ddots & & \\ g_{-N} & g_{-N+1} & g_{-N-1} & & & & g_0 & g_{-2N} \\ g_N & g_{N+1} & g_{N-1} & \dots & & & g_{2N} & g_0 \end{bmatrix} \quad (3.10)$$

Returning to the circuit equations, we can write:

$$\begin{bmatrix} Y_T(\omega) & 0 & 0 & 0 \\ 0 & Y_T(-\omega_0 + \omega) & 0 & 0 \\ 0 & 0 & Y_T(\omega_0 + \omega) & \vdots \\ 0 & 0 & \dots & 0 & Y_T(N\omega_0 + \omega) \end{bmatrix} \begin{bmatrix} \Delta V_{DC} \\ \Delta V_1^{1*} \\ \Delta V_1^u \\ \Delta V_2^{1*} \\ \Delta V_2^u \\ \vdots \\ \Delta V_N^{1*} \\ \Delta V_N^u \end{bmatrix} +$$

$$+ \begin{bmatrix} g_0 & g_1 & g_{-1} & g_2 & \dots & \dots & g_N & g_{-N} \\ g_{-1} & g_0 & g_{-2} & g_1 & & & g_{N-1} & g_{-N-1} \\ g_1 & g_2 & g_0 & g_3 & & & & \vdots \\ g_{-2} & g_{-1} & g_{-3} & g_0 & & & & \vdots \\ \vdots & & & & \ddots & & & \vdots \\ \vdots & & & & & \ddots & & \vdots \\ g_{-N} & g_{-N+1} & g_{-N-1} & & & & g_0 & g_{-2N} \\ g_N & g_{N+1} & g_{N-1} & \dots & & & g_{2N} & g_0 \end{bmatrix} \begin{bmatrix} \Delta V_{DC} \\ \Delta V_1^{1*} \\ \Delta V_1^u \\ \Delta V_2^{1*} \\ \Delta V_2^u \\ \vdots \\ \Delta V_N^{1*} \\ \Delta V_N^u \end{bmatrix} = \begin{bmatrix} \Delta I_{g_{DC}} \\ \Delta I_{g_1^{1*}} \\ \Delta I_{g_1^u} \\ \vdots \\ \Delta I_{g_N^{1*}} \\ \Delta I_{g_N^u} \end{bmatrix} \quad (3.11)$$

Simplifying:

$$\{[Y_T] + [G]\} \Delta \bar{V} = \Delta \bar{I}_g \quad (3.12)$$

The conversion matrix analysis is relevant in mixer circuits, which involves a radiofrequency signal (RF) with small amplitude and a local oscillator signal (LO) that represent the large signal. In a first step, we obtain the large signal response of the circuit with the harmonic balance, just working with the LO signal. Then the circuit has to be linearized around the large signal response and apply the RF signal. The analysis carried out by introducing the RF signal is linear. Because of the amplitude of the signal is small, the operating point of the system is not affected.

This kind of circuits could also be analyzed using the harmonic balance method using two tones. However, the conversion matrix method reduces the computation time and offer more accurate results.

## **Chapter 4:**

# **SIW Cavity-Backed Patch Antenna design**

This chapter presents a compact, passive substrate integrated waveguide (SIW) cavity-backed patch antenna design. The selected structure is a rectangular-patch antenna using substrate integrated waveguide (SIW) technology due to its benefits such as good performance, low cost and small size. Further details about the selection of the antenna structure will be given in this chapter.

In order to analyze the SIW Cavity-Backed Patch Antenna structure, Ansoft HFSS software was used. HFSS is an industry-standard simulation tool for 3D full-wave electromagnetic field simulation. By means of HFSS one can obtain E- and H-fields, currents distributions, S-parameters and near and far field results. HFSS will generate an appropriate, efficient and accurate mesh for solving the problem using the proven finite element method (FEM).

This chapter presents the process used to simulate the SIW Cavity-Backed Patch Antenna, the most important design parameters in the selected structure and the obtained results.

### **4.1. SIW Cavity-Backed Patch Antenna Structure**

In order to design the SIW Cavity-Backed Patch Antenna, it is important to select a SIW Cavity-Backed Patch Antenna structure and determine its most important design parameters. This allows us to simulate the structure in an easy and fast way, knowing the key parameters that we have to be changed in order to obtain the desired results. In the next two subsections, the used structure and the most relevant parameters of the SIW Cavity-Backed Patch Antenna are presented.

#### **4.1.1. Description**

The selected operation frequency for the antenna design was 9.9 GHz. In order to achieve this objective frequency, a rectangular-patch antenna that allows an easy fabrication process was selected. Furthermore, rectangular-patch antennas have many profits, such as low

profile, light-weight, easy integration with linear or planar arrays and can generate linear polarization. However, rectangular-patch antennas suffer from surface wave propagation. This is a serious problem in rectangular-patch antennas because surface wave reduce the antenna efficiency and gain, limit the bandwidth, increase end-fire radiation, increase cross-polarization radiation and limit the applicable frequency range (as mentioned in chapter 2).

To overcome these issues, a cavity backed patch antenna based on substrate integrated waveguide (SIW) technology combined with grounded coplanar waveguide (GCPW) structure was chosen. Metalized via holes were used to construct conventional metal waveguide in a planar substrate to suppress unwanted modes and to form a shielding cavity around the patch element. The patch is placed on one side of the substrate and it is isolated from the ground plane by a narrow gap typically about two substrate thicknesses wide. The square SIW cavity is formed using four rows of metalized vias. In order to obtain a behavior similar to a conventional metallic cavity, the conditions  $D/b > 0.5$  and  $D/\lambda_0 < 0.1$  must be satisfied, where  $\lambda_0$  denote free space wavelength,  $D$  is the diameter of the holes and  $b$  is the spacing between the hole. With these conditions, the attenuation constant is small enough and leakage from clearance between two neighboring vias can be neglected. A  $50 \Omega$  grounded coplanar waveguide is adopted as feeding element. Two stubs are etched perpendicular to the coplanar feed line on the top metal as shown in Figure 4-2. The transverse stub is necessary to increase the coupling efficiency.

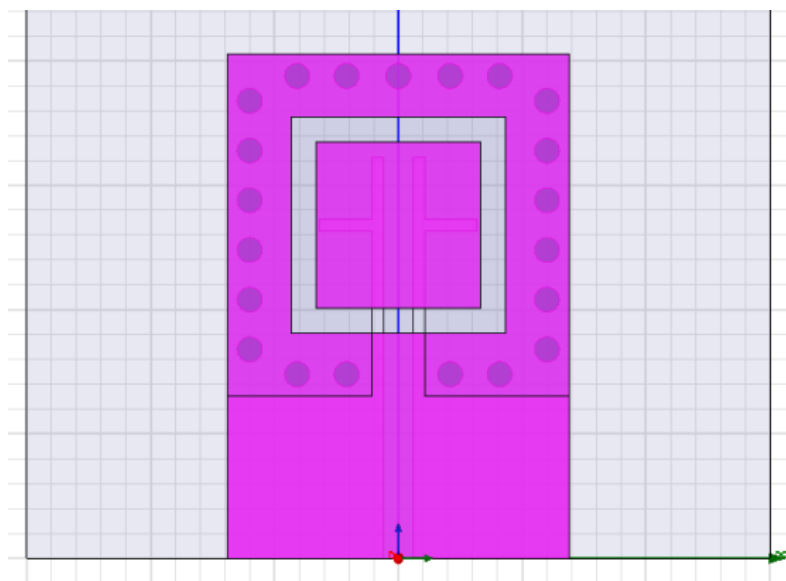


Figure 4.1: Front view

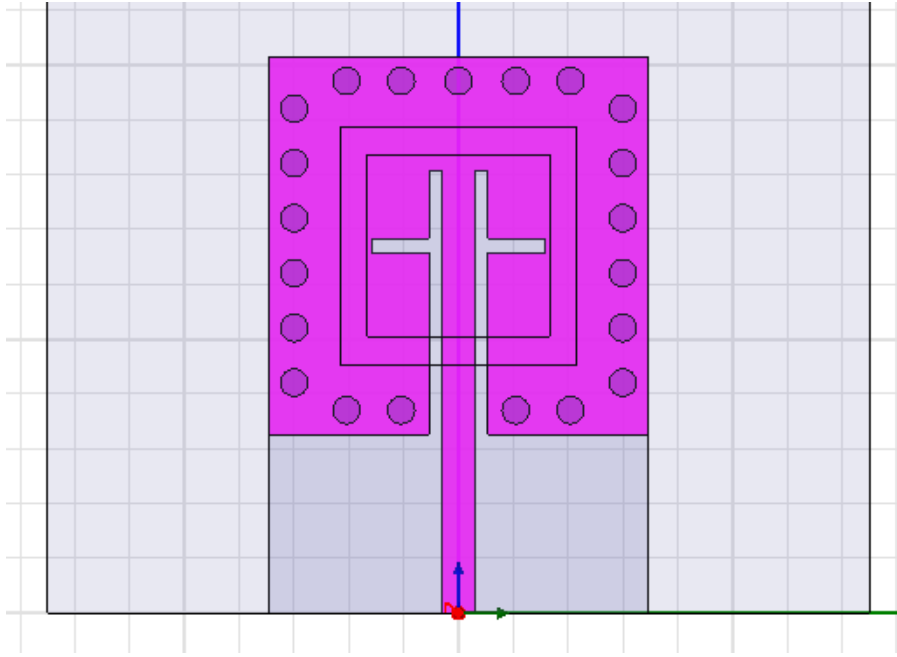


Figure 4.2: Rear view

The selected material for the antenna design was Arlon 25 N (A25N) whose parameters are shown in Table 4.1.

	A25N
$E_r$ (Dielectric constant)	3.38
TanD (Dissipation factor)	0.0025
H (thickness)	0.508 mm
Cond (Copper)	$5.813 \times 10^7$

Table 4.1: Substrate parameters

#### 4.1.2. Relevant parameters of SIW Cavity-Backed Patch Antenna

In order to make a fast and easy simulation, one needs to know about the most important parameters of the SIW cavity-backed antenna structure. Therefore, a brief description of the most important parameters, their characteristics and their relevance in the SIW cavity-backed antenna design is presented next:

- Antenna substrate dielectric constant: This parameter affects the bandwidth and radiation efficiency of the antenna, with lower permittivity giving wider impedance bandwidth and reduced surface wave excitation.
- Antenna substrate thickness: This parameter affects bandwidth and coupling level. A thicker substrate results in wider bandwidth, but less coupling for a given aperture size.
- Rectangular patch dimensions: The length of the patch radiator determines the resonant frequency of the antenna. The width of the patch affects the resonant resistance of the antenna, with a wider patch giving a lower resistance.
- Feed line size: Besides controlling the characteristic impedance of the feed line, the width of the feed line affects the coupling to the patch antenna. It allows us to modify the  $S_{11}$  parameter changing its length.
- Transverse stub in the feed line: This parameter is necessary to increase the coupling efficiency. It allows us to modify the resonant frequency changing its length.
- Metallized via arrays: This parameter has to fulfill the SIW technology requirements. These requirements are exposed in chapter 2. Adding more via holes, we can obtain a better  $S_{11}$  parameter.

From these parameters, the substrate dielectric constant and the substrate thickness are given by the selected material (Table 4.1). One can only modify the rest of the parameters previously mentioned in order to obtain an optimized design of the antenna.

## 4.2. Simulation Setup and Design Process

In this section, the procedure to simulate the SIW cavity-backed patch antenna in HFSS is presented. The dimension of the antenna used in this section corresponds to the end design values. The design process followed to select these dimensions is described in section 4.3.

### 4.2.1. Antenna dimensions

In Figure 4.3, the selected antenna structure is presented. Table 4.2 shows the dimensions of the antenna ( $L_{ind}$  and  $L_{slot}$  are the parameters that will be varied to find the adequate antenna structure) .

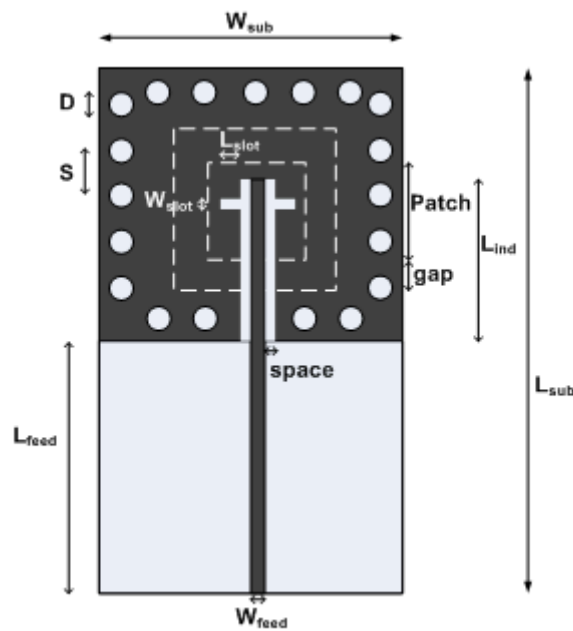


Figure 4.3: Passive antenna structure

Par	Dim (mm)	Par	Dim (mm)	Par	Dim (mm)
$W_{sub}$	13.8	$W_{feed}$	1.16	$L_{ind}$	<b>9.5-9.9</b>
$L_{sub}$	20.3	$L_{feed}$	6.5	space	0.5
$D$	1	$L_{slot}$	<b>1.9-2.1</b>	Patch	6.65
$s$	2	$W_{slot}$	0.5	gap	1

Table 4.2: Antenna dimensions

## 4.2.2. Design and Simulation process

First of all, we have to create a “new project” in HFSS. After that, HFSS only needs that the geometry and the material properties of the antenna structure are specified. The first step is to build the SIW cavity-backed structure, starting with the substrate (Arlon 25N). To specify the substrate structure, a box has to be drawn in a correct coordinate origin. Figure 4.4 shows the box that model the substrate structure.

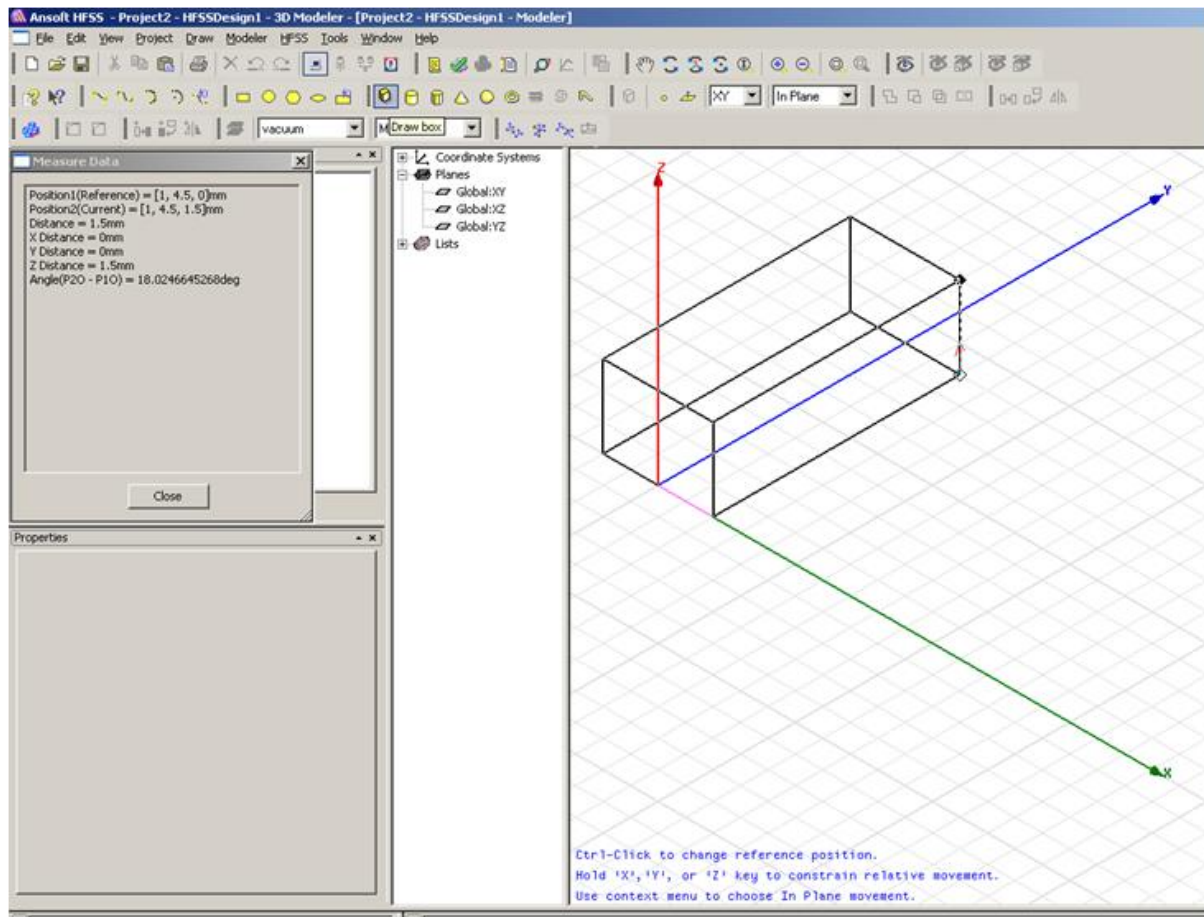


Figure 4.4: Box that represents the substrate structure

As Figure 4.4 shows, the box dimensions are not the same as the dimensions described in subsection 4.2.1. To assign these values to the box dimensions, we have to create variables that allow us to have all the antenna's parameters in an orderly way. This procedure is shown in Figure 4.5.

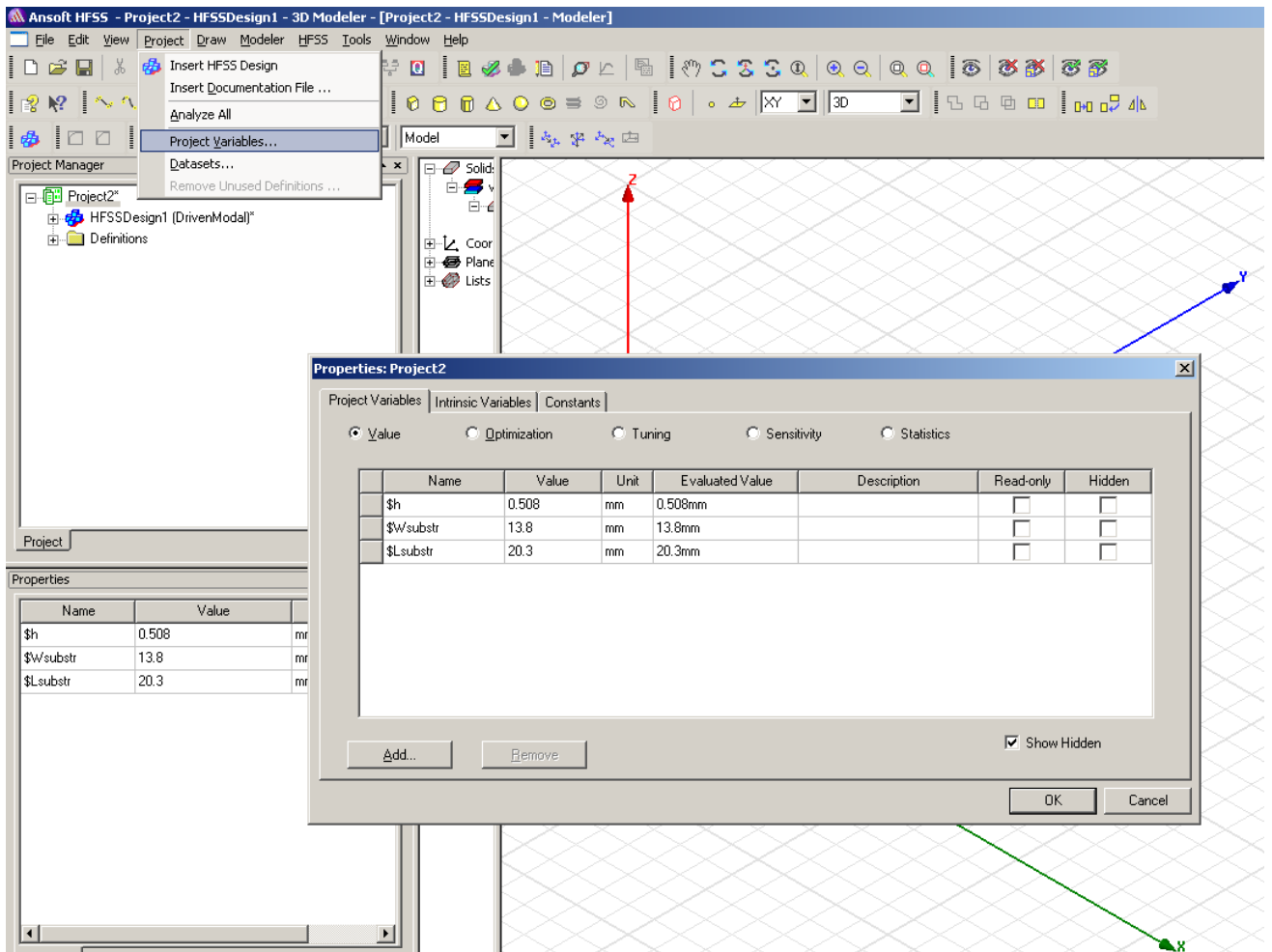


Figure 4.5: Adding project variables

Now that the substrate variables have been created, the substrate structure can be dimensioned. To do that, we have to right-click on the box and choose *edit/properties*. The substrate has to be placed in an adequate reference position. In the attribute tab, the material of the substrate can be chosen. In this case, we have to choose Arlon 25N (HFSS has the properties of the Arlon 25N, so we only have to assign the substrate with this material). Figure 4.6 and 4.7 show the properties of the substrate and the final result is shown in Figure 4.8.

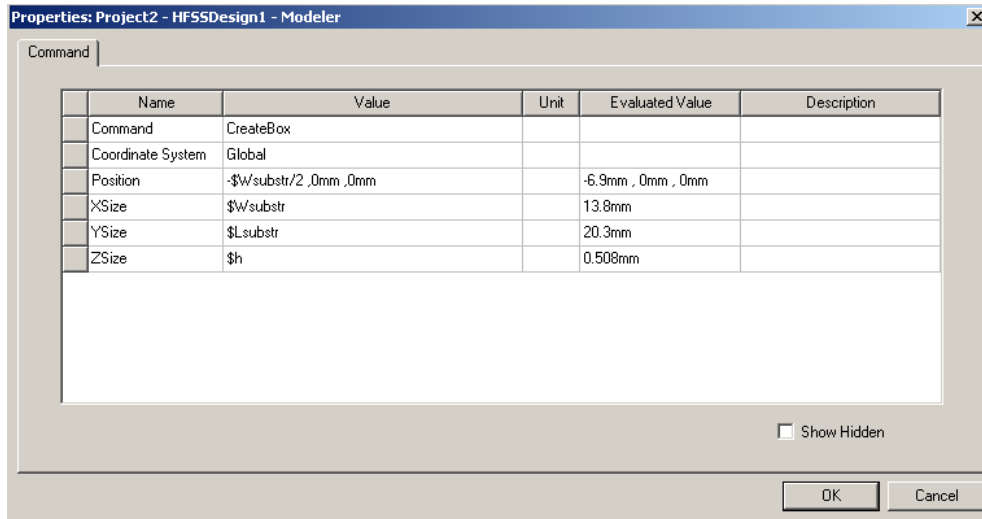


Figure 4.6: Substrate dimensions and position

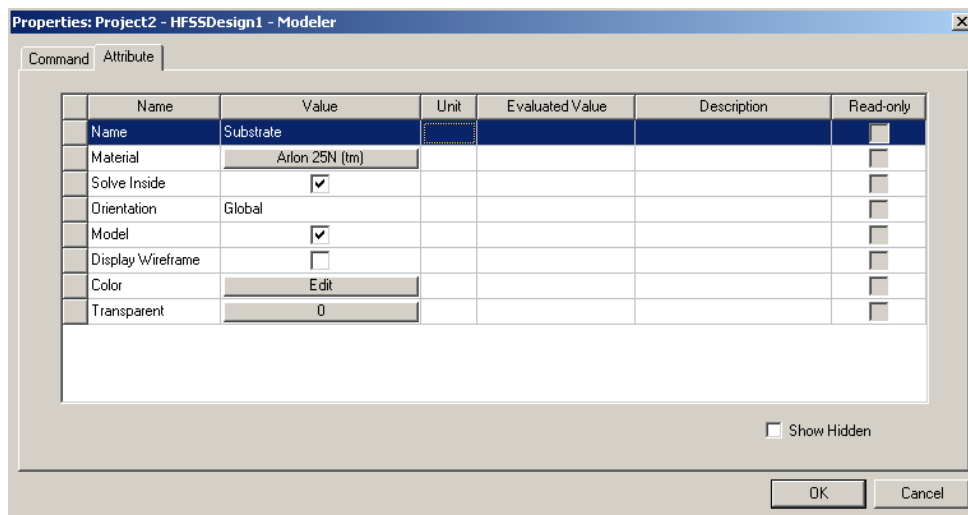


Figure 4.7: Substrate attributes

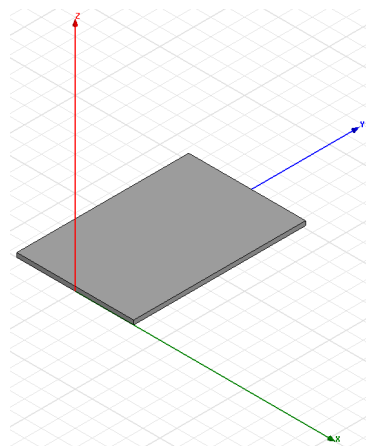


Figure 4.8: Substrate structure

In order to create the patch and the ground plane, two rectangles have to be drawn on the top of the substrate. Then the necessary variables have to be created and the material properties have to be assigned. To make the ground plane, a rectangle with the same dimensions of the substrate and a smaller rectangle with 8.65 x 8.65 mm size have to be created. Then, the smaller rectangle is subtracted from the big one. In order to do the subtraction, the two rectangles have to be placed at the same Z level. Then, both rectangles have to be selected and choose *edit/Boolean/Subtract* (as is shown in Figure 4.9 and Figure 4.10). Finally, a rectangle is drawn and placed in the center of the gap resulting from the subtraction (Figure 4.11). This rectangle will correspond to the radiating patch antenna element.

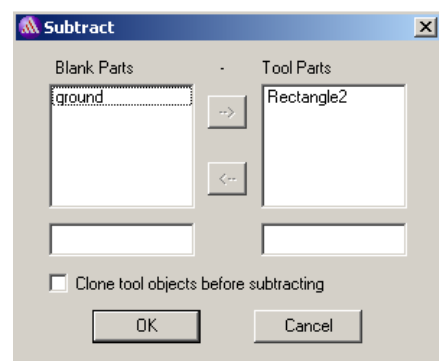
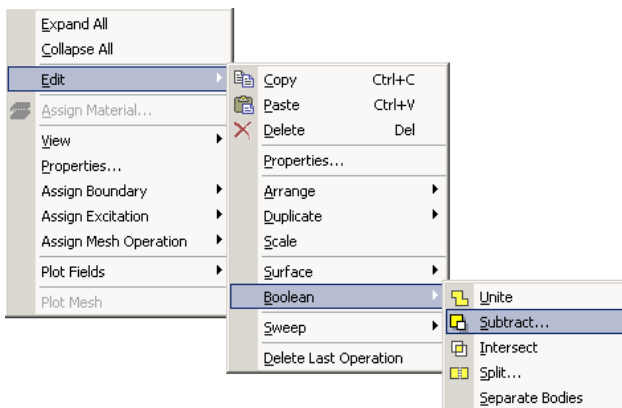


Figure 4.9: Subtracting the rectangles

Figure 4.10: Defining the subtraction

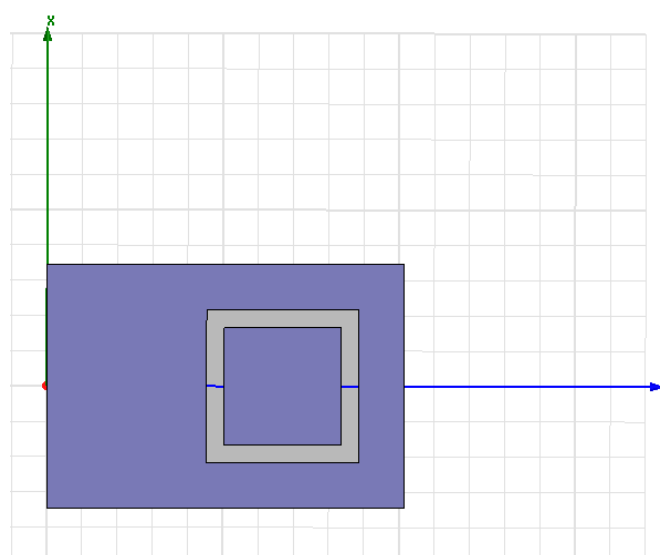


Figure 4.11: Ground plane and patch

In order to complete the top part, it is necessary to assign the appropriate material. The ground plane and the patch antenna are assigned perfect conductor. This procedure is made selecting the ground plane and the patch antenna and choosing *Assign Boundary / Perfect E* (as is shown in Figure 4.12).

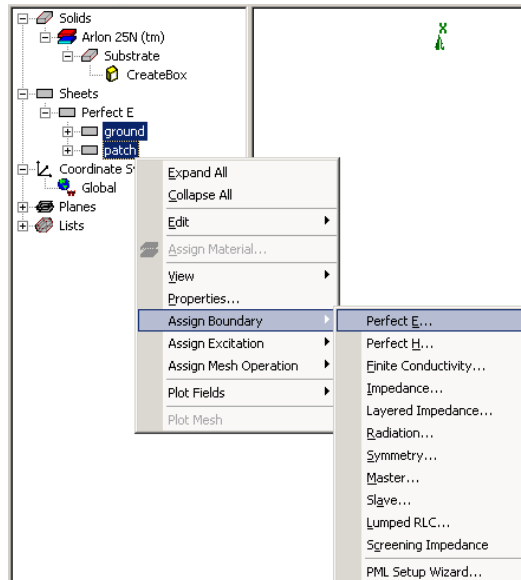


Figure 4.12: Assign the correct behavior

To make the feed line, the transverse stubs and to complete the SIW cavity, some rectangles are drawn to represent the feed line and the cooper plane and some cylinders are drawn to represent the metalized via holes. Before that, the corresponding variables have to be created. Figure 4.13 presents the variables that are used. Then we can draw the rectangles and change their properties (size, position and behavior), in the same way that was described for the top part.

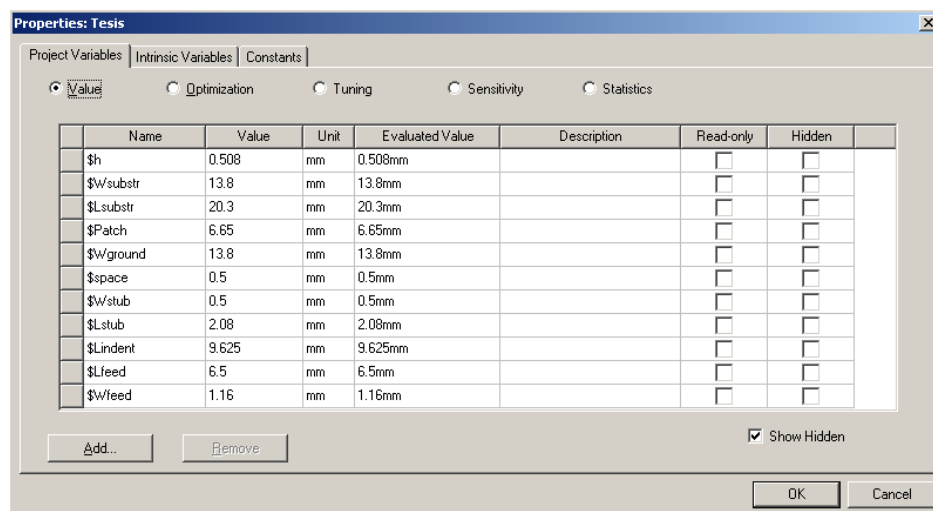


Figure 4.13: Variables for the cooper plane design and feed line design

In order to design the other side of the SIW cavity backed antenna, six rectangles are used. One of them (R1) correspond to the feed line, two of them (R2 and R3) are used to obtain the transverse stubs and the last three rectangles (R4, R5 and R6) are used to create the rectangular conductor needed to obtain the cavity. Figure 4.14 presents the six rectangles (top) used to design the cavity side of the antenna and the radiating element side (bottom) which design has been previously explained.

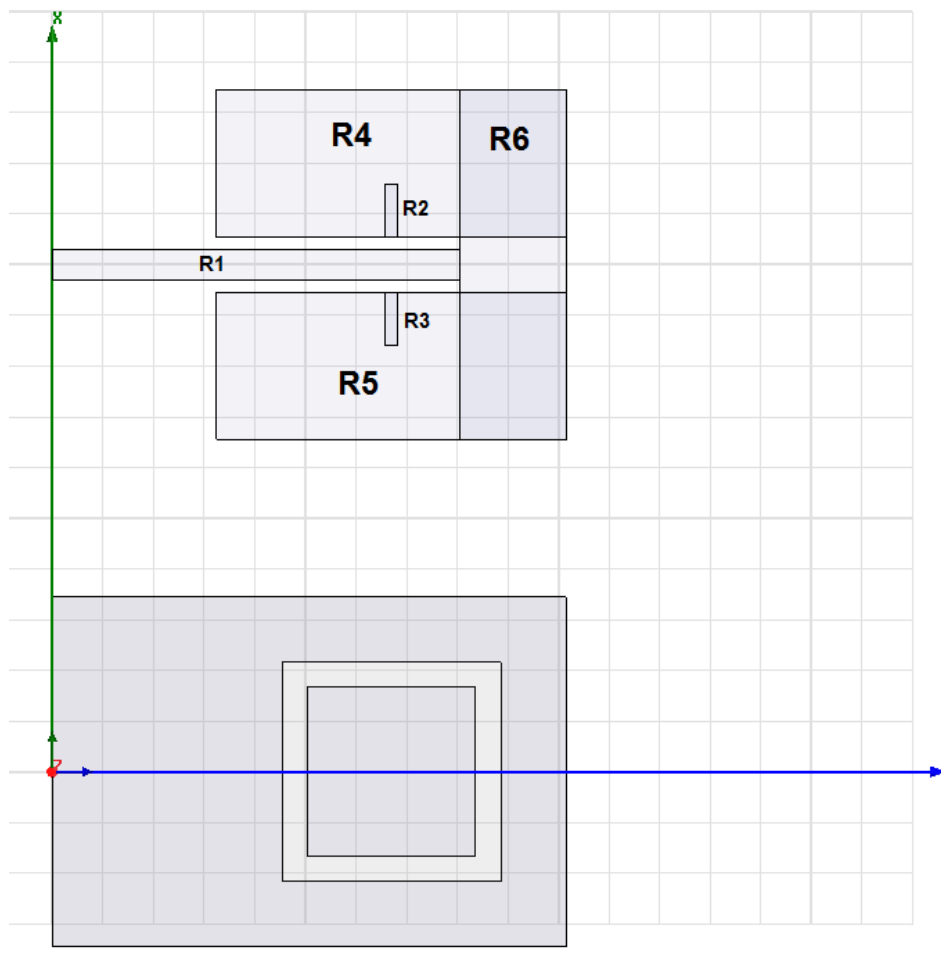


Figure 4.14: Rectangles that represent the feed line and the ground plane

To create the transverse stubs, the two small rectangles (R2 and R3) are subtracted from the two big rectangles that are oriented horizontally (R4 and R5). In order to do so, the four rectangles have to be selected and we have to follow the process described in Figure 4.9 and 4.10. Once this is done, the resulting structure together with the remaining rectangles is selected and merged using *edit/Boolean/Unit* (as is shown in Figure 4.15). Finally, the perfect conductor behavior (as is shown in Figure 4.12) is assigned to the final structure. In Figure 4.16, we can see the resulting structure that falls in the bottom part of the substrate.

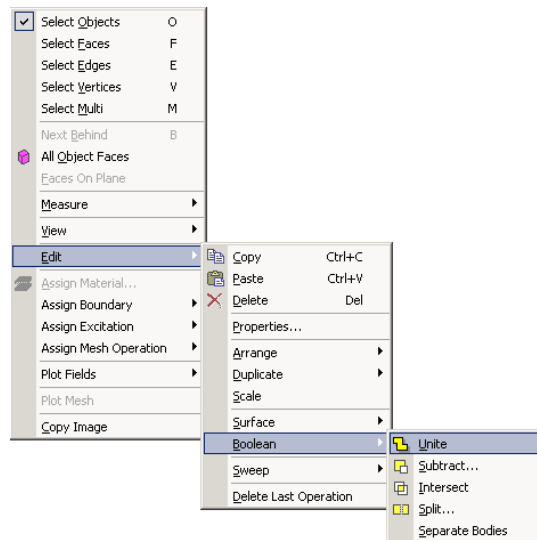


Figure 4.15: Joining the rectangles

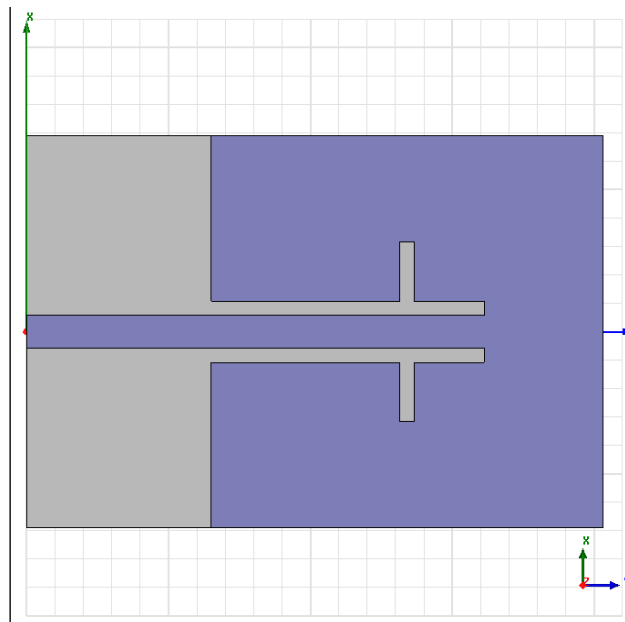


Figure 4.16: Bottom part of the substrate

The last step required to create the cavity is to make the metalized via holes. The size and placement of these via holes is made parametric by creating the corresponding variables. In this case, it is necessary to define the radius and the height. The height is defined by variable \$h, that correspond to the height of the substrate, as the via holes have to cross from the upper to the lower side of the structure. The other variable \$r correspond to the radius. With these variables, the size of the cylinders can be modified. Additional variables are created to place the cylinders in the correct position. All these variables allow us to place the cylinders in a correct position and modify the characteristics of the SIW cavity-backed antenna in a fast way to simulate different structures designs. These variables are described in Figure 4.17 and the final

position of the metalized via holes is described in Figure 4.18. The metalized via holes are assigned perfect conductor (Figure 4.19). The final design of the SIW cavity backed patch antenna element is shown in Figure 4.20.

The screenshot shows a software dialog box titled "Properties: Tesis" with three tabs: "Project Variables", "Intrinsic Variables", and "Constants". The "Project Variables" tab is active, showing a table of variables. The table has columns for Name, Value, Unit, Evaluated Value, Description, Read-only, and Hidden. Below the table are buttons for "Add...", "Remove", "Show Hidden", "OK", and "Cancel".

Name	Value	Unit	Evaluated Value	Description	Read-only	Hidden
\$Wfeed	1.16	mm	1.16mm		<input type="checkbox"/>	<input type="checkbox"/>
\$r	0.5	mm	0.5mm		<input type="checkbox"/>	<input type="checkbox"/>
\$Dist	12	mm	12mm		<input type="checkbox"/>	<input type="checkbox"/>
\$b	2*[2*\$r]		2mm		<input type="checkbox"/>	<input type="checkbox"/>
\$Hx	0.4	mm	0.4mm		<input type="checkbox"/>	<input type="checkbox"/>
\$Hy	1.4	mm	1.4mm		<input type="checkbox"/>	<input type="checkbox"/>
\$Vx	0.51	mm	0.51mm		<input type="checkbox"/>	<input type="checkbox"/>
\$Vy	0.9	mm	0.9mm		<input type="checkbox"/>	<input type="checkbox"/>

Figure 4.17: Variables for the metalized via holes design

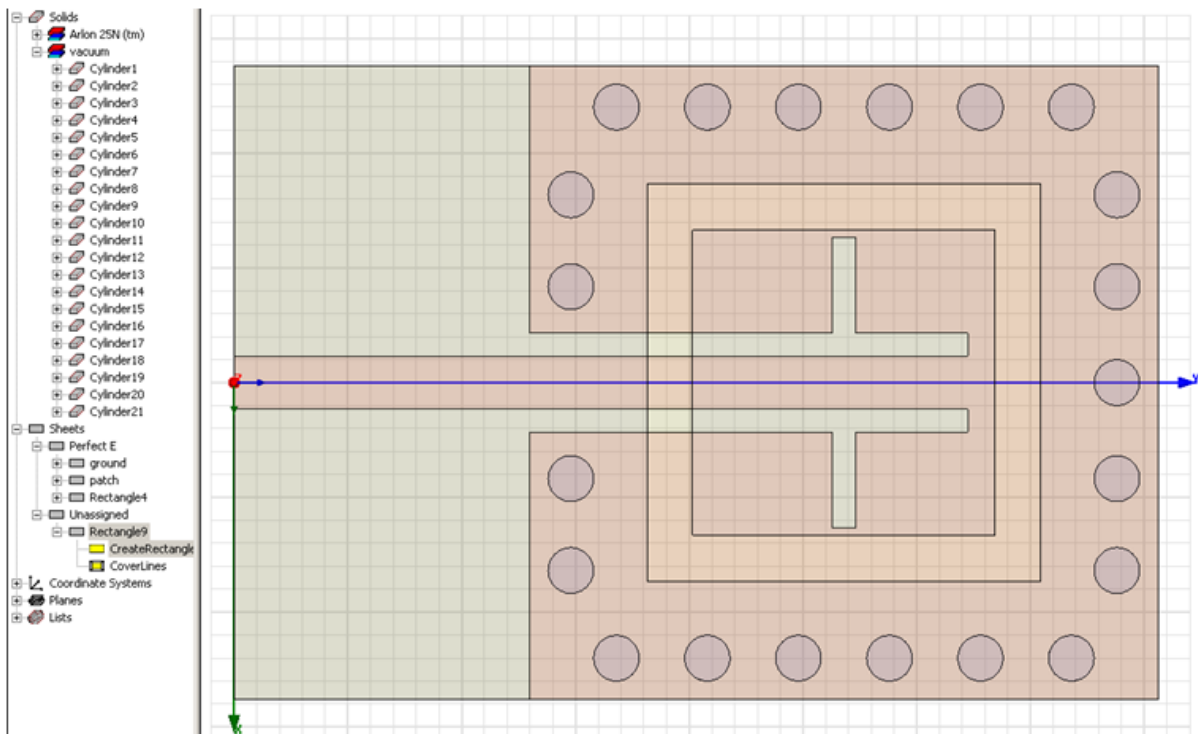


Figure 4.18: Representation of the metalized via holes

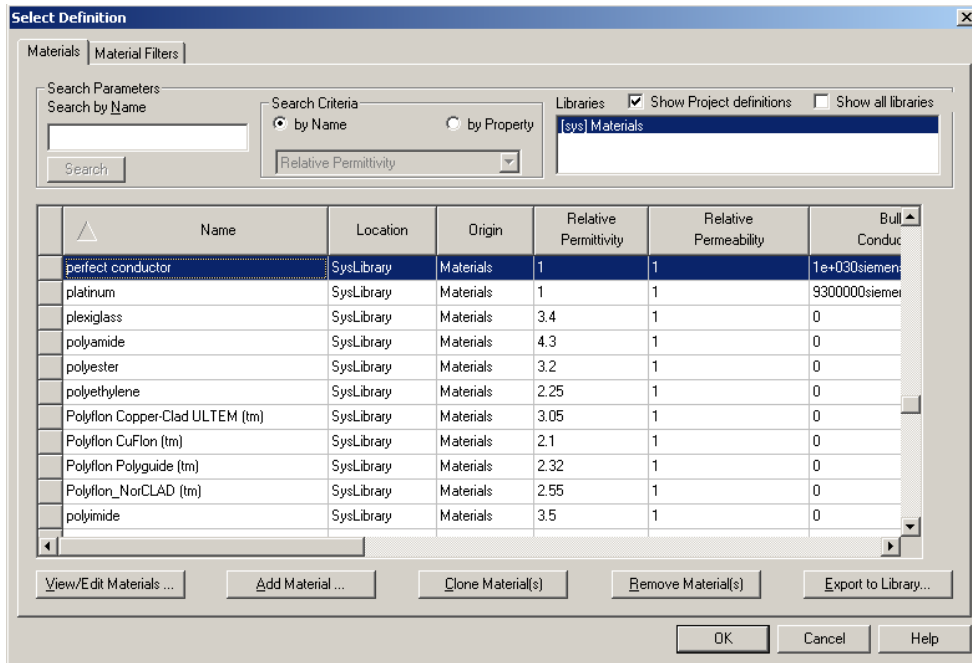


Figure 4.19: Metalized via hole attribute (Perfect conductor)

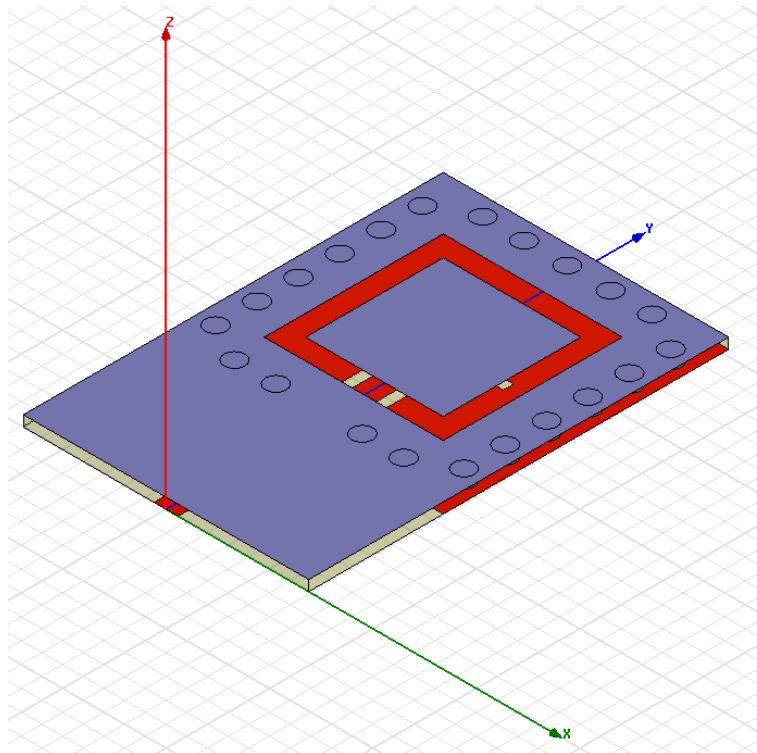


Figure 4.20: Preview of the SIW cavity-backed antenna

In order to setup the simulation environment, we have to introduce a wave port and the radiation space. To do that, a rectangle is made that represents the exciting port and a box is drawn to represent the radiation space. The box has to surround the complete SIW cavity-backed structure. To ensure a proper calculation of the radiation pattern the box should be  $\lambda/4$  from each of the edges of the radiating structure. The wave port has to be wide enough to cover the feed line, as show in Figure 4.21. Figure 4.22 shows the assignment made for both the radiation box and the wave port.

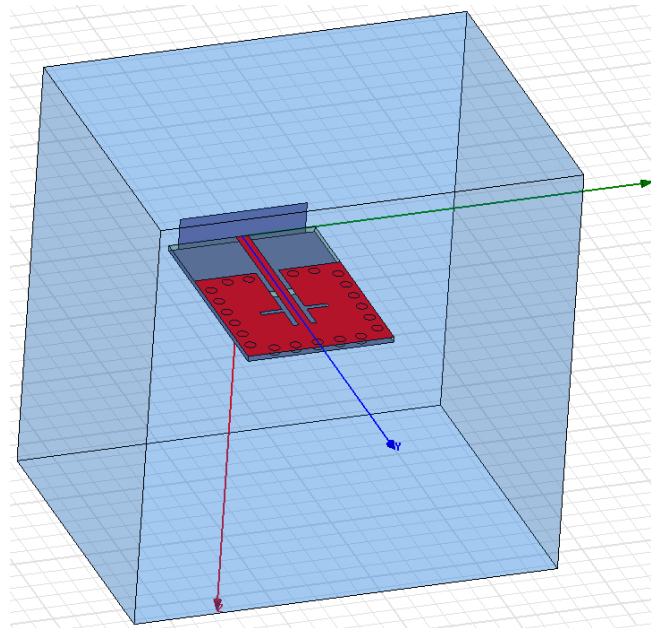


Figure 4.21: Air box and wave port representation

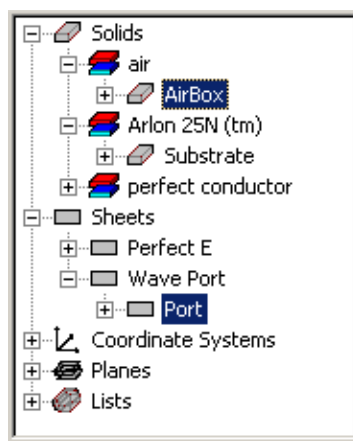


Figure 4.22: Box and rectangle attributes

Now the SIW cavity-backed patch antenna structure is finished one can start the simulation process. First of all, we have to add a solution setup. Figures 4.23 and 4.24 present the correct way to configure the solution setup.

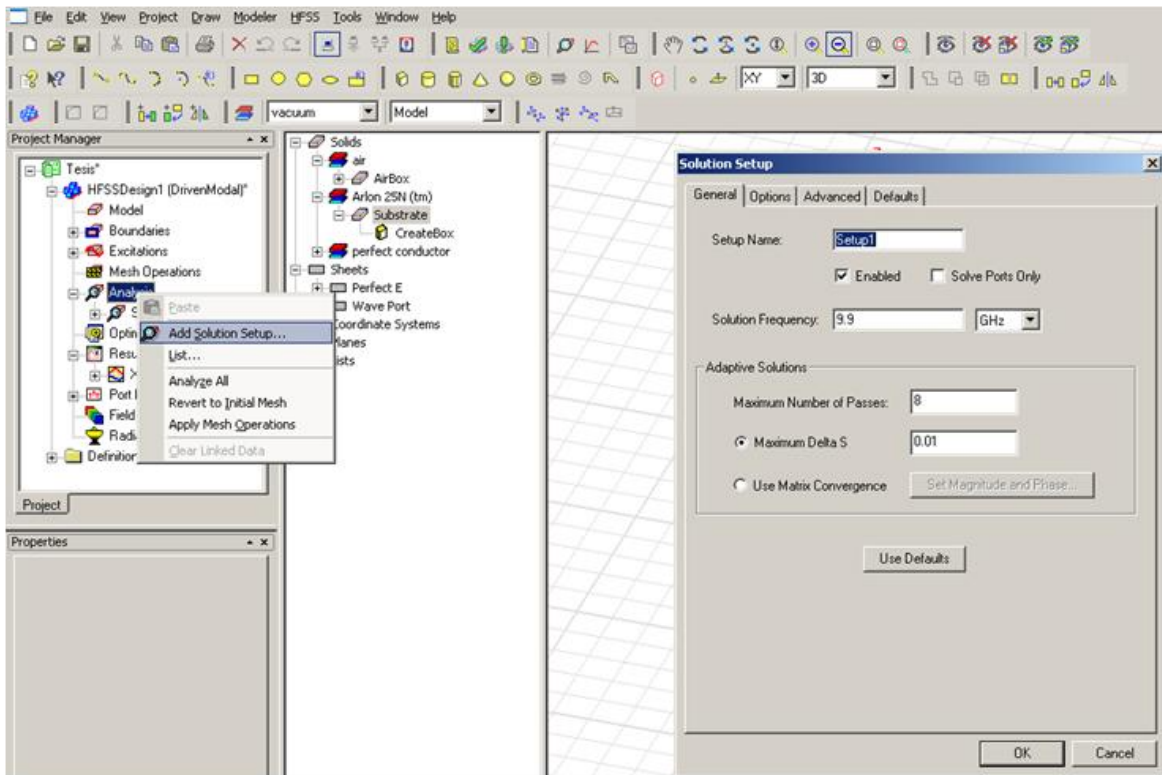


Figure 4.23: Adding a solution setup

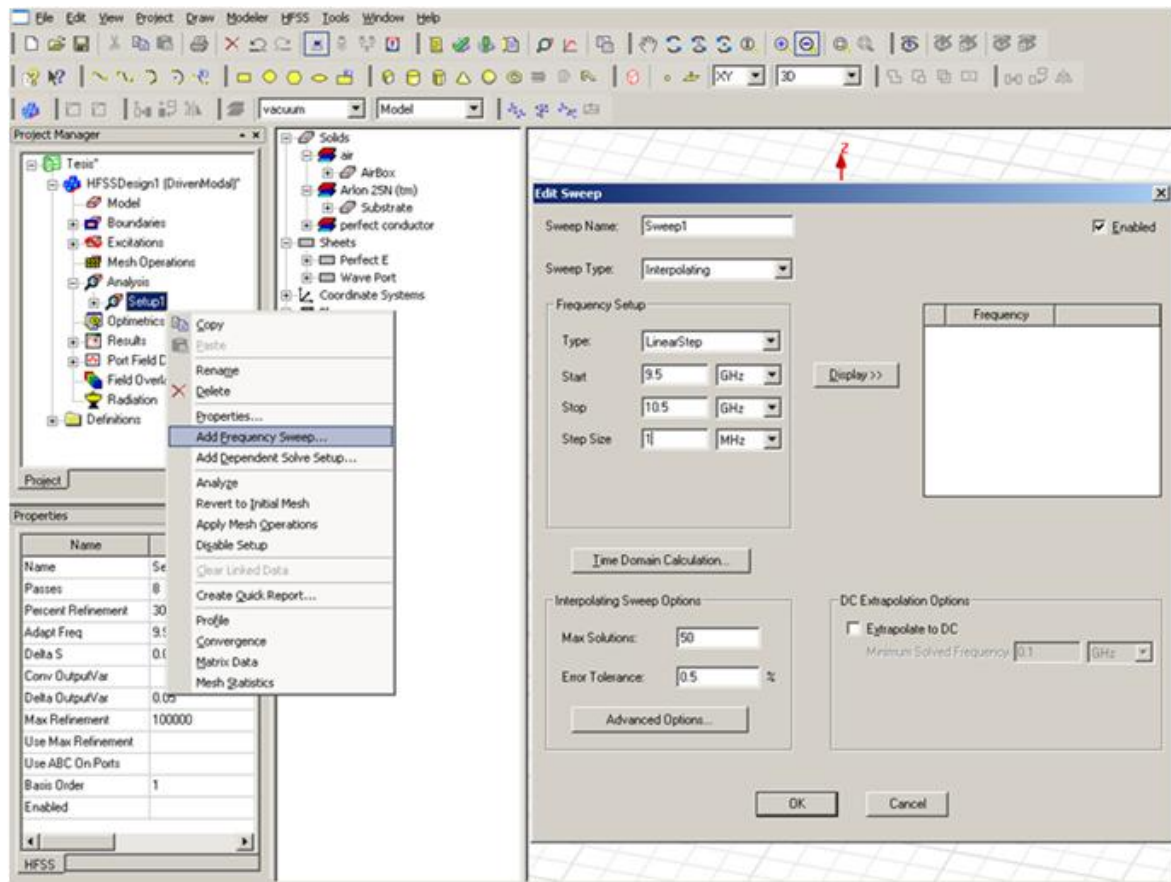


Figure 4.24: Adding a frequency sweep

To evaluate radiated fields in the far-field region, we must set up an infinite sphere that surrounds the radiating object and that will define how the radiation patterns are calculated in HFSS. The steps to create a Far Field Radiation Sphere are:

1. Radiation>Insert Far Field Setup>Infinite Sphere.
2. Introduce the ranges of  $\phi$  and  $\theta$  angles to define the sphere

Figure 4.25 presents the Radiation Sphere Setup.

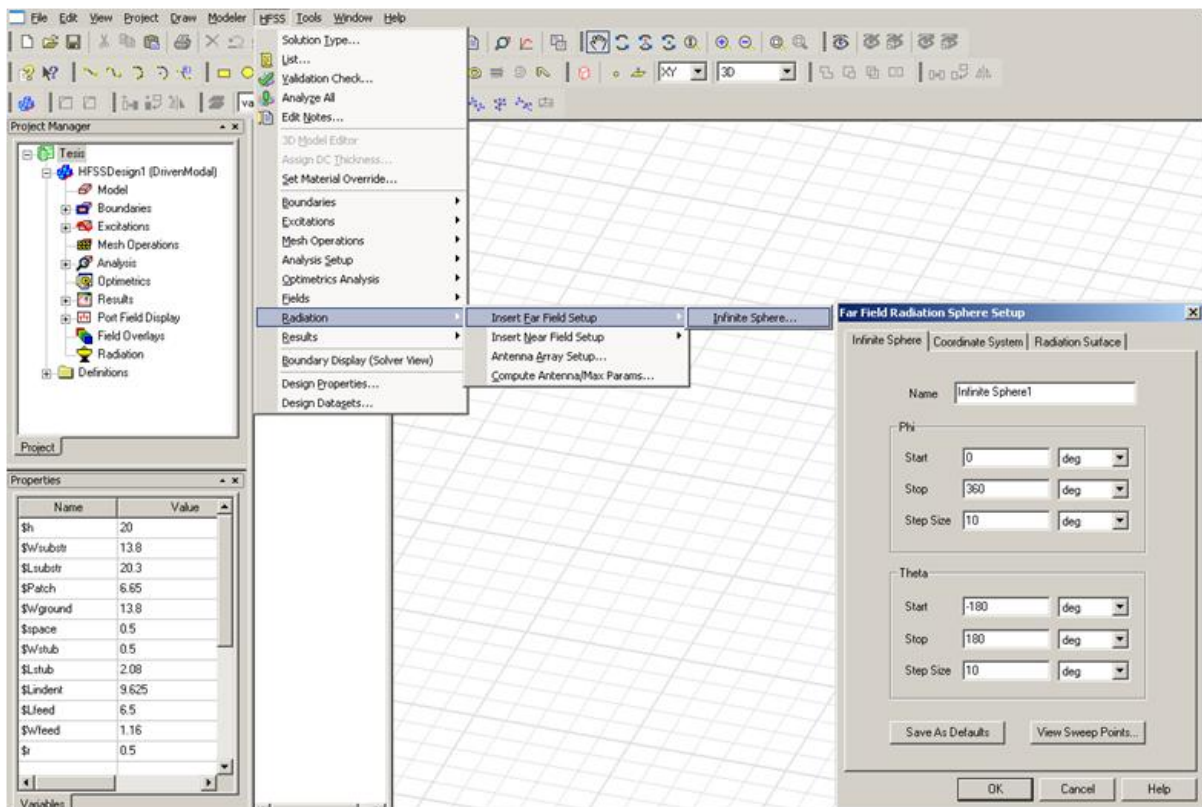


Figure 4.25: Far field radiation sphere setup

Once the structure to analyze has been modeled and the simulation setup has been adjusted, the SIW cavity backed patch antenna element is ready to be simulated and its performance optimized.

### 4.3. Simulation Results

In this section, the obtained simulation results are presented. In order to obtain a good design of the antenna, we need to have good matching at the desired resonant frequency (9.9 GHz). This implies that the  $S_{11}$  parameter at 9.9 GHz should be the lowest possible.

Once that we have an adequate structure that satisfy a good  $S_{11}$ , all the characteristics of this optimized structure are analyzed to compare them with the measured results (chapter 6).

#### 4.3.1. Finding a good SIW Cavity-Backed Patch Antenna Structure

As mentioned previously, the antenna requirements are a resonance frequency of 9.9 GHz which means a low  $S_{11}$  parameter value at this frequency. To achieve these objectives, different antenna structures were simulated. In Table 4.2, the parameters that were modified to obtain the desirable results are shown.

The first step is to obtain the resonance at 9.9 GHz. To obtain it, we only have to modify the size of the transverse stubs. Changing their length, we will change the resonant frequency. In Figure 4.26, the variation of the resonance frequency versus the stubs length is shown.

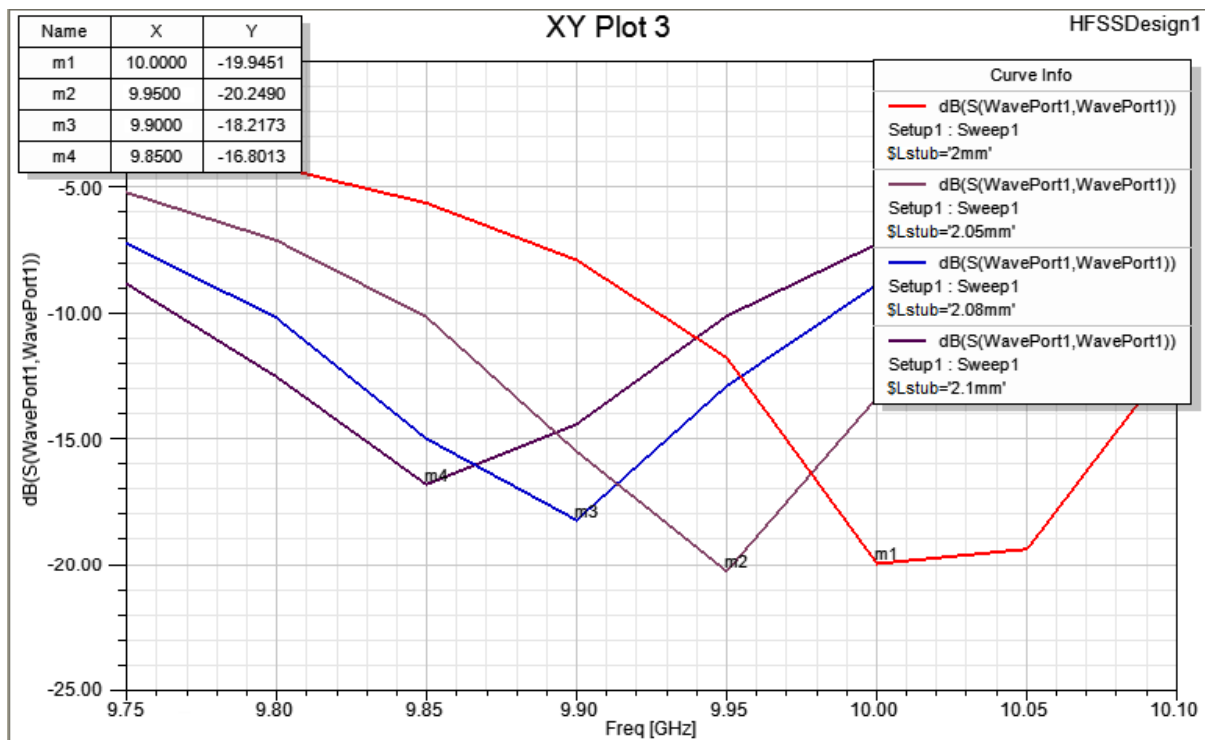


Figure 4.26: Resonant frequency variation versus the stub length

Once the resonant frequency is achieved (selecting  $L_{stub} = 2.08\text{mm}$ ), we have to minimize the value of the  $S_{11}$  parameter. In order to do that, we have two alternatives. The first

one is to add more via holes. Due to the fix substrate size, this option is not possible. The second alternative is to modify the size of the feed line. This allows changing the  $S_{11}$  parameter. In Figure 4.27, the variation of the feed line length ( $L_{indent}$ ) and the adequate value to obtain the best  $S_{11}$  parameter is presented. It can be seen that there is an optimum value  $L_{indent}=9.625$  mm for minimum  $S_{11}$ .

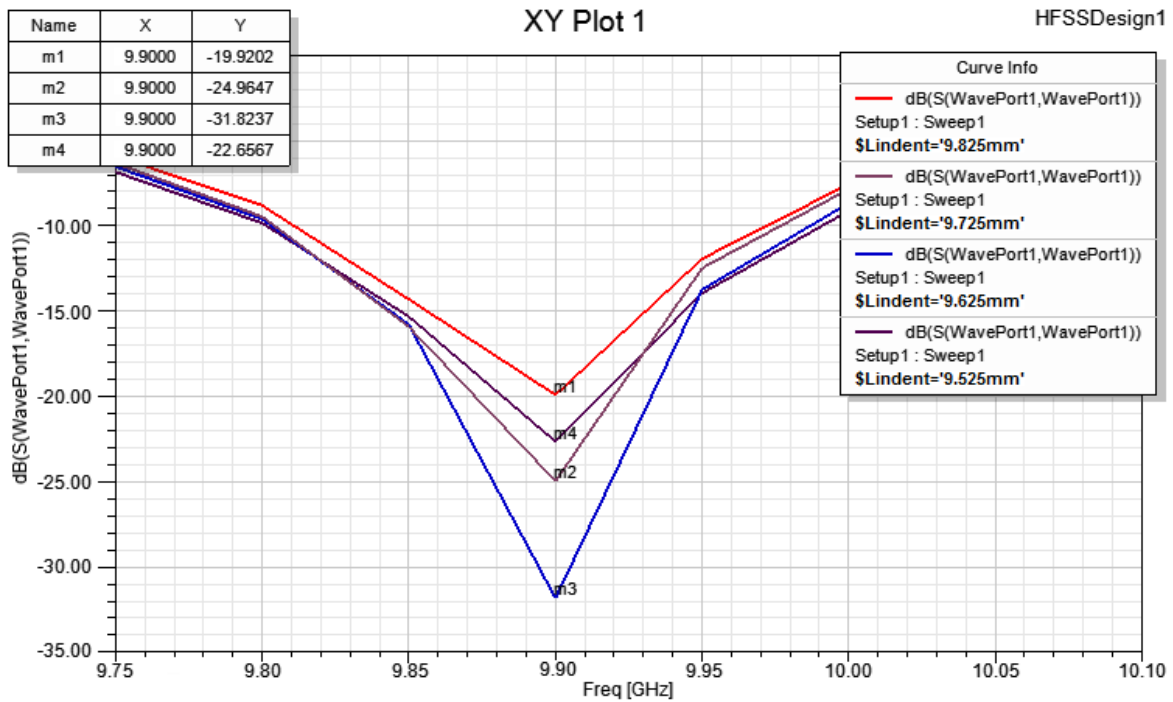


Figure 4.27: Changing feed line length

After obtaining an optimized design of the SIW cavity-backed patch antenna in term of  $S_{11}$  and resonance frequency, its performance in terms of radiation pattern, gain and directivity will be analyzed.

### 4.3.2. Results of the SIW Cavity-Backed Patch Antenna Structure

In this subsection, the results of the final SIW cavity-backed patch antenna design are presented. The results that are shown are going to be compared with the measured results after the fabrication.

In Figure 4.27 the return loss ( $S_{11}$  parameter) of the selected structure corresponds to the blue curve. For the resonant frequency of 9.9 GHz the  $S_{11}$  parameter has a value of -31.82 dB. This structure presents a -10 dB impedance bandwidth of 186 MHz.

The radiation patterns corresponding to 9.9 GHz are calculated with HFSS that allows representing E-plane co-polar, E-plane cross-polar, H-plane co-polar and H-plane cross-polar, as well as the 3D radiation pattern. Figure 4.28 shows the 3D radiation pattern.

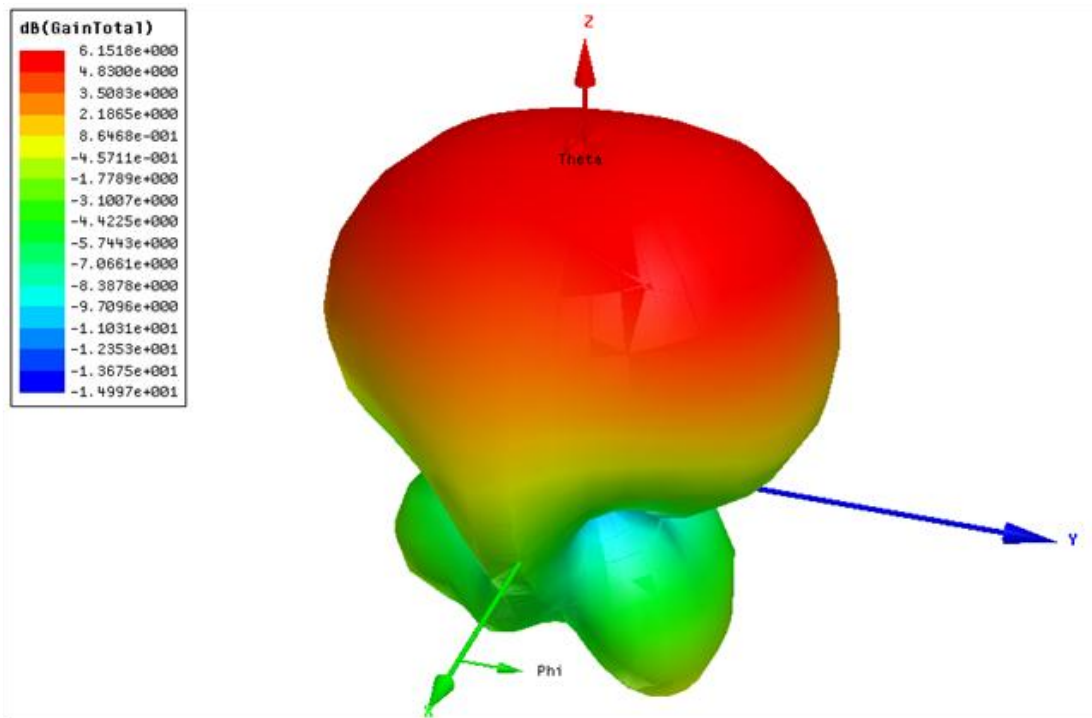


Figure 4.28: Simulated 3D radiation pattern

From the E-plane co-polar, one can obtain some characteristics, as the half-power beam width at -3 dB (HPBW), beam width between first nulls (FNBW), front-to-back ratio (FRB) and the gain. These results are shown in Table 4.3. Next the simulated radiation patterns for the different radiation planes are represented.

Name	Theta	Ang	Mag
m1	0.0000	0.0000	5.6012

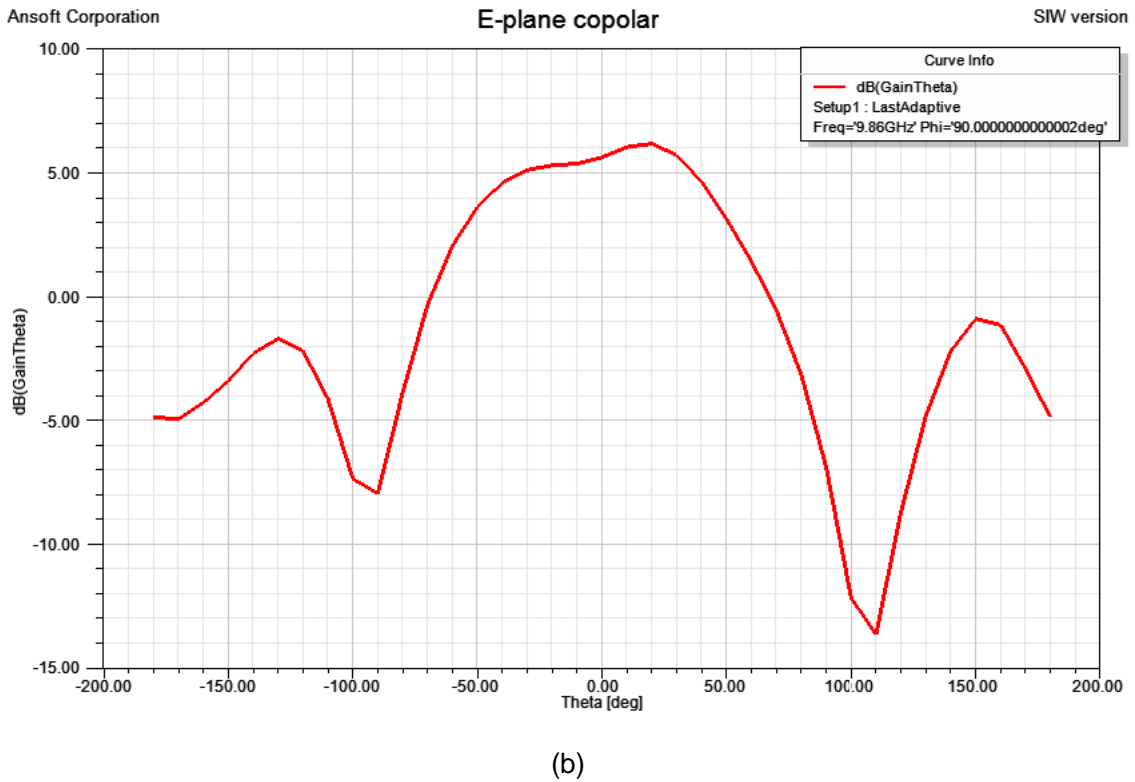
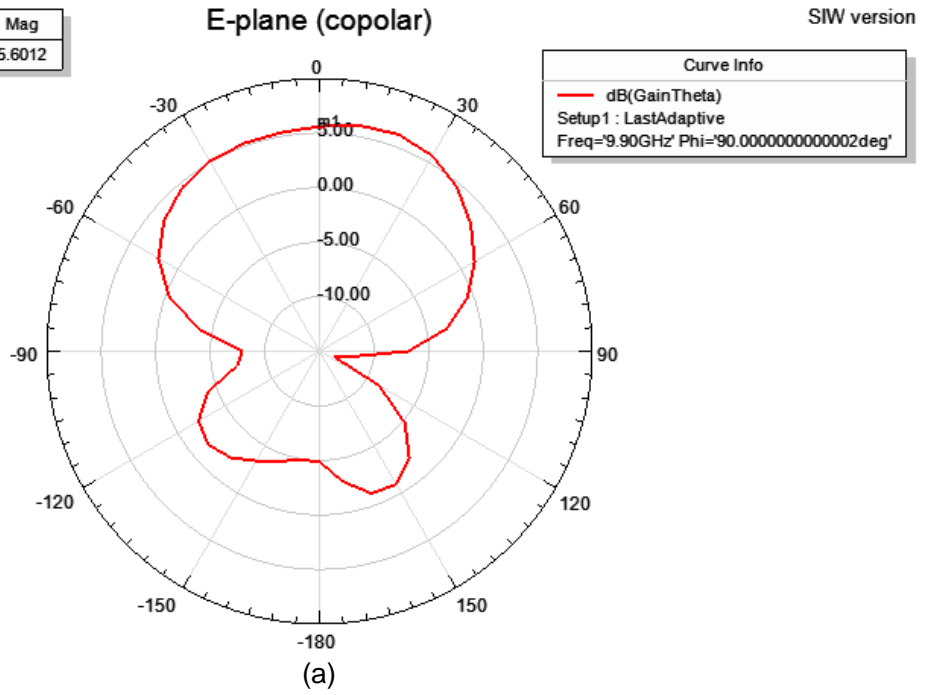
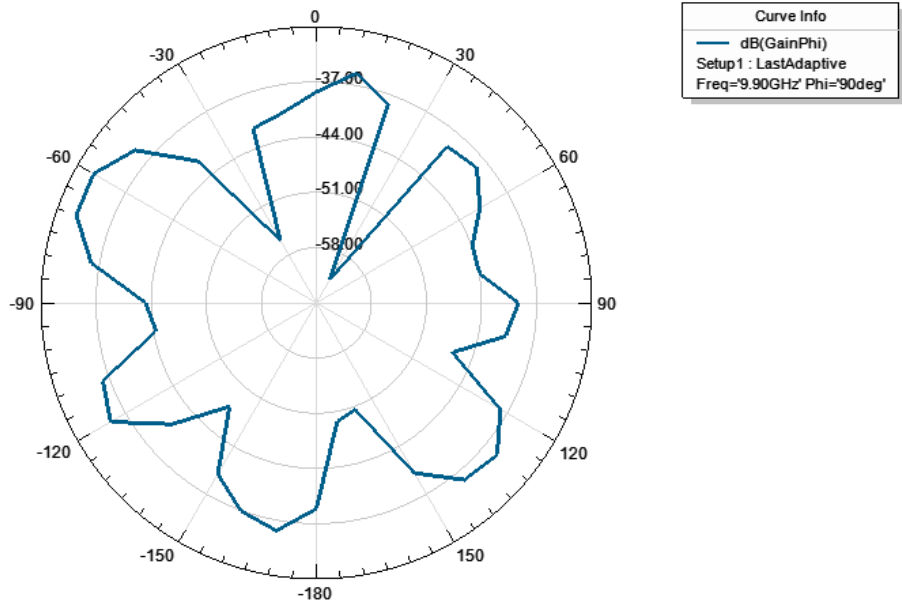


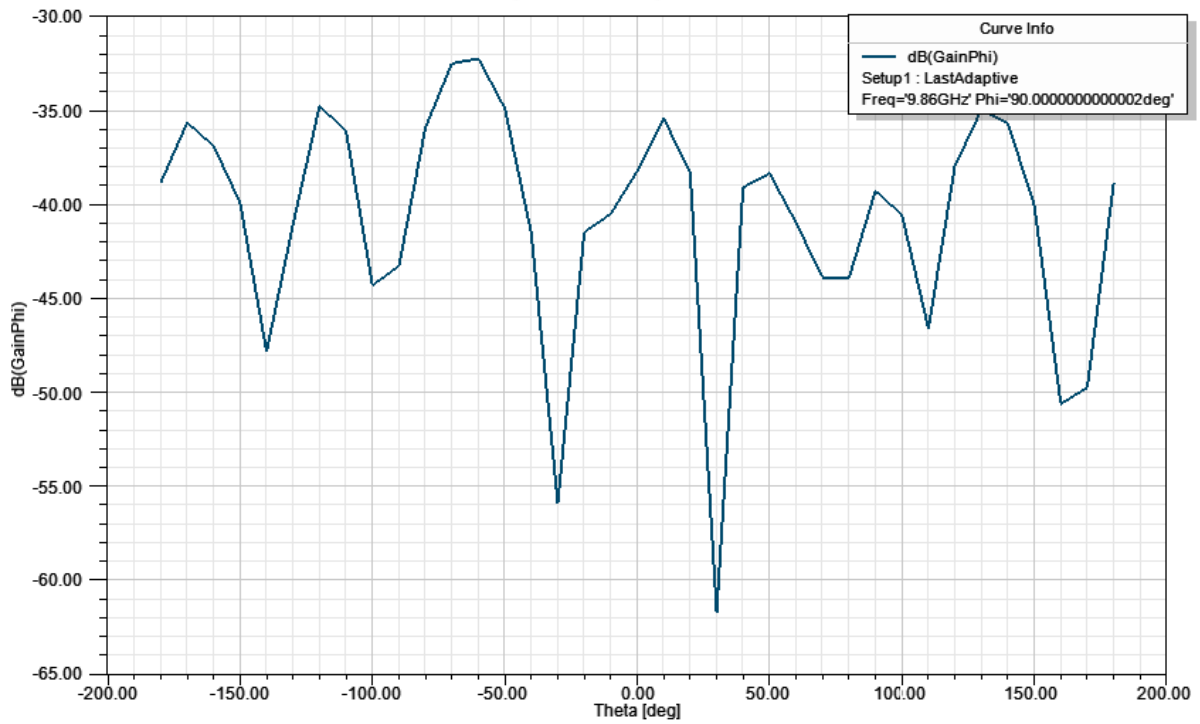
Figure 4.29: Simulated E-plane co-polar radiation pattern in a polar plot (a) and rectangular plot (b)

### E-plane (crosspolar)



(a)

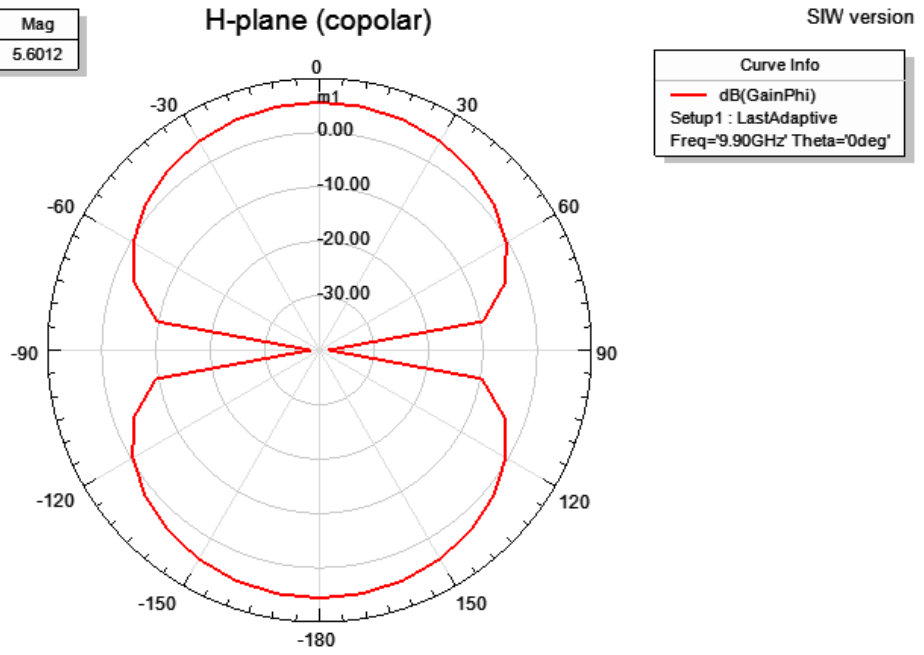
### E-plane crosspolar



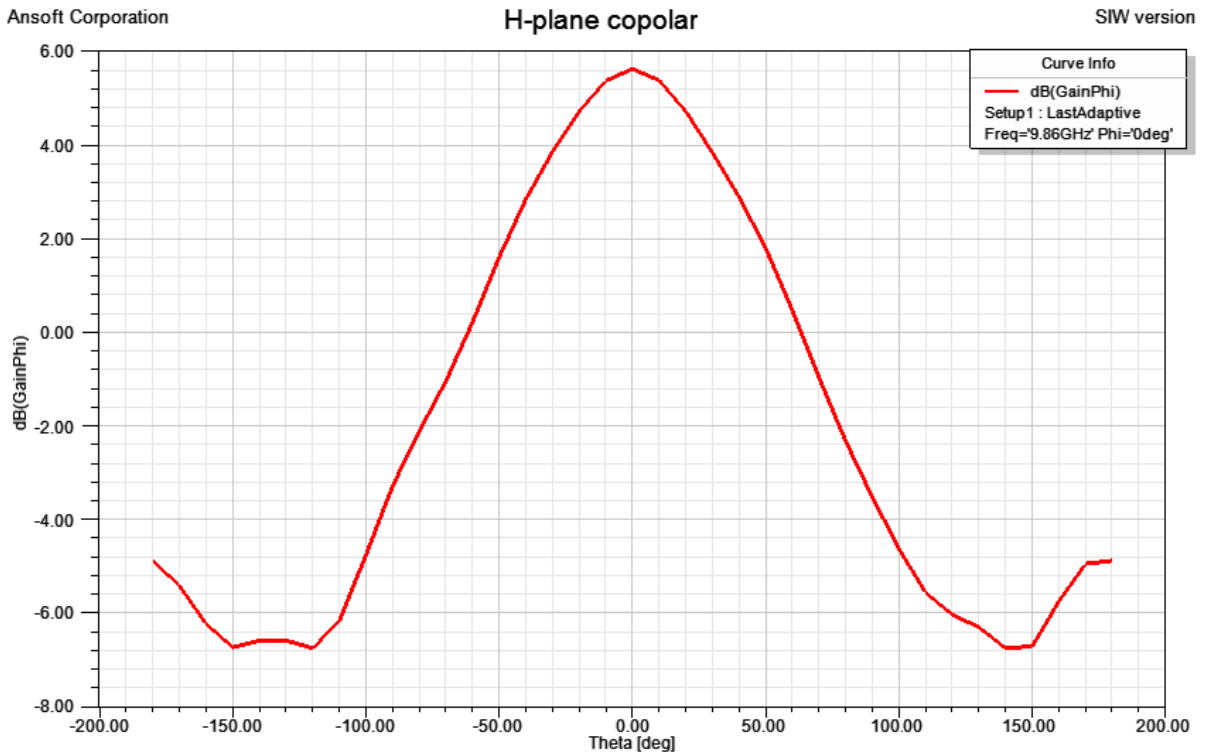
(b)

Figure 4.30: Simulated E-plane cross-polar radiation pattern in a polar plot (a) and rectangular plot (b)

Name	Phi	Ang	Mag
m1	360.0000	-0.0000	5.6012



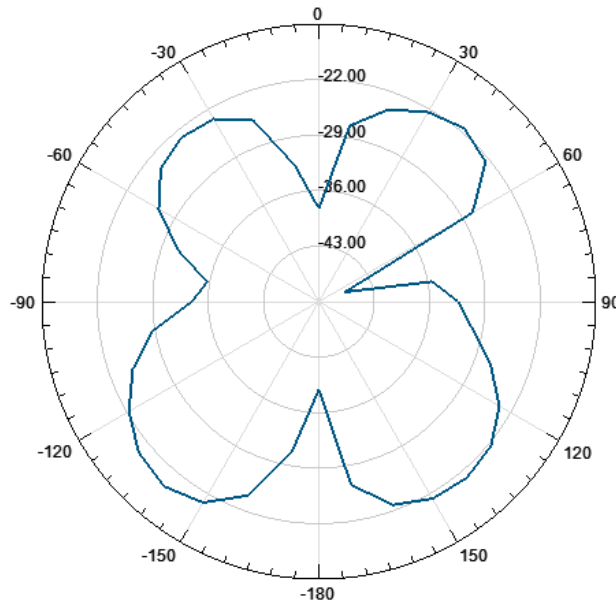
(a)



(b)

Figure 4.31: Simulated H-plane co-polar radiation pattern in a polar plot (a) and rectangular plot (b)

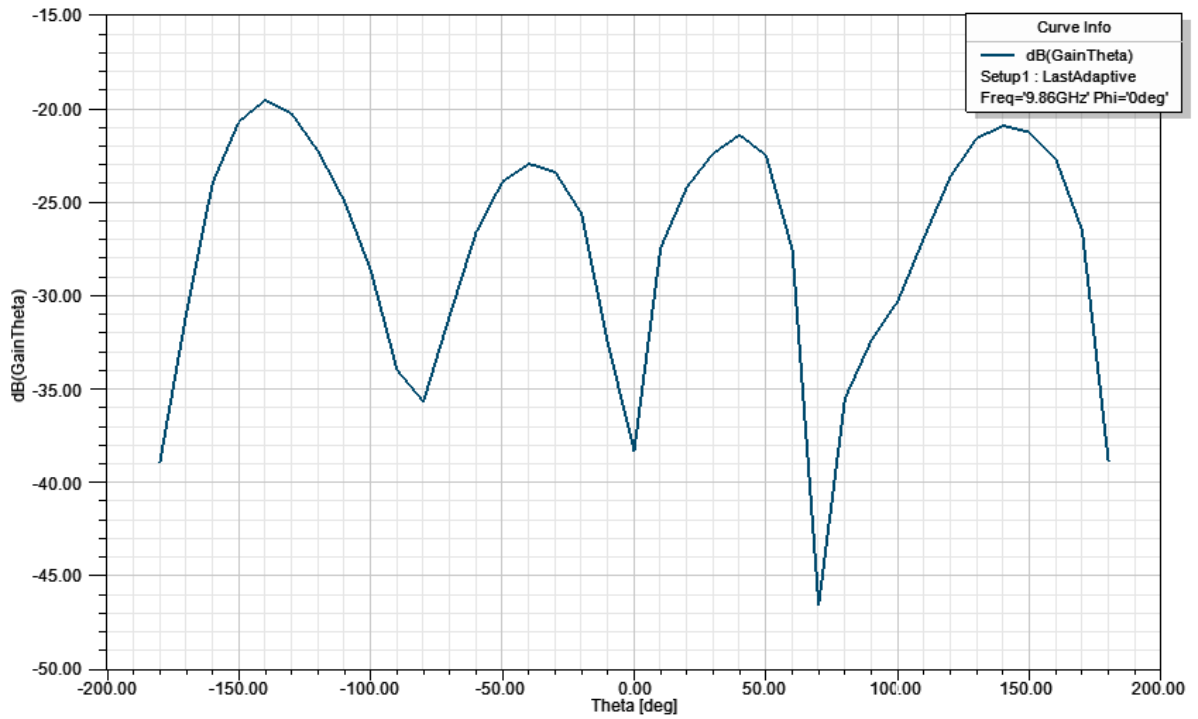
### H-plane (crosspolar)



Curve Info	
—	dB(GainTheta)
Setup1 : LastAdaptive	
Freq=9.90GHz' Phi=0deg'	

(a)

### H-plane crosspolar



Curve Info	
—	dB(GainTheta)
Setup1 : LastAdaptive	
Freq=9.86GHz' Phi=0deg'	

(b)

Figure 4.32: Simulated H-plane cross-polar radiation pattern in a polar plot (a) and rectangular plot (b)

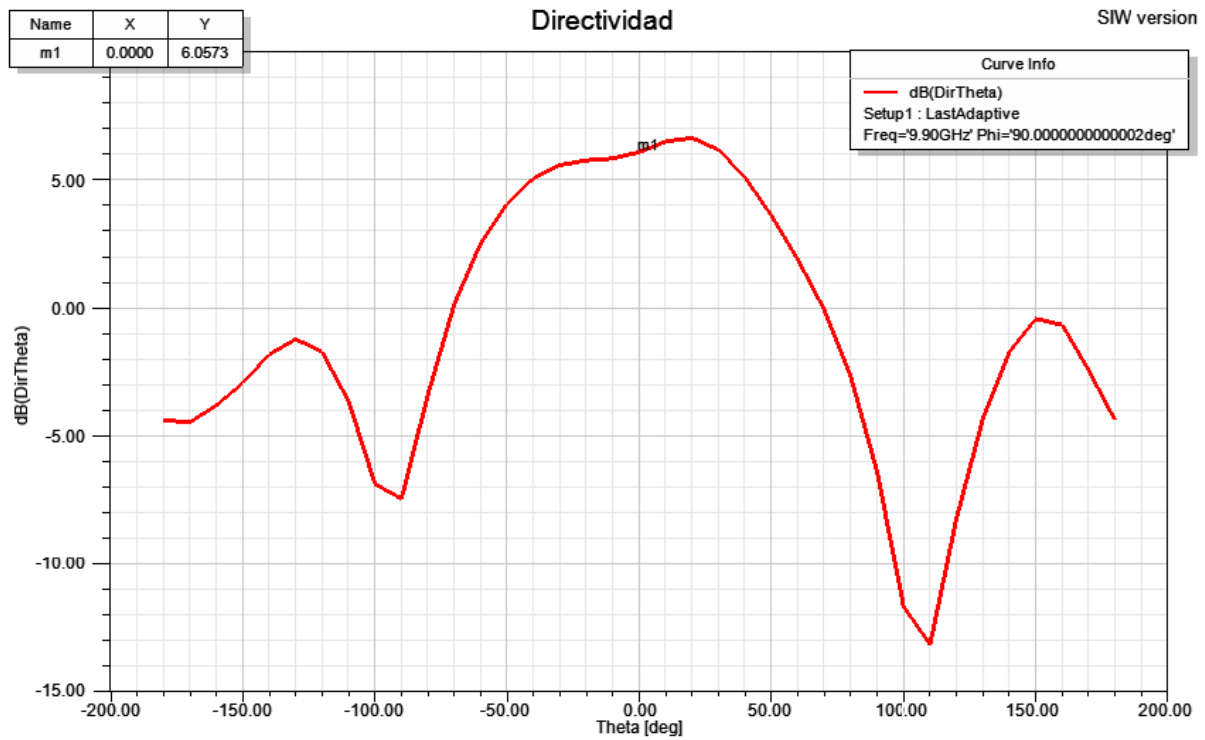


Figure 4.33: Directivity

Antenna Parameter	
Gain	5.6 dB
Polarization	linear
Directivity	6.05 dB
HPBW	112°
FNBW	200°
FRB	10.6 dB

Table 4.3: Relevant characteristics of the designed antenna

It is important to keep in mind these values, because once that we fabricate the antenna, we will be able to compare the measurement values against the design values; with that, we can determine how good is the antenna and how good was the manufacturing process.

## **Chapter 5:**

# **SOM Active Integrated Antenna design**

This chapter presents the design of a self-oscillating mixer (SOM) integrated into a SIW cavity-backed patch antenna for down conversion applications. This integration allows us to reduce considerably the size of the down converter circuit. Furthermore, the use of SIW technology permits us to implement in an easy way the active antenna. The integration of the self-oscillating mixer and the passive antenna is explained in this chapter.

In order to analyze the self-oscillating mixer integrated into the SIW cavity-backed patch antenna, Agilent ADS (Advanced Design System) software was used. ADS was selected because it permits us to use Harmonic Balance and Conversion Matrix simulations. These two simulation methods allow us to find the steady state oscillating solution and to perform small signal analysis of the mixer.

This chapter will explain all the steps followed to simulate the SOM active integrated antenna and the most important results obtained.

### **5.1. SOM Active Integrated Antenna structure**

The SOM Active Integrated Antenna has been designed combining the results obtained from HFSS for the passive SIW cavity-backed patch antenna with the circuit simulator Agilent ADS for simulating the active antenna. In the next two subsections the designed active antenna structure is presented.

#### **5.1.1. Description**

One important objective of this project is to obtain an optimized design of an active antenna based on SOM. To achieve this objective, a NE3210S01 HJFET was used as the active device. The SOM generates the local oscillator (LO) and at the same time it performs the mixing process of this LO with an external incoming radiofrequency (RF) signal. Because of this double function, the designed circuit is compact and simplified. Another advantage of the SOM is the capability to achieve conversion gain due to the use of an active device.

Due to the passive antenna structure and its characteristics, the resonant frequency of the antenna was used as the RF value (9.9 GHz). It allows us to work using the best performance of the antenna. The local oscillation (LO) frequency selected was 6.64 GHz and the output intermediate frequency ( $f_{IF}$ ) was 3.38 GHz. To obtain this  $f_{IF}$ , the incoming RF signal has to be mixed with the second harmonic of the local oscillation 13.28 GHz.

The first step of the design is to synthesize the core oscillator. In order to obtain the desired oscillation frequency of 6.64 GHz, a reflection type oscillator is used. In this case, the gate of the transistor is connected to the cavity feed line and two parallel stubs are used to achieve the oscillation frequency at 6.64 GHz. The stubs (Lss1 and Lss2 in Figure 5.1) are used to eliminate unwanted parasitic oscillations and additionally fine tune the oscillation frequency. To complete the circuit, a self-bias configuration is used. This configuration is made by placing two resistors from the source terminals to ground and placing a biasing DC voltage source in the drain terminal. This circuit has frequency stability and low phase noise oscillation.

Once the oscillation frequency is obtained, we do not have to change the structure of the circuit to obtain the self-oscillating mixer. In this second step the complete circuit is optimized in order to be oscillating at the desired oscillation frequency 6.64 GHz and at the same time to obtain conversion gain at the IF frequency of 3.38 GHz.

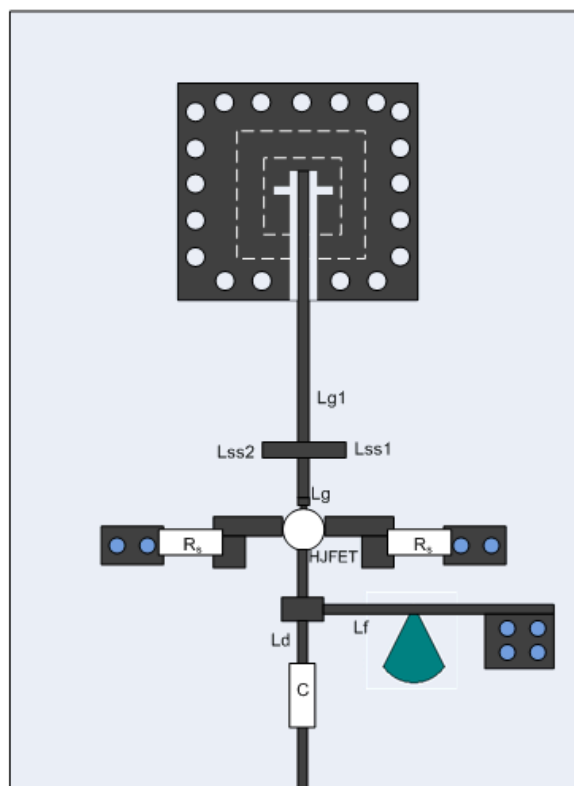


Figure 5.1: Active antenna oscillating mixer structure

## 5.2. Simulation Setup and Design Process

This section presents the procedure to simulate the SOM Active Integrated Antenna in Agilent ADS. First of all, we have to create a new project. Once it was made, we can start to build all the circuit structure. Before this process, it is necessary to import HFSS S-parameter data of the SIW cavity backed antenna to use them in the circuit simulator. Figure 5.2 presents the schematic of the SOM Active Integrated Antenna in Agilent ADS.

### 5.2.1. Circuit dimensions

The first element one can see in the schematic of Figure 5.2 is the S-parameter block corresponding to the SIW cavity-backed antenna. Then the HJFET transistor is connected to the radiating element through its gate terminal (G). The self-bias configuration is made by placing two resistors  $R_S$  from the source terminals (S) to ground and placing a biasing DC voltage source in the drain terminal (D). Additionally, the electromagnetic simulations both for the transistor pad and for the via-ground structure use to connect  $R_S$  to ground have been introduced in the circuit simulation to better model the real performance of the active SOM antenna.

The transmission line dimensions in the design will be optimized in order to obtain an oscillating solution at 6.64 GHz and at the same time to achieve conversion gain at 3.38 GHz. Table 5.1 shows the values of all the microstrip lines and junctions that were used. The parameters that were optimized to obtain the best circuit performance are marked in bold in Table 5.1. The procedure to obtain an optimized design is described in the next section.

Gate terminal			Drain terminal			Source terminal		
Element	Length variable	Value	Element	Length variable	Value	Element	Length variable	Value
Microstrip line	<b>Lg1</b>	<b>0.1 - 13 mm</b>	Microstrip line	Lf	0.5 - 5 mm	Resistor	Rs	12 - 50 $\Omega$
Stub	Lss1	0.1 - 4 mm	Microstrip line	Ld	0.1 - 5 mm	Resistor	Rs	13 - 50 $\Omega$
Stub	Lss2	0.1 - 4 mm	Microstrip line	---	5mm			
Microstrip line	<b>Lg</b>	<b>0.1 - 1.5 mm</b>	Voltage source	Vdd	1.5 v			
			Microstrip line	---	2 mm			
			Capacitor	---	1 pF			
			Resistor	---	50 $\Omega$			

Table 5.1: Parameters of the circuit

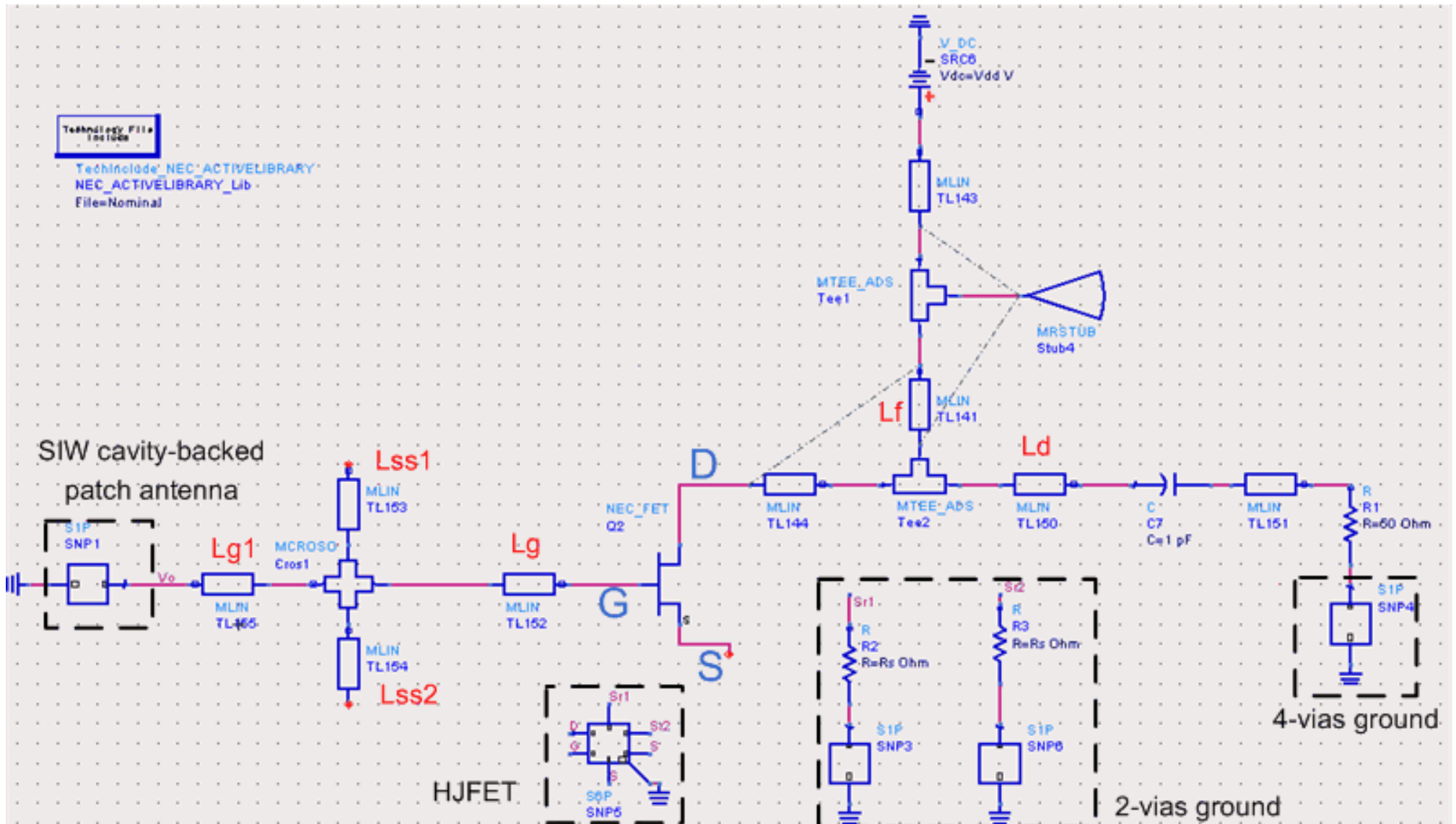


Figure 5.2: Active antenna oscillating mixer structure

## 5.2.2. Design and Simulation process

Once the basic circuit structure is prepared the first step is to obtain the frequency of oscillation. To do that, both the small signal simulation of the oscillator (using ADS OscTest tool) and the Harmonic Balance (HB) simulation (large signal simulation) are used. After the oscillation frequency of 6.64 GHz was obtained, the conversion gain of the SOM is optimized always maintaining the oscillation frequency to 6.64 GHz. The conversion gain optimization is made using a combined HB and conversion matrix (CM) analysis.

### 5.2.2.1. Finding the oscillation frequency

#### OscTest:

The first analysis used for the design of the SOM was the small signal tool OscTest (Figure 5.3). This probe has internally a scattering parameter termination port. It is connected to the circuit to calculate the loop gain of the oscillator. The simulation will give us  $S_{11}$  parameters and we have to plot the magnitude and phase of  $S_{11}$  ( $\text{dB}[S_{11}]$  and  $\text{phase}[S_{11}]$ ). The oscillation occurs when  $\text{dB}[S_{11}]$  is higher than 0 dB and  $\text{phase}[S_{11}]$  crosses the  $0^\circ$  with negative slope.

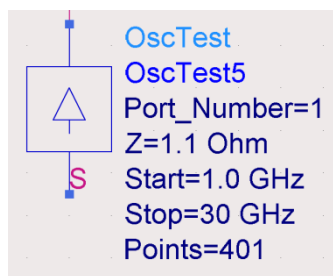


Figure 5.3: OscTest element

The OscTest is used to have a general vision of the potential oscillations in the circuit. It is done for fixed values of the circuit parameters. As an example, for the selected values in Table 5.2 the results of the OscTest simulation are the ones in Figure 5.4.

From Figure 5.4 one can see that there is a possible oscillation near 6.51 GHz. It means that using the parameters values in Table 5.2 we can obtain the desired oscillation frequency. In order to obtain a more accurate value of the oscillation frequency (6.64 GHz), we have to tune the variables and in order to know the actual value of the steady state oscillation frequency use a large signal analysis as the harmonic balance.

Gate terminal			Drain terminal			Source terminal		
Element	Length variable	Value	Element	Length variable	Value	Element	Length variable	Value
Microstrip line	Lg1	0.24 mm	Microstrip line	Lf	3.1 mm	Resistor	Rs	30 Ω
Stub	Lss1	0.4 mm	Microstrip line	Ld	5 mm	Resistor	Rs	30 Ω
Stub	Lss2	0.39 mm	Microstrip line	---	5mm			
Microstrip line	Lg	0.53 mm	Voltage source	Vdd	1.5 v			
			Microstrip line	---	2 mm			
			Capacitor	---	1 pF			
			Resistor	---	50 Ω			

Table 5.2: Values for the OscTest simulation

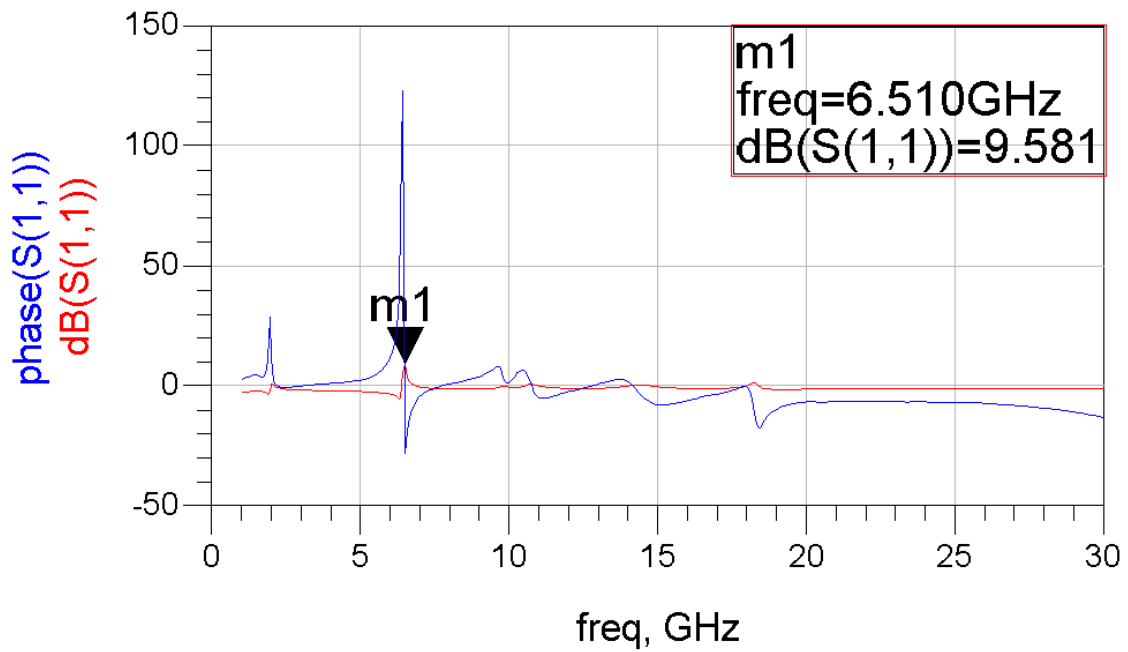


Figure 5.4: Osc Test results representation

### Harmonic Balance simulation:

The harmonic balance simulation is a large signal analysis that allows us to obtain the steady state solution of the circuit. A simplified explanation of the HB simulations follows: the HB simulation makes Kirchhoff equations of the circuit under analysis at the different harmonics specified in the HB parameters. Then it uses Newton Raphson algorithm to solve these equations. The initial vector used in the Newton Raphson is taken from the external generators that are present in the circuit schematic. This means, in an oscillator, the vector of initial conditions will be obtained from the DC voltage source. This means the frequency of the obtained solution will be 0 Hz (also known as trivial solution) and not the desired oscillating solution. In order to solve this problem, an auxiliary generator (AuxG) with frequency  $f_0$  is connected to a circuit node in the schematic. This will allow HB to converge to an oscillating solution.

The schematic of the used AuxG is shown in Figure 5.5. It is formed by band-pass filter at the frequency of interest  $f_0$ , and a generator defined by an amplitude, a phase and a frequency  $f_0$ . The auxiliary generator probe allows us to have an equation that includes  $f_0$  (the oscillation frequency) and that will give the Newton Raphson the necessary vector of initial conditions to find the oscillating solution. The band-pass filter forces the AuxG to work only at  $f_0$ . In order to avoid the perturbation of the final steady state solution due to the presence of the AuxG, it must fulfill a condition that correspond to  $Y=0$  (admittance at the AuxG node must be zero). This condition is introduced in ADS using two design goals in the optimization process (Figure 5.6). These goals introduce two more equations in the HB system of equations.

It is important to note that in this case the probe is placed at G (gate terminal) of the transistor. It can be placed anywhere in the circuit, but in order to analyze the possible oscillations of the circuit, it is better to place it directly in the terminals of the transistor (S, G, D).

Using HB in combination with an optimization process allows calculating the circuit parameters in order to obtain a selected performance. This way one can optimize the desired frequency, phase and amplitude in the oscillator. The optimization option has to be enabled in the variables (Figure 5.7).

The typical parameters that are controlled are the frequency, the power and the current consumption. Figure 5.8 presents the simulation results obtained after using the optimization process to design the core oscillator. It has an oscillation frequency of 6.639 GHz, an output power around 6dBm and a current consumption of 13mA.

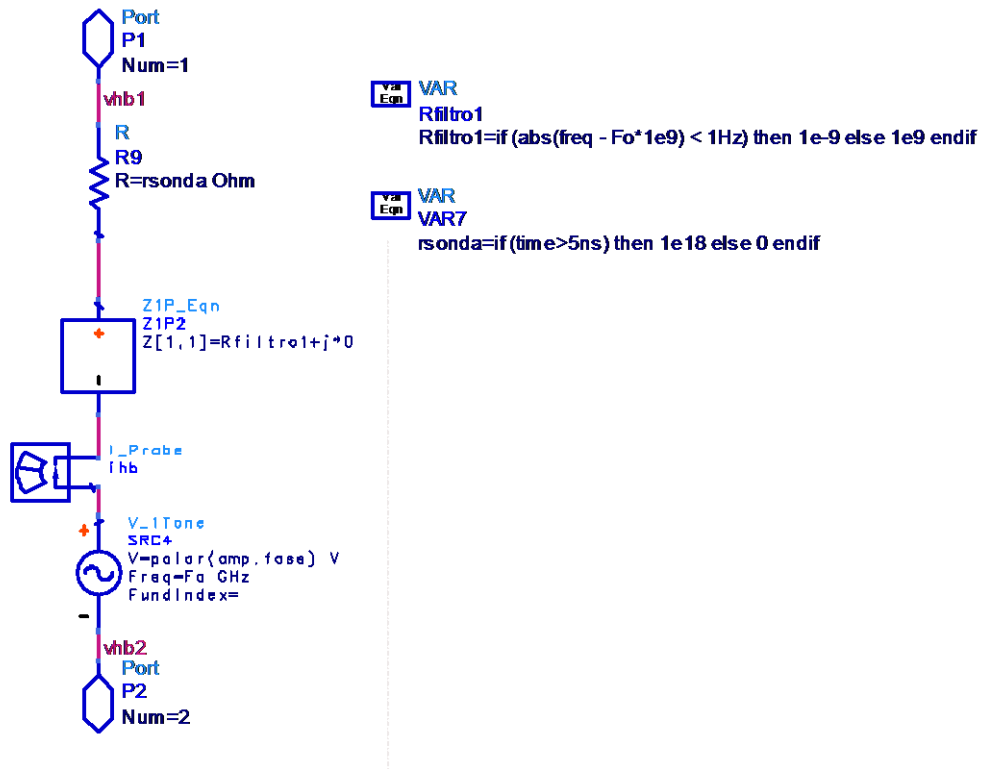


Figure 5.5: Auxiliary generator schematic

**HARMONIC BALANCE**

HarmonicBalance  
HB1  
Freq[1]=ffund GHz  
Order[1]=7  
FundOversample=4  
OscSteps=20.0

**GOAL**

Goal  
OptimGoal2  
Expr="imag(Ys1)"  
SimInstanceName="HB1"

**GOAL**

Goal  
OptimGoal1  
Expr="real(Ys1)"  
SimInstanceName="HB1"

AuxG  
Xx1  
amp=amp1  
fase=pho  
Fo=ffund

[Meas Eqn] MeasEqn  
Admittance2  
Ys1=Xx1.ihb.i[1]/G[1]

[Var Eqn] VAR  
VAR176  
amp1=0.98 {o}  
pho=0 {o}

[Var Eqn] VAR  
VAR175  
ffund=6.64 {o}

Figure 5.6: AuxG conditions setup in Harmonic Balance

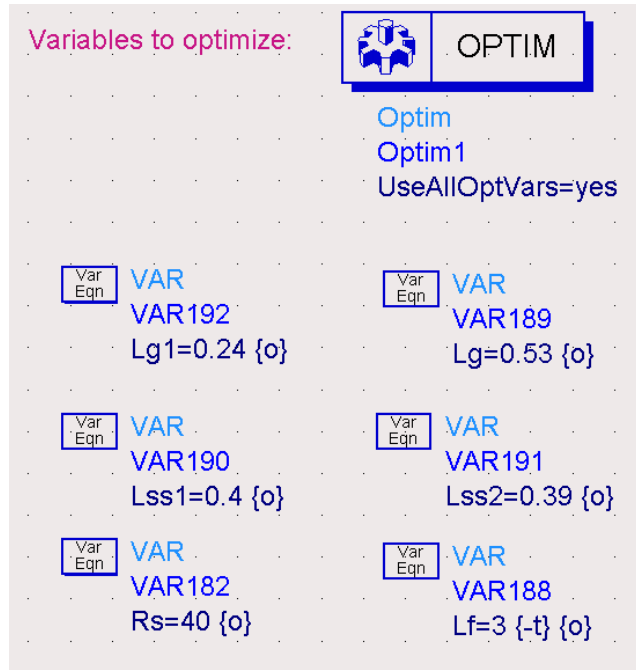


Figure 5.7: Variables to optimize

Gate terminal			Drain terminal			Source terminal		
Element	Length variable	Value	Element	Length variable	Value	Element	Length variable	Value
Microstrip line	Lg1	0.24 mm	Microstrip line	Lf	3.1 mm	Resistor	Rs	40 Ω
Stub	Lss1	0.4 mm	Microstrip line	Ld	5 mm	Resistor	Rs	40 Ω
Stub	Lss2	0.39 mm	Microstrip line	---	5mm			
Microstrip line	Lg	0.53 mm	Voltage source	Vdd	1.5 v			
			Microstrip line	---	2 mm			
			Capacitor	---	1 pF			
			Resistor	---	50 Ω			

Table 5.3: Optimized variables

freq	dBm(Vo)	abs(SRC6.i)
	optlter=1	optlter=1
0.0000 Hz	-106.565	0.013
6.639 GHz	6.824	0.007
13.28 GHz	-4.616	0.001
19.92 GHz	-17.877	0.001
26.56 GHz	-36.557	2.620E-4
33.19 GHz	-29.209	4.195E-5
39.83 GHz	-36.527	5.753E-6
46.47 GHz	-45.265	1.103E-5

FinalEF
4.234E-12

Figure 5.8: Harmonic Balance results after the optimization

Once the core oscillator has been designed to present an oscillation frequency of approximately 6.64 GHz, the optimization of its performance as SOM will be optimized.

### 5.2.2.2. Self-Oscillating Mixer simulation

The simulation process follow to design the SOM combines the large signal HB with the small signal CM analysis. It is a two level optimization routine. In a first step the oscillation frequency is calculated with HB analysis and in the second step a perturbation is introduced around that oscillating solution and the mixing product are calculated through CM. The HB block set up to perform this analysis is shown in Figure 5.9.

The intermediate frequency ( $f_{IF}$ ) has to be indicated in the harmonic balance. In this case, the variable fsweep represents the RF incoming frequency.  $f_{IF}$  is calculated as  $2*ffund-fsweep$ , where  $ffund$  is the oscillation frequency. To validate this configuration, a small signal source has to be used (Figure 5.10). The lower sideband small-signal voltage source allows us to make the small signal analysis on the circuit.

The conversion gain is formulated in terms of the IF delivered output power and the RF available power. Equation 5.1 shows the conversion gain and Figure 5.11 defines equation 5.1 in the ADS.

$$G_c = \frac{\frac{V_{out}^2}{2R_L}}{\frac{V_{in}^2}{8R_g}} = \frac{4V_{out}^2}{V_{in}^2} \quad (5.1)$$

$V_{out}$ : IF output power

$V_{in}$ : RF input power

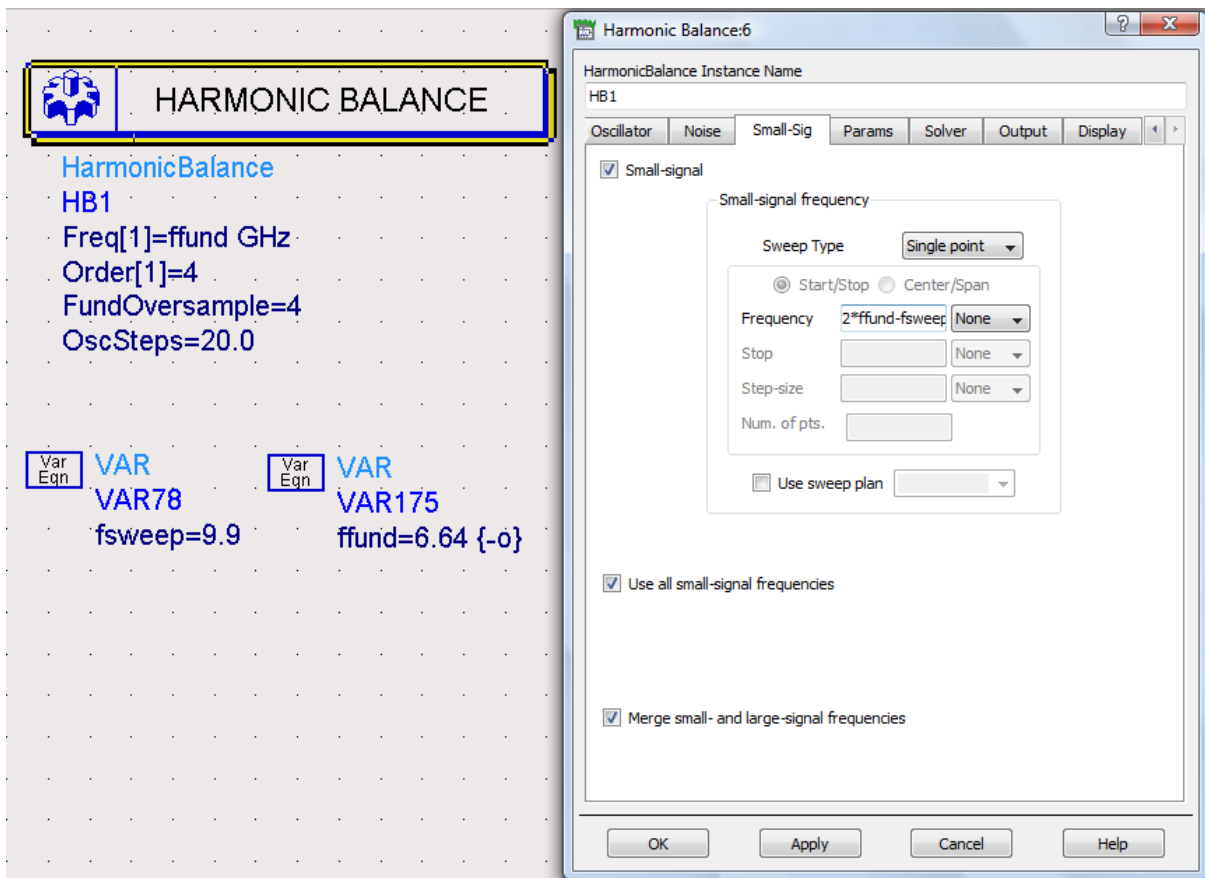


Figure 5.9: Small signal set up

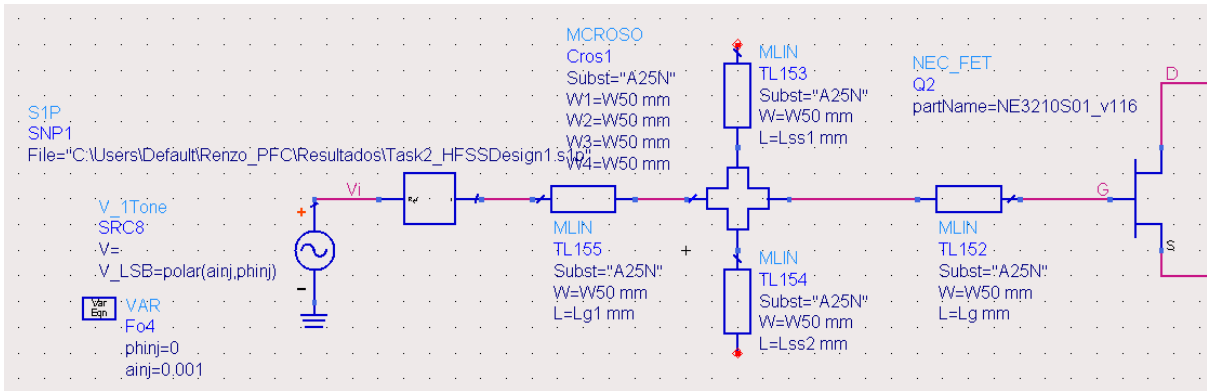


Figure 5.10: Small-signal voltage source

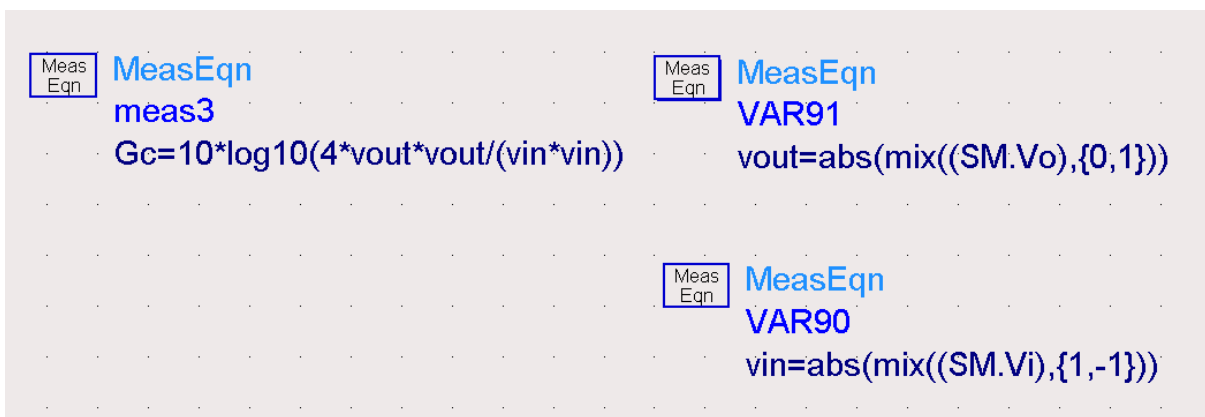


Figure 5.11: Defining gain equation

A new goal is introduced into the circuit to optimize the conversion gain (Figure 5.12). Table 5.4 presents all the variables values that are optimized in the process until a reasonable conversion gain was obtained. The best obtained result was -1.5 dB (Table 5.4).



Figure 5.12: Gain goal

Once an optimum design has been obtained, the layout of the circuit is prepared to be fabricated (Figure 5.14). In the ADS, we can generate automatically the layout of the circuit. Figure 5.13 shows how we can generate it. Once we had the layout, we have to export the file into a Gerber file type. The complete process is explained in detail in chapter 6.

simulation	ffund	Gc	Lg1	Lg	Lss1	Lss2	Rs	Ld	Lf	FinalEF
1	6.64	<b>-8.350</b>	0.382	0.31	0.41	0.42	14.21	1.9	3	1.05E-16
2	6.64	<b>-7.678</b>	0.39	0.26	0.45	0.45	13.13	1.51	2.95	1.12E-13
3	6.64	<b>-6.382</b>	13.19	0.9	1.9	0.39	13.44	1.5	2.87	7.88E-14
4	6.64	<b>-5.914</b>	13.2907	0.91	1.53	0.41	13.34	1.5	2.87	5.69E-14
5	6.64	<b>-5.497</b>	13.28	0.0907	1.53	0.41	13.54	1.5	2.87	4.54E-13
6	6.64	<b>-5.000</b>	13.17	1.01544	1.53	0.41	14.13	1.5	2.87	2.55E-12
7	6.64	<b>-4.666</b>	13.04	1	1.99	0.41	14.03	1.5	2.79	5.53E-12
8	6.64	<b>-4.305</b>	13.04	0.99	2	0.41	13.67	1.5	2.71	6.00E-12
9	6.64	<b>-3.254</b>	13.1092	1	2.05	0.41	13.7	1.51	2.09	7.04E-17
10	6.64	<b>-2.971</b>	13.24	0.85	2	0.46	12.26	1.5	1.97	7.01E-12
11	6.64	<b>-2.900</b>	13.24	0.85	2	0.45	12.33	1.5	1.97	9.86E-10
12	6.64	<b>-2.633</b>	13.24	0.85	1.2	1.35	12.33	1.5	1.97	3.03E-13
13	6.64	<b>-2.500</b>	13.23	0.84	1.22	1.33	12.33	1.4	1.97	4.45E-12
14	6.64	<b>-2.344</b>	13.252	0.83	1.22	1.33	12.33	1.3	1.97	5.23E-12
15	6.64	<b>-2.242</b>	13.251	0.83	1.22	1.33	12.33	1.21	1.97	2.63E-13
16	6.64	<b>-2.200</b>	13.251	0.83	1.22	1.33	12.33	1.17	1.97	4.95E-12
17	6.64	<b>-1.514</b>	13.23	0.827	1.22	1.4	12.29	0.5	1.97	1.29E-12

Table 5.4: Optimized variables in order to obtain a reasonable conversion gain

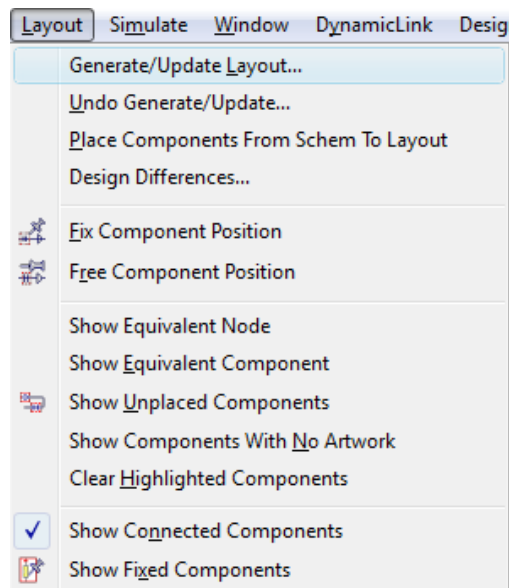


Figure 5.13: Generating the layout

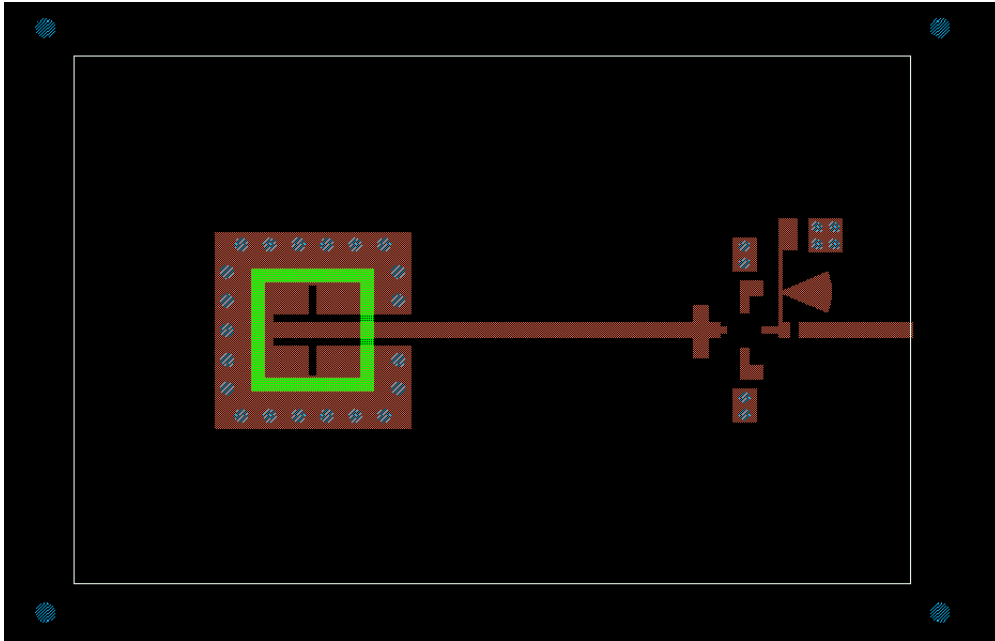


Figure 5.14: Circuit layout

## Chapter 6:

# Fabrication and measurements

This chapter presents the fabrication process of the SIW cavity-backed patch antenna and the active antenna self-oscillating mixer, the measurement procedure and the obtained results. Furthermore, the measurement results are compared with the simulation results, analyzing their similitude and differences.

### 6.1. Fabrication process

The fabrication process is the same for both SIW cavity-backed patch antenna and active antenna self-oscillating mixer. They were fabricated at the “CTTC facilities”. The steps are the following:

- 1) First of all, we need to export the layouts from Agilent ADS momentum simulation into a Gerber file type. This type of file allows us to work with the LPKF milling machine software (Figure 6.1).
- 2) The A25N substrate has to be fixed into the work surface of the LPKF milling machine. It allows making the feed line, transverse stubs, patch and the ground plane contours (Figure 6.2).
- 3) All unwanted copper was removed using a cutter and following the contours made by the LPKF milling machine (Figure 6.3 and 6.4).
- 4) In order to fabricate via holes that form the SIW cavity, a plastic material is stick to both sides of the circuit. Then a conductive paste is extended over the surface of the circuit and absorbed in the vias. Then the plastic is removed and the circuit introduce into the oven.
- 5) After the SOM Active Integrated Antenna structure is fabricated, the capacitors, connector and resistors are soldered. In the case of the passive antenna, there is no extra component to be soldered (only the connector). In Figures 6.5 and 6.6 one can see both fabricated circuits.

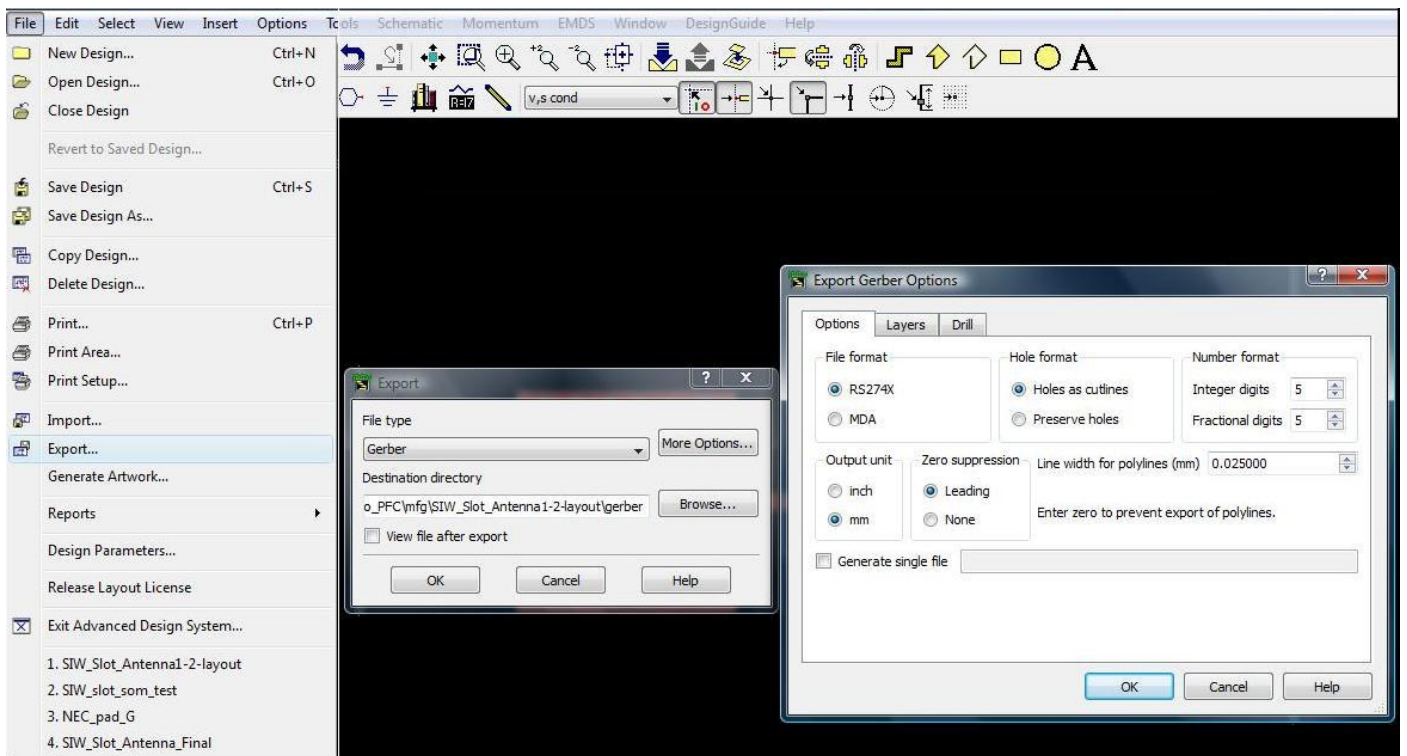


Figure 6.1: Exporting all data into a Gerber file type



Figure 6.2: Fixing A25N substrate into the work surface of the LPFK milling machine

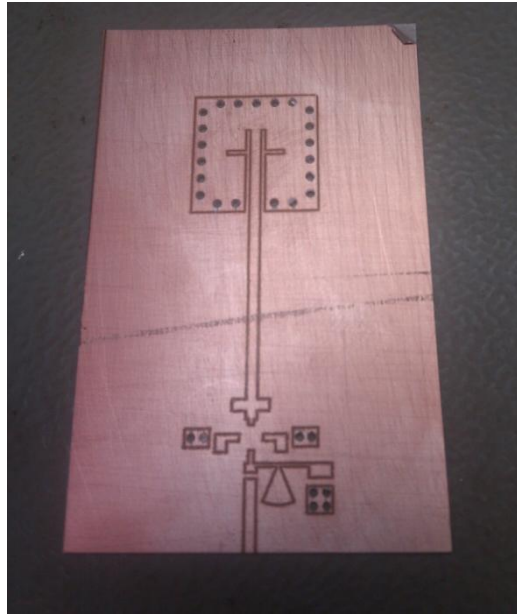


Figure 6.3: Before I removed the unwanted cooper

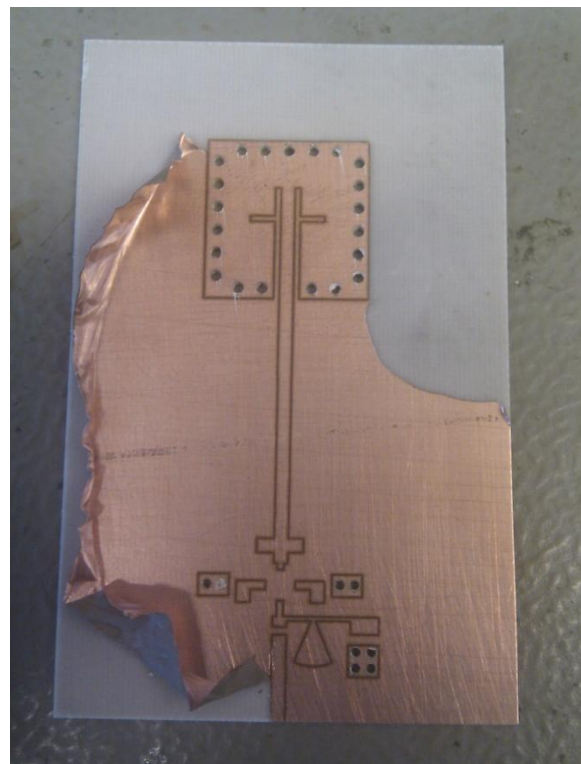
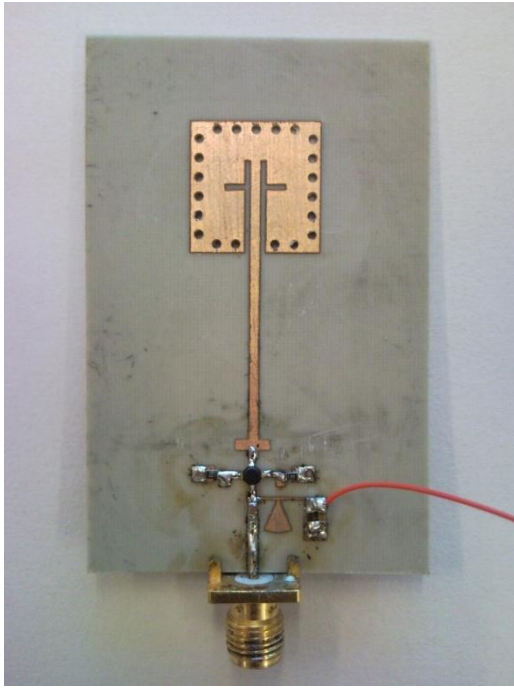


Figure 6.4: Removing the unwanted copper using a cutter and following the marks made by the milling machine

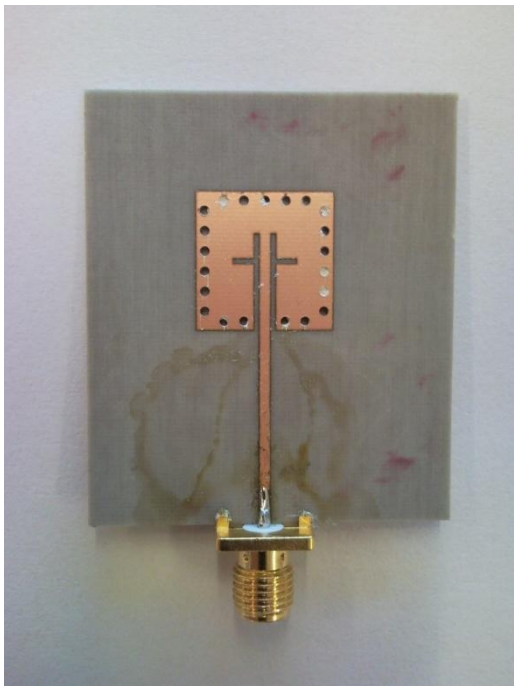


(a)

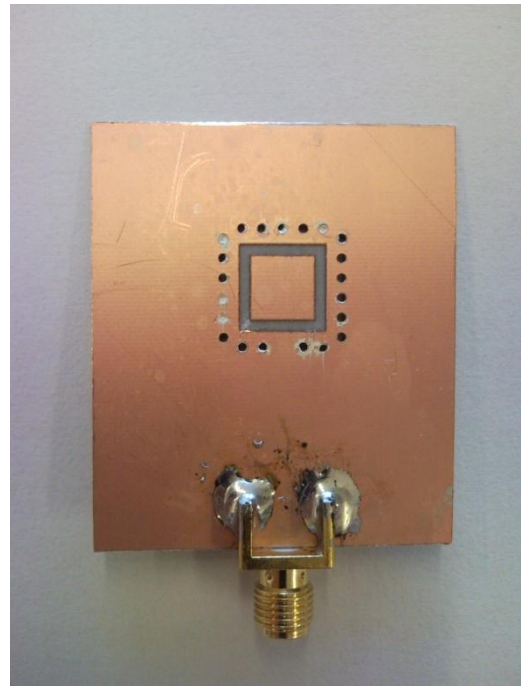


(b)

Figure 6.5: SOM Active Integrated Antenna: Rear view (a) and front view (b)



(a)



(b)

Figure 6.6: SIW cavity-backed antenna: Rear view (a) and front view (b)

## 6.2. Measurement results

This section presents all the results of the measurement. The order that the results are presented is designated according to the measurement process. Furthermore, the measurement process is described.

### 6.2.1. $S_{11}$ Parameter of the Passive Antenna

The first parameter measured was the return losses of the passive antenna ( $S_{11}$  parameter). In order to obtain this parameter, the passive antenna was connected to the Rohde & Schwarz ZVA24 vector network analyzer. Previously, the vector network analyzer had to be calibrated. In this project, Matlab was used to process all the data exported from the vector network analyzer. In this case, it allows us to plot the  $S_{11}$  parameter. Figure 6.7 shows the  $S_{11}$  parameter. It presents a value of -20 dB and 10 dB impedance bandwidth of 160 MHz.

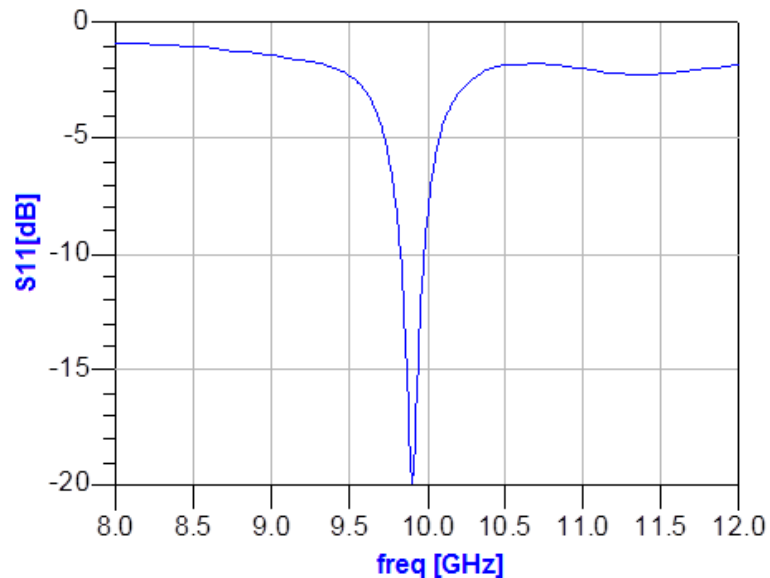


Figure 6.7:  $S_{11}$  parameter plot

Comparing Figure 6.7 and Figure 4.27, one can see that the fabrication result of the  $S_{11}$  parameter is lower than the simulation result but it is still having a good value. These mean that the fabrication process can be considered good.

## 6.2.2. Oscillation frequency of the SOM

Once the  $S_{11}$  parameter was measured and verified that its value is adequate to not have considerable reflection losses, we can start to measure the oscillation frequency of the SOM. In order to obtain this measured, the SOM was connected to a spectrum analyzer. The oscillation frequency varies according to the voltage injected to the drain terminal. Figure 6.8 shows the variation of the oscillation frequency versus the drain bias voltage.

Figure 6.9 and 6.10 show the output spectrum of the oscillation at two different values of drain bias voltage. The actual drain biasing selected for the design was 1.5 V. In simulation 1.5 V of biasing correspond to an oscillation frequency of 6.64 GHz. In measurements this frequency is slightly shifted to 6.525 GHz.

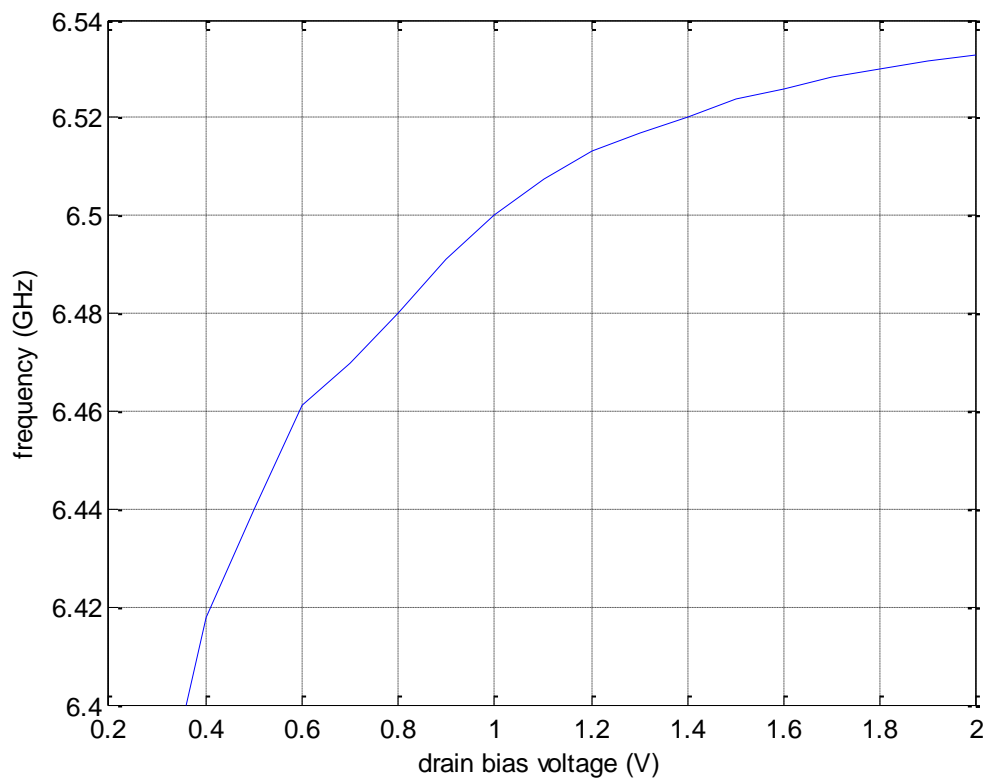


Figure 6.8: Oscillation frequency's behavior according the drain voltage

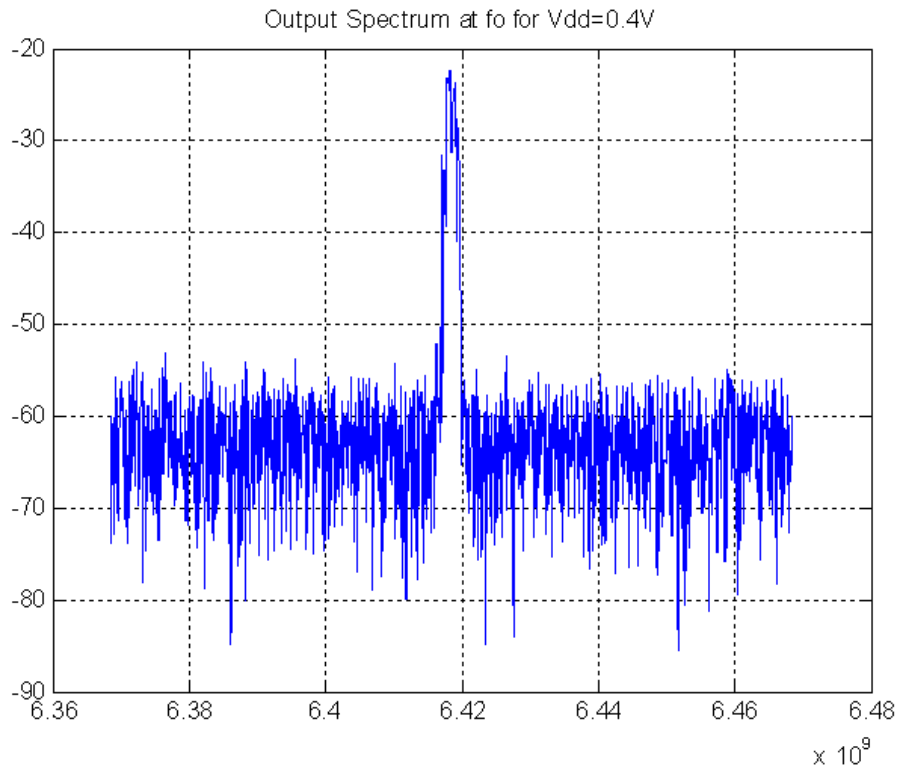


Figure 6.9: Oscillation frequency injecting 0.4 volt in the drain terminal

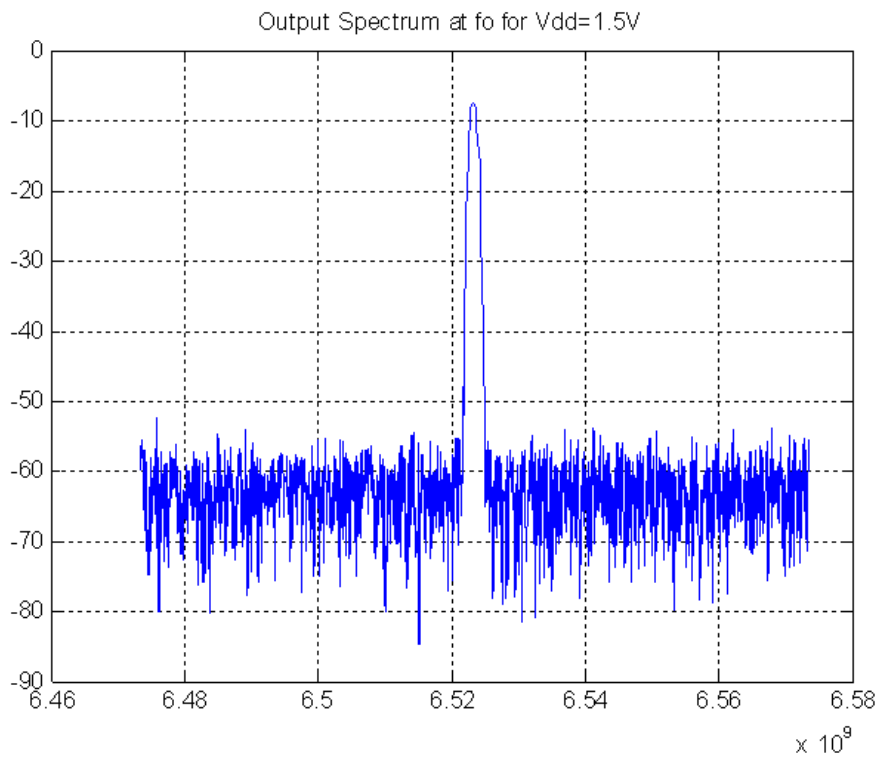


Figure 6.10: Oscillation frequency injecting 1.5 volts in the drain terminal

### 6.2.3. Radiation Pattern Measurements Process and Results

This section presents the process to obtain the radiation patterns of the passive and active antennas and the obtained results. These measurements were obtained in an anechoic chamber.

In order to obtain the radiation patterns, two different antennas under test (AUT) were considered: the passive SIW cavity-backed patch antenna (AUT 1) and the SOM Active Integrated Antenna (AUT 2). In the next subsections, the procedure used to measure the radiation patterns, the gain values of the antennas and the conversion gain of the SOM is explained.

#### 6.2.3.1. Comparison procedure

To obtain the radiation pattern and the gain of the ATU 1 and ATU 2, both elements and a third one have to be measured. The third element is a standard horn antenna. This horn antenna allows us to obtain the specific values of the ATU 1 gain and ATU 2 gain, because its gain is already known. In the process shown below, the followed steps to obtain ATU 1 gain and ATU 2 gain are presented.

##### Step 1: Standard Gain Horn measurement

In this first step, the horn received power is measured using a spectrum analyzer. The relationship between the transmitted and received power is given by Friis formula. Figure 6.11 presents the used set-up.

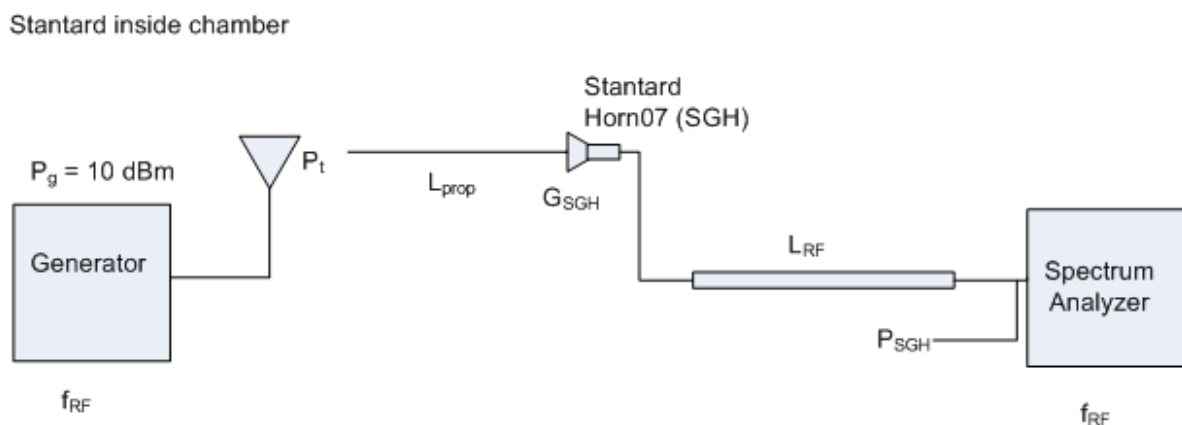


Figure 6.11: Transmission and reception scheme for standard horn antenna measurement

Where:

- $L_{prop}$ : Propagation losses
- $L_{RF}$ : Cable losses at  $f_{RF}$
- $G_{SGH}$ : Gain of the standard horn antenna (known from the specifications)
- $P_{SGH}$ : Measured power with the standard horn antenna

Using Friis equation:

$$P_{SGH} = P_t - L_{prop} + G_{SGH} - L_{RF} \quad (6.1)$$

Step 2: AUT 1 measurement

In this second step, the AUT 1 received power is measured. To relate all the transmission and reception parameter, the Friis equation is used (as in step 1). Figure 6.12 presents the set-up used.

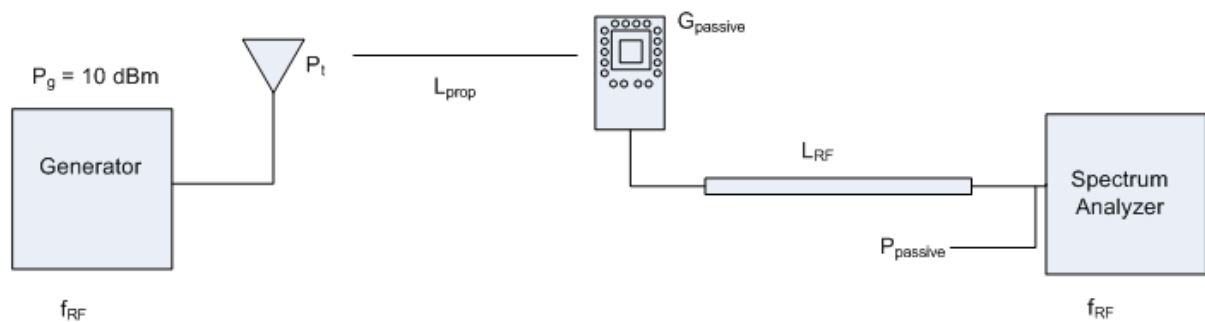


Figure 6.12: Transmission and reception scheme to SIW cavity-backed antenna measurement

Where:

- $G_{passive}$ : gain of the passive antenna
- $P_{passive}$ : measured power with the passive antenna

Using Friis equation:

$$P_{passive} = P_t - L_{prop} + G_{passive} - L_{RF} \quad (6.2)$$

From equations 6.1 and 6.2, we can obtain  $G_{passive}$ :

$$\begin{aligned} G_{passive} &= P_{passive} - (P_t - L_{prop} - L_{RF}) \\ &= P_{passive} - (P_{SGH} - G_{SGH}) \\ &= P_{passive} - P_{SGH} + G_{SGH} \end{aligned} \quad (6.3)$$

$P_{SGH}$  and  $G_{SGH}$  are known, so  $G_{passive}$  can be calculated

### Step 3: AUT 2 measurement

In this third step, the AUT 2 received power is measured. To relate all the transmission and reception parameter, the Friis equation is used (as in step 1 and 2). Figure 6.13 presents the used set-up.

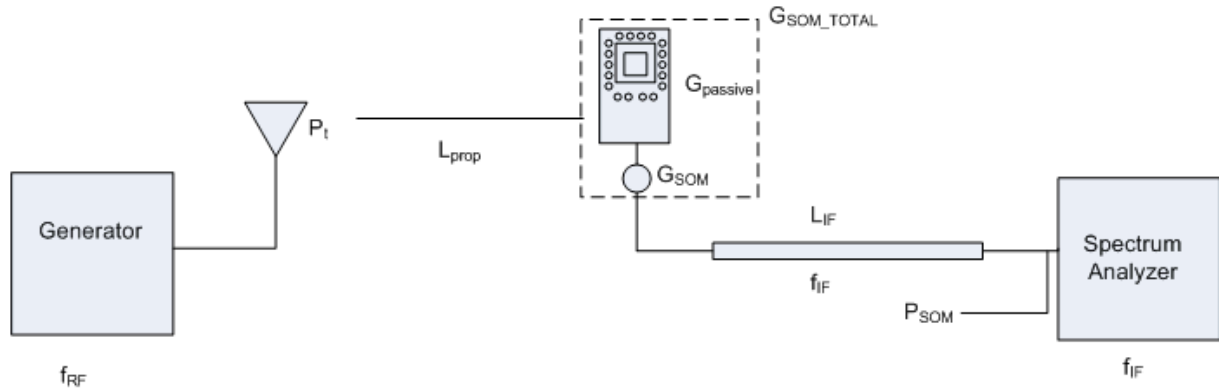


Figure 6.13: Transmission and reception scheme for SOM Active Integrated Antenna measurement

Where:

- $L_{IF}$ : Cable losses at  $f_{IF}$
- $G_{SOM}$ : Gain of the self-oscillating mixer
- $G_{SOM\_TOTAL}$ : Gain of the active Antenna
- $P_{SOM}$ : measured power with the active antenna

Using Friis equation:

$$P_{SOM} = P_t - L_{prop} + G_{SOM\_TOTAL} - L_{IF} \quad (6.4)$$

From equations 6.1 and 6.4, we can obtain  $G_{SOM\_TOTAL}$ :

$$\begin{aligned} G_{SOM\_TOTAL} &= P_{SOM} - (P_t - L_{prop} - L_{IF}) \\ &= P_{SOM} - (P_{SGH} - G_{SGH} + L_{RF}) - L_{IF} \\ &= P_{SOM} - P_{SGH} + G_{SGH} - L_{RF} - L_{IF} \end{aligned} \quad (6.5)$$

And from equation 6.2 and 6.4, we can obtain  $G_{SOM}$ :

$$\begin{aligned} G_{SOM} &= P_{SOM} - (P_t - L_{prop} + G_{passive} - L_{IF}) \\ &= P_{SOM} - (P_{passive} + L_{RF}) + L_{IF} \\ &= P_{SOM} - P_{passive} - L_{RF} + L_{IF} \end{aligned} \quad (6.6)$$

The problem of equations 6.5 and 6.6 is that we do not have  $L_{RF}$  and  $L_{IF}$  values. To obtain them, and later  $G_{SOM}$  and  $G_{SOM\_TOTAL}$  values, we have to measure their values, as is shown in Figure 6.14. When the generator injects a 0 dBm signal, the  $L_{RF}$  and  $L_{RF}$  are obtained directly in the spectrum analyzer.

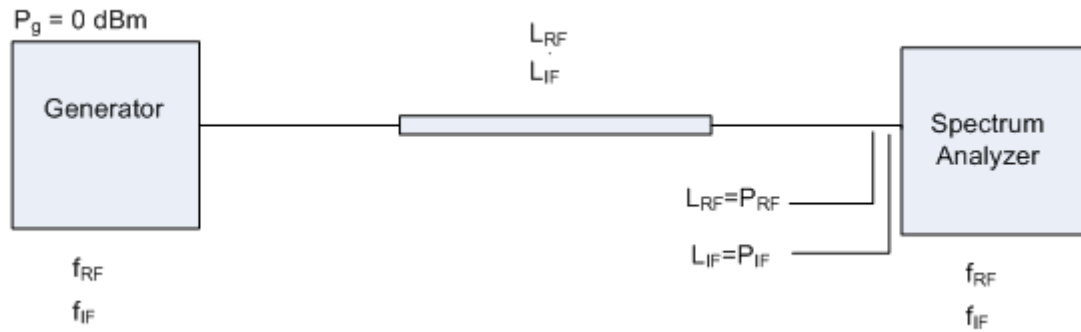


Figure 6.14:  $L_{IF}$  and  $L_{RF}$  measurement

Finally, with all these steps, we can obtain the gain values of the passive and active antennas. With them, we can plot the radiation pattern with their respectively values. Matlab was used to process all the data obtained.

### 6.2.3.2. Measurement Process of the Radiation Pattern

For 2D radiation pattern measurements, we have to work at the anechoic chamber (Figure 6.19). To obtain the E-plane co-polar, E-plane cross-polar, H-plane co-polar and H-plane cross-polar, we have to place the passive antenna and the active antenna in different ways. This section explains the followed procedure to obtain all these measurements (the procedures are the same for both antennas).



Figure 6.15: Measuring E-plane co-polar

E-plane co-polar: In this case, we have to inject the signal from the generator to the transmitting antenna with its E-field parallel with E-field of the receiving antenna. This allows us to obtain the E-plane while the antenna is rotated (as shown in Figure 6.15).



Figure 6.16: Measuring E-plane cross-polar

E-plane cross-polar: In this case, we have to inject the signal from the generator to the transmitting antenna with its E-field transversal with E-field of the receiving antenna. This allows us to obtain the E-plane co-polar while the antenna is rotated (as shown in Figure 6.16).



Figure 6.17: Measuring H-plane co-polar

H-plane co-polar: In this case, we have to inject the signal from the generator to the transmitting antenna with its H-field parallel with H-field of the receiving antenna. This allows us to obtain the H-plane co-polar while the antenna is rotated (as shown in Figure 6.17).

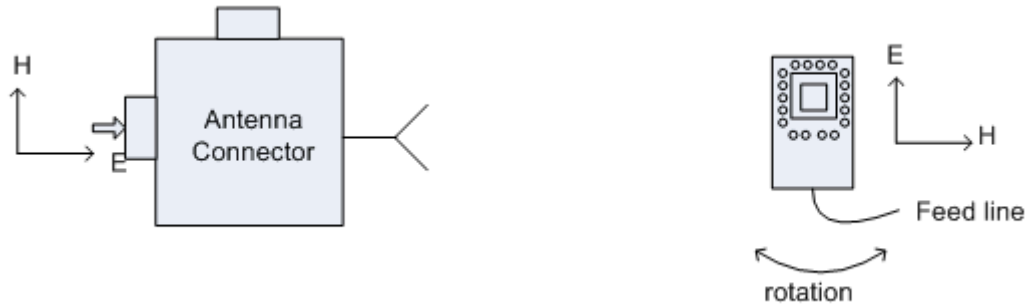


Figure 6.18: Measuring H-plane cross-polar

H-plane cross-polar: In this case, we have to inject the signal from the generator to the transmitting antenna with its H-field transversal with H-field of the receiving antenna. This allows us to obtain the H-plane cross-polar while the antenna is rotated (as shown in Figure 6.18).

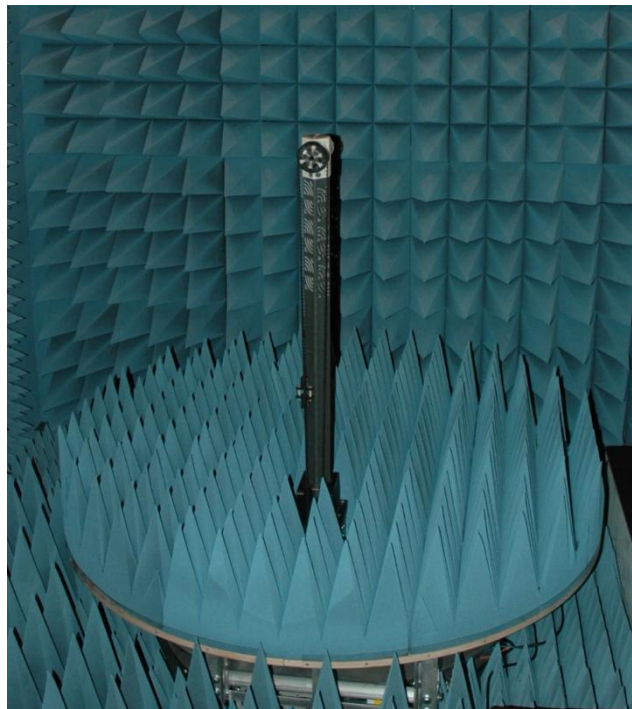


Figure 6.19: Rotational platform of the anechoic chamber

### 6.2.3.3. Passive Antenna

In Figures 6.20, 6.21, 6.22 and 6.23 we can see the E-plane and the H-plane radiation pattern of the antenna (co-polar and cross-polar). In this case, Matlab was used to process all the data exported. It allows us to plot the radiation patterns presented below:

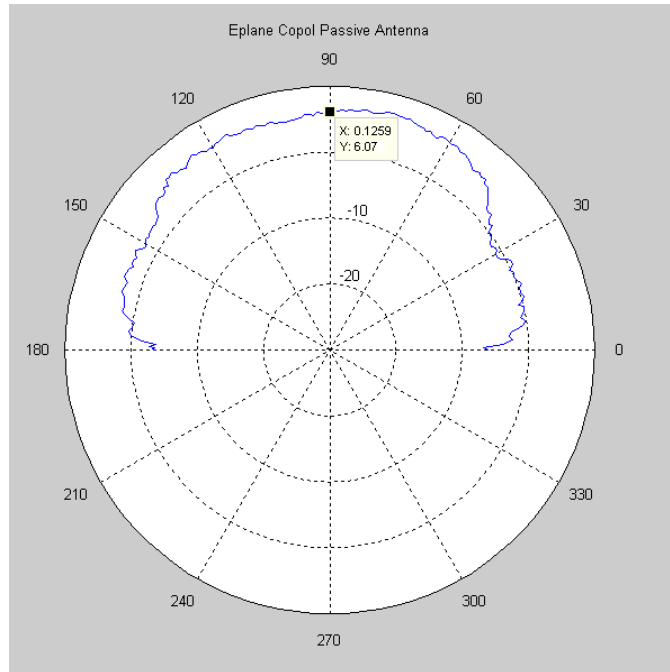


Figure 6.20: Measured E-plane co-polar radiation patter

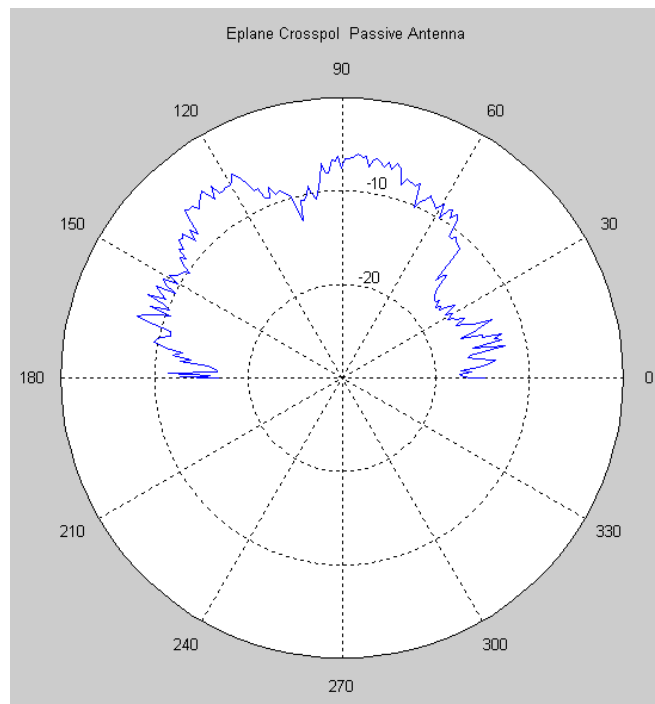


Figure 6.21: Measured E-plane cross-polar radiation pattern

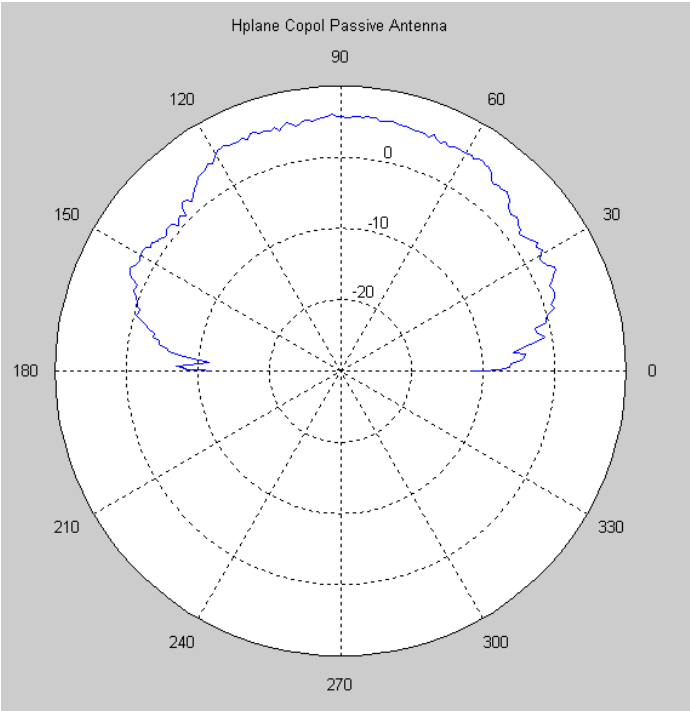


Figure 6.22: Measured H-plane co-polar radiation pattern

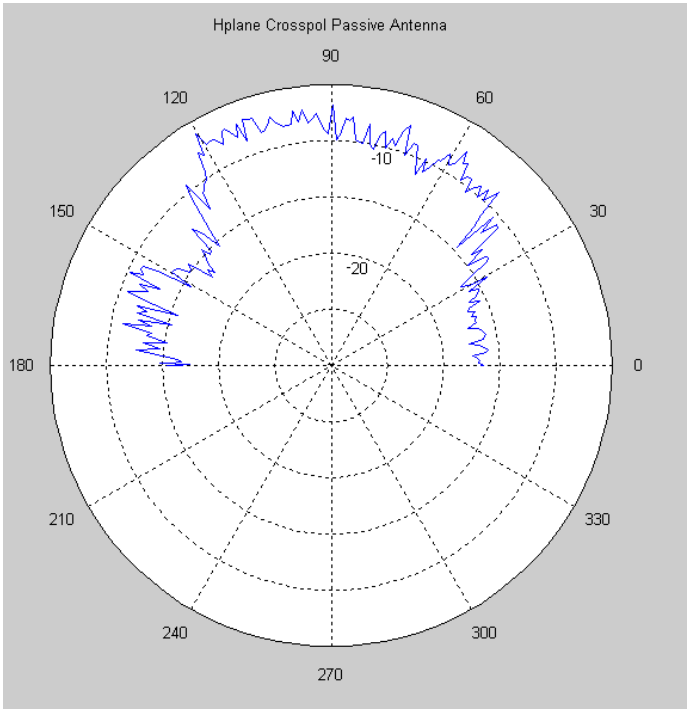


Figure 6.23: Measured H-plane cross-polar radiation pattern

From the E-plane co-polar, we can obtain some characteristics, as the half-power beam width at -3 dB (HPBW), beam width between first nulls (FNBW) and the gain. These results are shown in Table 6.1. The fabrication results are very similar with the simulation results of the passive antenna.

Antenna Parameter	
Gain	6.07 dB
Polarization	linear
Directivity	6 dB
HPBW	108°
FNBW	188°

Table 6.1: Passive antenna results

#### 6.2.3.4. Active antenna

In Figure 6.24, 6.25, 6.26 and 6.27, we can see the E-plane and the H-plane radiation pattern of the active antenna (co-polar and cross-polar). In this case, Matlab was used again to process all the data exported. It allows us to plot the radiation patterns presented below:

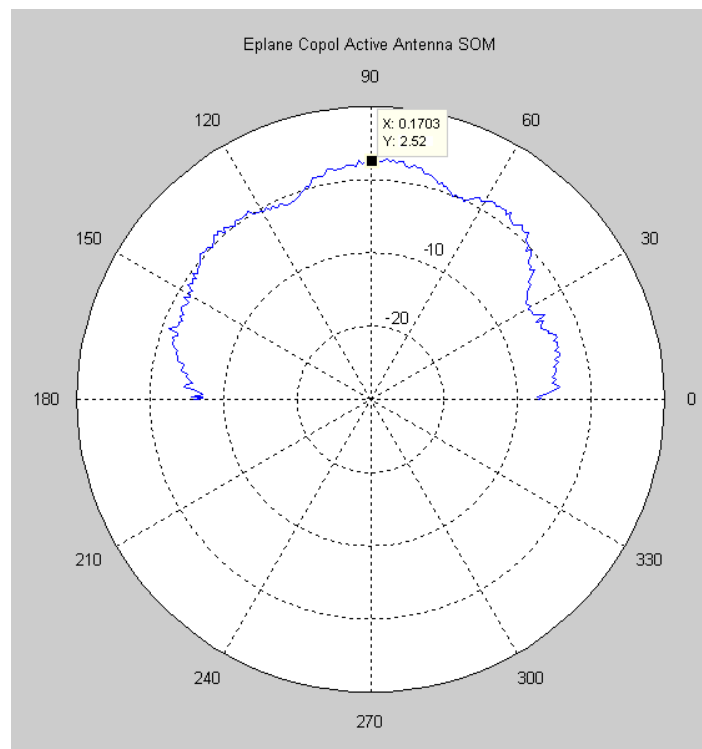


Figure 6.24: Measured E-plane co-polar radiation pattern

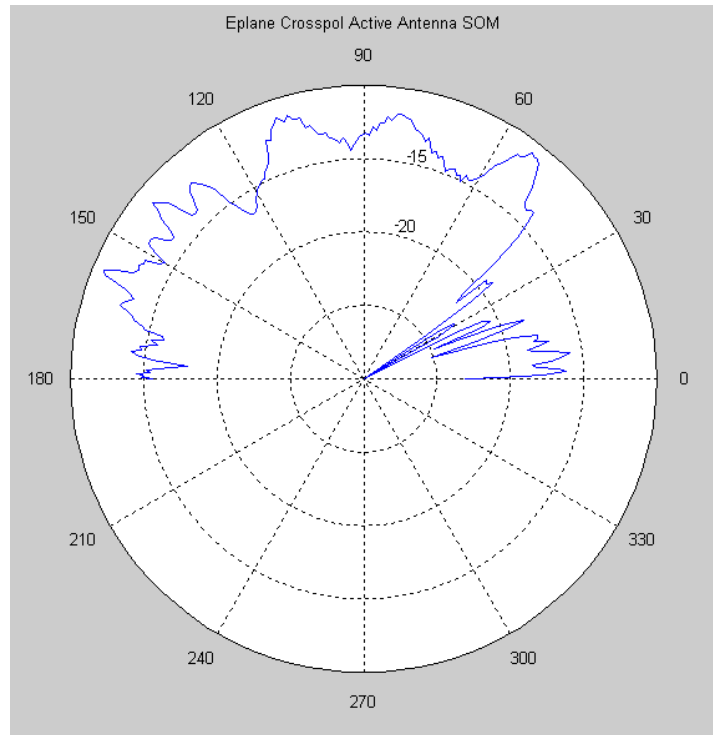


Figure 6.25: Measured E-plane cross-polar radiation pattern

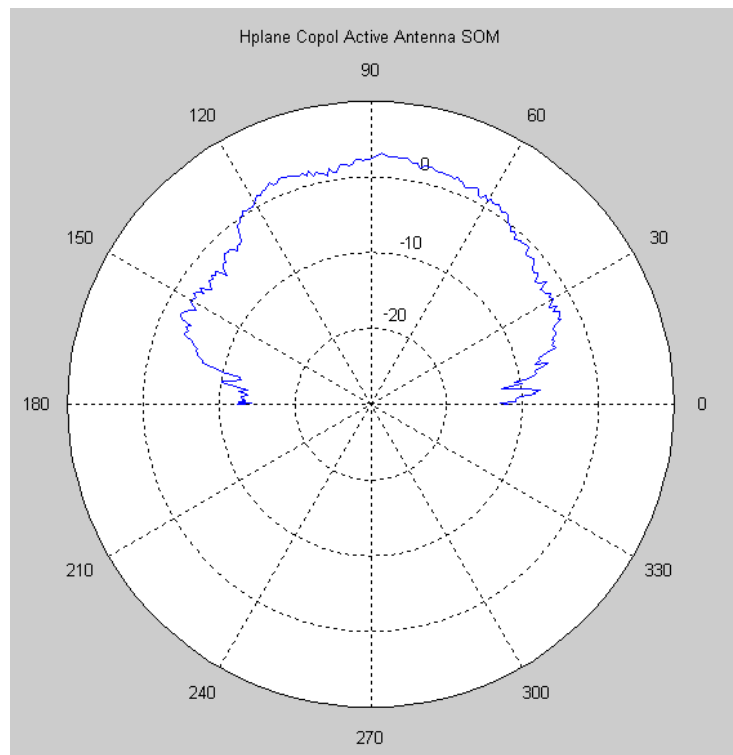


Figure 6.26: Measured H-plane co-polar radiation pattern

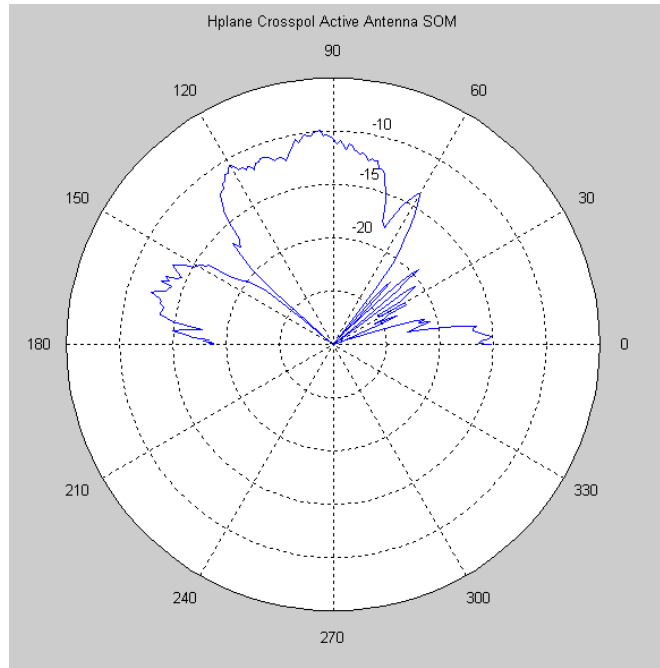


Figure 6.27: Measured H-plane cross-polar radiation pattern

#### 6.2.4. Gain of the SOM

Finally, after all radiation patterns were measured and verified their values are correct according with the simulations results, the conversion gain can be calculated. To obtain this value, Equation 6.6 has to be used. Figure 6.28 presents the measured conversion gain versus the selected IF frequency. This selection is made by modifying the input RF frequency. The maximum conversion gain measured value -3.8 dB. If we compare this value with the simulated conversion gain, we can see that there is a 1.8 dB loss. However one has to take into account that the measured oscillation frequency is shifted from the simulated value also, which is the main cause for the loss of gain.

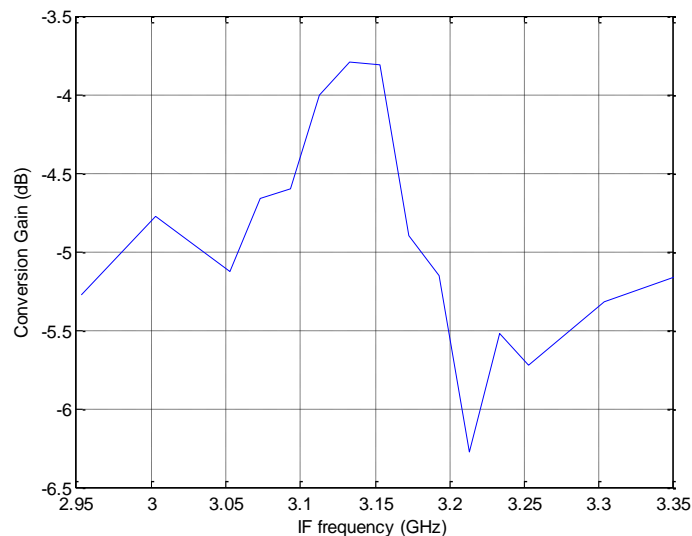


Figure 6.28: Conversion Gain of the self-oscillating mixer

## Chapter 7:

# Conclusions and future work

A single substrate, compact SIW cavity-backed active patch antenna self-oscillating mixer has been designed. Its use is intended for receiving phased arrays based on coupled self-oscillating mixers. The proposed topology allows implementing the patch antenna and the active circuitry on different sides of the substrate allowing for high integration and an efficient and low cost fabrication.

A combination of electromagnetic, harmonic balance and conversion matrix analysis techniques was used in order to optimize the oscillation frequency of the core oscillator and the conversion gain of the self-oscillating mixer.

As future lines within this research topic, we can highlight:

- Refinement of the self-oscillating mixer design in order to obtain conversion gain
- Design a tunable self-oscillating mixer
- Design a receiving phased array using this SIW cavity backed patch antenna self-oscillating mixers

# Bibliography

- [1] Maurizio BOZZI, Luca PERREGRINI, Ke WU, Paolo ARCIONI. *Current and Future Research Trends in Substrate Integrated Waveguide Technology*. Radioengineering, VOL.18, No 2, June 2009
- [2] Ke WU, Dominic DESLANDES and Yves CASSIVI. *The Substrate Integrated Circuits – A New Concept for High-Frequency Electronics and Optoelectronics*. Telsiks 2003.
- [3] Constantine A. Blanis. *Antenna theory*. John Wiley and Sons, Ney York 2nd edition, 1997
- [4] David Pozar, *Microstrip antenna aperturecoupled to a microstripline*. ELECTRONICS LETTERS, pages 49-50, 1985.
- [5] Nemaï Chandra Karmakar. *Investigations into a Cavity-Backed Circular-Patch Antenna*, IEEE Transactions on Antennas and Propagation, Vol 50, No 12, 2002
- [6] J. T. Aberle, “*On the use of metallized cavities backing microstrip antennas*,” in 1993 IEEE AP-S Int. Symp. Dig., 1993, pp. 60–63.
- [7] M. Lye, R. B. Waterhouse, D. Novak, F. Zavosh, and J. T. Aberle, “*Design and development of printed antenna remote units for optically distributed mobile communications*,” IEEE Microwave Guided Wave Lett., vol. 8, pp. 432–434, Dec. 1998.
- [8] M. E. Bialkowski, S. T. Jellett, and R. Varnes, “*An electronically steered antenna system for the Australian mobilesat™*,” Proc. Inst. Elect. Eng. Microwaves Antennas Propagat., vol. 143, no. 4, pp. 347–352, Aug. 1996.
- [9] F. Zavosh and J. T. Aberle, “*Improving the performance of microstrippatch antennas*,” IEEE Antennas Propagat. Mag., vol. 38, pp. 7–12, Aug. 1996.
- [10] ----, “*Design of high gain microstrip antennas*,” Microwave J., vol. 42, no. 9, pp. 138–148, Sept. 1999.
- [11] M. A. Gonzalez, J. A. Encinar, and J. Zapata, “*Radiation pattern computation of cavity-backed and probe-fed stacked microstrip patch arrays*,” IEEE Trans. Antennas Propagat., vol. 48, pp. 502–509, Apr. 2000.

- [12] M. J. Tsai and B. Rulf, "A simple double-slot radiator for E-plane beam control," presented at the Proc. 2000 Int. Union of Radio Science (URSI), Salt Lake City, UT, July 2000.
- [13] A. Boag, Y. Shimony, A. Boag, and R. Mittra, "Dual band cavity-backed quarter-wave patch antenna," in Proc. 1995 IEEE Antennas and Propagation Int. Symp. Dig., Newport Beach, CA, June 1995, pp. 2124–2127.
- [14] S. Noghianian and L. Shafai, "Control of microstrip antenna radiation characteristics by ground plane size and shape," Proc. Inst. Elect. Eng. Microwave Antennas Propagat., vol. 145, no. 3, pp. 207–212, June 1998.
- [15] Annex III—List of Cost 245 Temporal Documents [Online]. Available: <http://www.inet.uni2.dk/home/cost260/cost245/temporal.html>
- [16] J. L. Volakis and J. M. Jin, "A scheme to lower the resonant frequency of the microstrip patch antenna," IEEE Microwave Guided Wave Lett., vol. 2, pp. 292–293, July 1992.
- [17] Herran, L.F., Ver Hoeye, S., Fernandez, M. , "Phase-shifter/down-converter cell for phased-array antennas," Electronics Letters , vol.42, no.4, pp. 193- 195, 16 Feb. 2006
- [18] Herran, L.F., Ver Hoeye, S., Fernandez, M.; Las Heras, F., , "Use of mutually coupled harmonic self-oscillating mixers for receiving phased-array antennas," Electronics Letters , vol.44, no.1, pp.11-12, January 3 2008
- [19] A. Collado, "Análisis y control práctico de bifurcaciones en circuitos de microondas. Aplicación a sistemas de osciladores acoplados", PhD dissertation, Universidad de Cantabria, ETSIT, 2007.
- [20] Almudena Suárez, Raymond Quéré, "Stability analysis of nonlinear microwave circuits", Artech House, 2003 - Technology & Engineering
- [21] Darrell W. Pepper, Juan C. Heinrich, "The finite element method: basic concepts and applications", Taylor & Francis, 1992
- [22] O. C. Zienkiewicz, R. L. Taylor, Robert Leroy Taylor, J. Z. Zhu, "The finite element method: its basis and fundamentals", Butterworth-Heinemann, 2005
- [23] J. Jin, The Finite Element Method: its basis and fundamentals. New York:Wiley, 1993.
- [24] J. Gong, J. L. Volakis, A. C. Woo, and H. T. G. Wang, "Scattering and radiation analysis of three-dimensional cavity arrays via a hybrid finite-element method," IEEE Trans. Antennas Propagat., vol. 41, no. 11, pp. 1580-1586, Nov. 1993.

- [25] S. Hudson, D. Pozar, "Grounded coplanar waveguide-fed aperture-coupled cavity-backed microstrip antenna," *Electronics Letters*, vol. 36, no. 12, pp. 1003-1005, June 2000.
- [26] J.-C. Cheng, N.I. Dib, L.P.B. Katehi, "Theoretical modeling of cavity-backed patch antennas using a hybrid technique," *IEEE Transactions on Antennas and Propagation*, vol. 43, no. 9, pp.1003-1013, Sep 1995.
- [27] F. Giuppi, A. Georgiadis, A. Collado, M. Bozzi, S. Via, and L. Perregrini, "An X band, Compact Active Cavity Backed Patch Oscillator Antenna Using a Substrate Integrated Waveguide (SIW) Resonator," *IEEE International Symposium on Antennas and Propagation (AP-S)*, Toronto, ON, Canada, July 11-17, 2010.
- [28] F. Giuppi, A. Georgiadis, M. Bozzi, A. Collado, and L. Perregrini, "Active Antenna Oscillator Systems in Substrate Integrated Waveguide (SIW) Technology," *EuCAP*, Apr. 2010, Barcelona (ES).